FR 1628

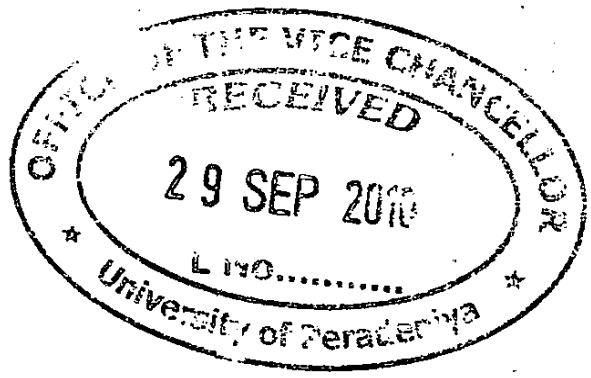

Final Report

On

Synthesis of Covalently linked Transition Metal Macrocyclic Complexes suitable for the Reduction of Water and Small Hazardous Molecules like CO_2.

Contract Number: RG/2006/FR/02

Principal Investigator:
Dr (Mrs.) M.Y.Udugala-Ganehenege

FINAL REPORT

Section 1

Information regarding Project/Project Personnel:

i) Contract Number: RG/2006/FR/02

ii) Title of the Project: **Synthesis of covalently linked transition metal macrocyclic and polypyridyl complexes suitable for the reduction of water and small hazardous molecules like CO_2.**

iii) Principal Investigator: Dr (Mrs.) M.Y.Udugala-Ganehenege

iv) Co-Investigators: None

v) Institute(s) where research was being carried out: University of Peradeniya

vi) Date of award: September 06, 2006

vii) Date of completion of Project: March 31, 2010

viii) Total allocation of funds (Rs): **25 86 484.00**

ix) Total spent (Rs): **25 84 852.45**

x) Number of Research Students employed: 05

xi) Post graduate degree completed with dates: 01 (Tentative date of the completion is in October, 2010 and he is writing the thesis of his M.Phil. Degree at present), 01 (has registered for an M.Phil. Degree)

xii) Number of Technical Assistants and/or laborers employed and period of service: 00

xiii) Publications/Communications arising from the project during the reporting period: 06 (published), 01 (accepted), 02 (submitted in September, 2010)

Section 2

Executive Summary of the Project:

Scientific background

Some face-to-face arranged metal macrocyclic complexes, shown in fig.1 and 2, synthesized by the chief investigator for her Ph.D. studies have shown remarkable affinities for trapping halides.[1,2] Redox behavior in such complexes is controlled by the nature of donor atoms, the ability of the ligands to adapt to coordination geometry changes, and the distance between metal centers. Many binuclear macrocyclic complexes have been synthesized in which these parameters are varied systematically, and the influence of these parameters on electron transfer and electronic and magnetic properties has been demonstrated.[3, 4] The relative orientation of the metal centers in binuclear complexes also plays a role in determining novel properties associated with the magnetic and electronic coupling between the metal centers through different bridging ligands. Many research have been carried out to convert or activate the bridging/coordinated ligand by using the novel properties associated with the redox and photochemical properties of the macrocyclic transition metal complexes.

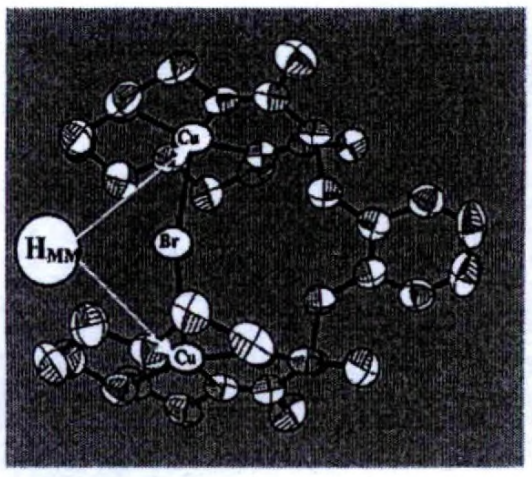

F.g.1. Br^- bridged dimeric Copper complex Udugala-Ganehenege, etal, *Inorg.Chem., 40(2), 2001, 1614-1625.*

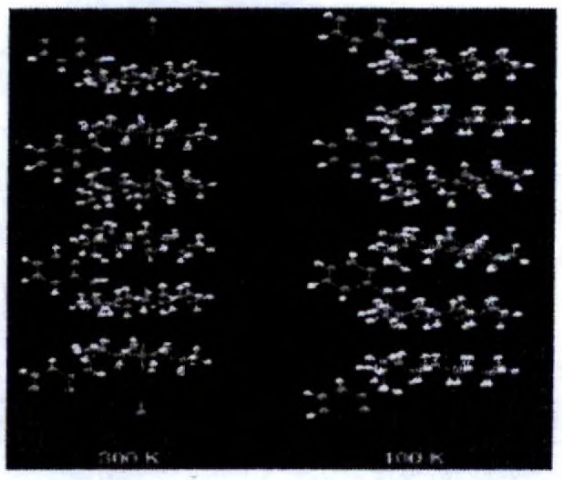

Fig.2. Br^- bridged dimeric Nickel complex Udugala-Ganehenege, etal, *Inorg.Chem., 44, 2005, 6019-6033.*

Objective

- The main objective of this research project was to synthesis novel macrocyclic metal complexes that were capable of trapping small molecules/ions for making use them
    - To mitigate Environmental Pollution caused by small hazardous molecules (like SO_2, NO, CO, CO_2, CH_4,etc) and heavy metal ions and anions
    - To produce Renewable Energy sources: Production of
        - H_2 from Water,
        - Fuels by CO_2 utilization/activation

Methodology

- The project pursued included a number of synthetic, spectroscopic and electrochemical studies of transition metal macrocyclic complexes.
- Electronic Absorption (UV-Visible, Luminescence, etc), Electrochemical potentials were used as measures of Coordination of small molecules/ions to transition metal centers and subsequent degradation of them regenerating the original metal complex.
- The different types of monomeric metal complexes having the structures shown in fig.3 were synthesized by using metal (Cu^{2+}, Ni^{2+}) salts, ethylenediamine and acetyl acetone and dithiozone (Rubeanic Acid).
- Attempts were made to synthesized dimeric structures shown in fig. 4 starting from the monomers in Fig. 3.
- The procedure were extended to synthesize structures similar to Fig. 5 by using natural sources (Chlorophyll-*a*) as the starting material.
- IR, CV,NMR, UV- visible, AAS, XRF, Single X-Ray and XRD techniques were used for the characterization and further analysis of the systems.

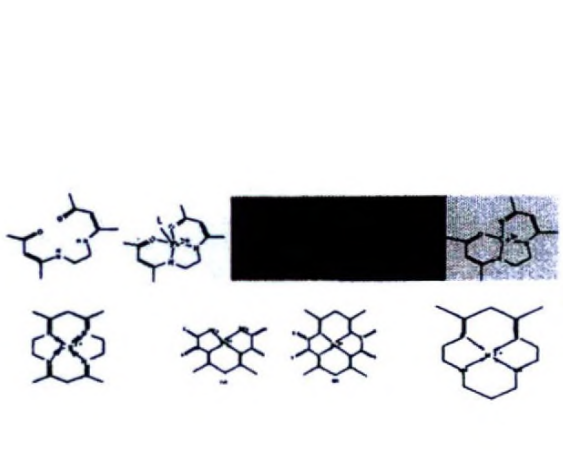

Fig.3

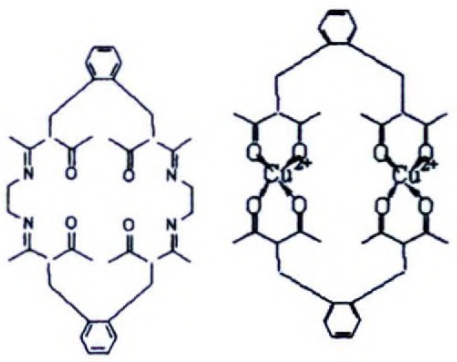

Fig.4

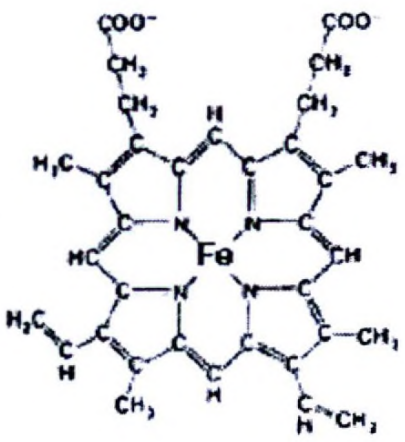

Fig.5

- Ion exchange properties of the systems were studied by using column chromatography techniques for the metal complexes that showed higher insolubility in almost all the solvents.
- CO_2 trapping capacities of the complexes of the type mentioned in Fig.3 and fig.5 were investigated by using a CO_2 detector which was sensitive to the IR radiation.
- Further, the nature of CO_2 binding with the temperature, complex concentration and the metal oxidation state of the complexes were studied.
- The fate of the bound CO_2 was studied by irradiation of the sample using a Xenon lamp(75 W), placing the sample container on a water bath to control temperature at a constant value (35^0-40^0 C).

Major findings

Complexes Synthesized and their Properties

1. Copper (II) complex with Dithiooxamide (Rubeanic acid) and acac.

(The possible structures are shown below in Fig.6 (a) and (b))

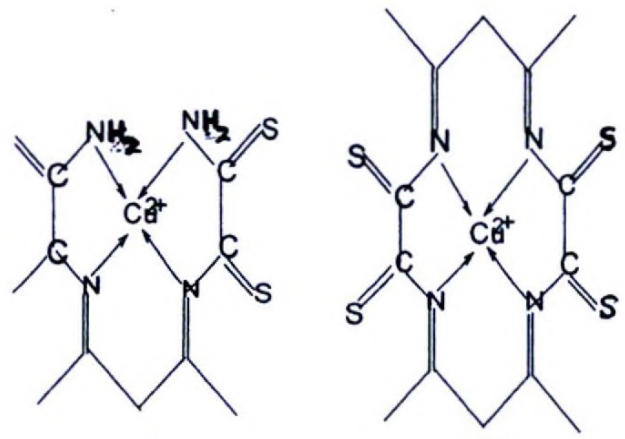

Fig.6

- The particle size of the complex is ~ 13.2 nm
- Complex can be used to trap Silver ions
- Ion exchange occurs at $[Ag^+] > 20$ ppm
- Specific affinity only for silver ions.

- This may be used for the application for specific trapping of some other noble ions like Au (I).

2. N,N- ethylenebis(acetylacetoneiminato)Cu(II) complex.

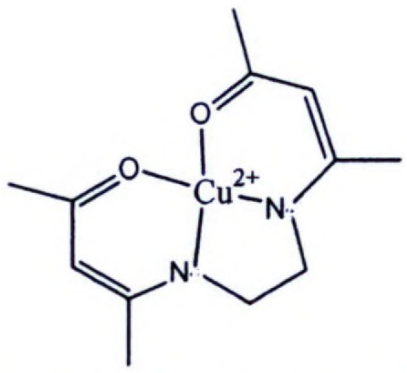

Fig.7. Structure based on X-ray data

- The complex shows
- An interesting acid base behavior; Reversible colour changes with H^+ & OH^-: qualitatively implies the possibility of making use of this compound as an acid-base indicator.
- A significant affinity for coordinating anions like SCN^-, Cl^-, Br^- and I^-
- The CO_2 binding capacity of the complex is about two times higher than the simple salt of Copper,($Cu(CH_3COO)_2$).
- This affinity CO_2 binding is higher at lower temperatures.

3. N,N- ethylenebis(acetylacetoneiminato)Ni(II) complex.

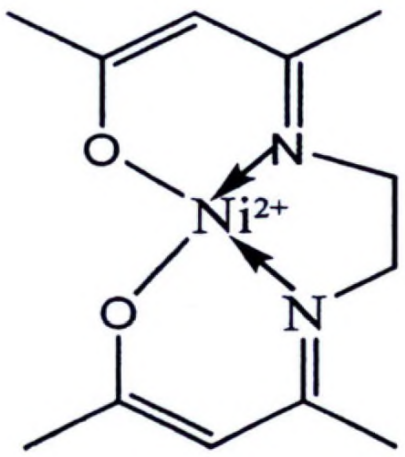

Fig.8. Structure based on X-ray data

- Appears as shiny, brownish red crystalline solid.
- It is highly soluble in organic solvent and mineral acid and forms a yellow colour solution. The solubility in water is poor.
- An interesting acid base behavior was seen.
- At room temperature, the complex shows ~ 35% more CO_2 absorption than nickel acetate, the starting material and the absorption capacity is not sensitive to the amount of complex present.

- When the temperature goes down to 4-5 °C the CO_2 absorption depends on the amount of complex present in the medium showing about 50% more CO_2 absorption than nickel acetate of the same concentration.

4. N,N- ethylenebis(acetylacetoneiminato)Fe(II) complex.

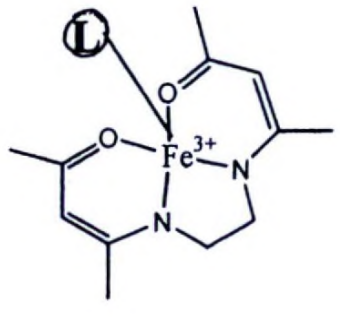

Fig.9. Expected structure

- The complex shows
  - An interesting acid base behavior
  - A significant affinity for coordinating anions like SCN^-, Cl^-, Br^- and I^- and converting them in to another useful forms.

    $I^- \longrightarrow I_2$

5. Conversion of Chlorophyll in to an M (II) Complex similar to Hemoglobin

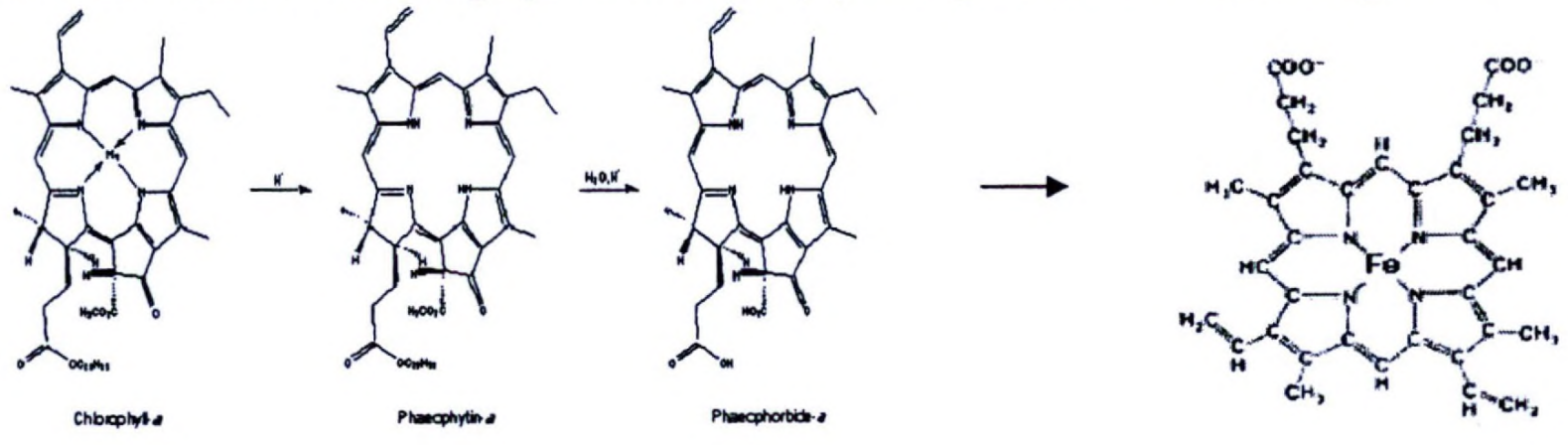

Fig.10. Steps in substituting Mg(II) center by transition metals(Fe, Co, etc)

1. When M= Fe (II/III)

- The complex is green
- The novel Fe(II) macrocyclic complex shows a significant higher capacity for CO_2 utilization than the chlorophyll *a* and simple Fe(II)/(III) salts (Fig.11)

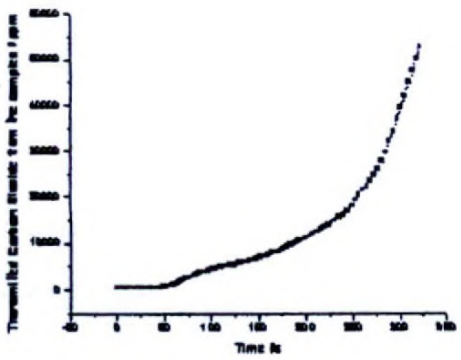

(a) CO_2 transmittance from Fe(II)complex with time

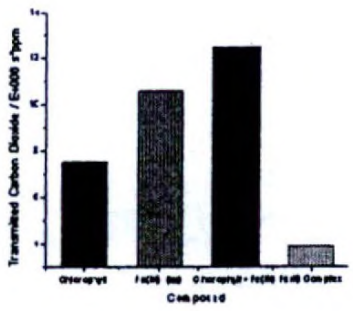

(b) CO_2 transmittance for complexes

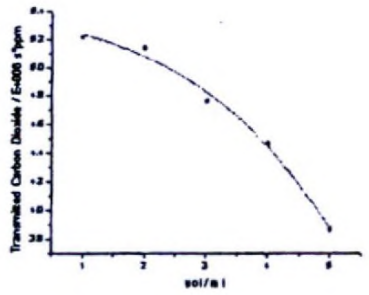

(c) CO_2 transmittance with increasing [Fe(II)complex]

Fig.11

2. When M = Co(II)

- The complex is dark green
- The novel iron (II) macrocyclic complex shows a significant higher capacity for CO_2 utilization than the chlorophyll *a* and simple Co(II) salts.(Fig.12 a)
- The compound showed an increased affinity for SCN^- coordination.
- The CO_2 trapping capacity in Co(II) complex gradually increases with the complex concentration (Fig.12 b)

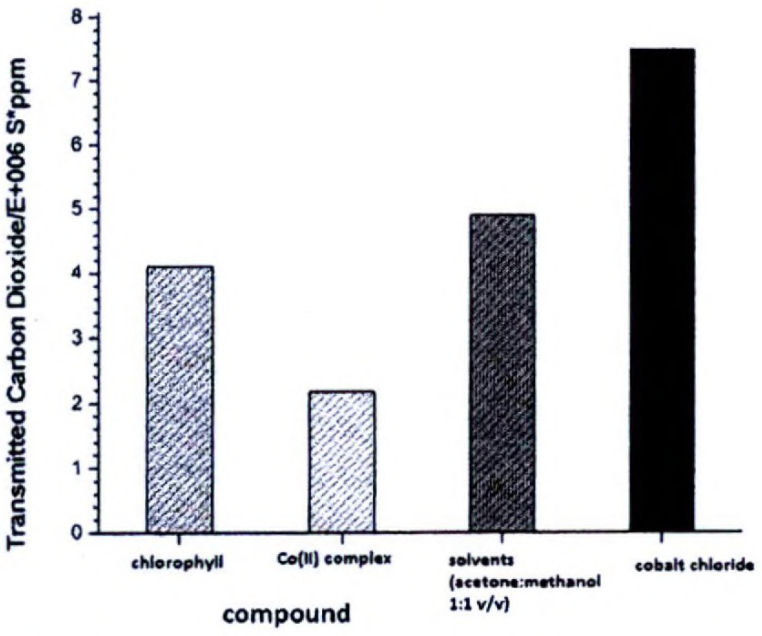

(a). CO_2 transmittance for different solutions

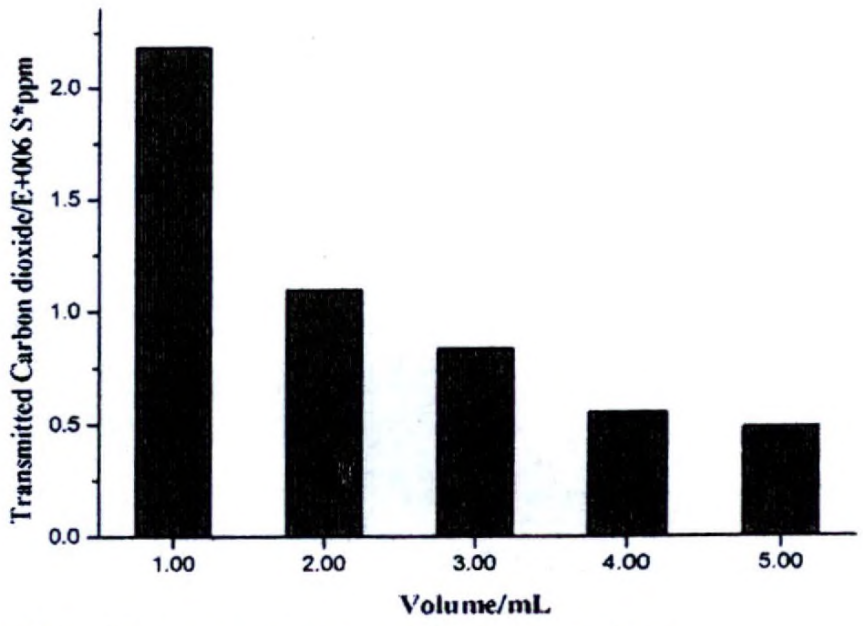

(b). CO_2 Transmittance with increasing [Co(II) complex]

Fig.12.

All the complexes of Cu (II), Ni (II), Fe (II/III) and Co(II) show higher CO_2 trapping capacity compared to the corresponding starting material of each complex.

Section 3
Report in detail:

i. Introduction/background

Global warming caused by increasing emission of greenhouse gasses such as CO_2, has been recognized as a serious environmental problem. Among the many options for the conversion and destruction of CO_2, the utilization of CO_2 has been received considerable attention recently. An increased use of CO_2 could be possible if the relatively inert CO_2 molecule could be activated. Among the numerous ways of CO_2 activation, coordination of CO_2 to transition metal macrocyclic complexes is currently under investigation. Many other gases like , N_2O, NO, H_2S, CO and unacceptable levels of some metal ions $Cr^{2+/3+}$, Cd^{2+}, Pb^{2+}, Hg^{2+} are also considered as environmental pollutants and the accumulation of those pollutants in the environment due to many anthropogenic activities has been increased in present. Many transition metal macrocyclic complexes have shown capability of binding various anions, cations and neutral molecules. Most of them are synthetic and the synthesis is highly expensive. Some face-to-face arranged transition metal macrocyclic complexes have shown remarkable affinities for trapping small molecules.[1,2] The redox properties of the metals of these complexes may be important for converting some hazardous small molecules present in our environment in to non-hazardous species. Thus, information from relatively simple systems would be very useful in evaluating those various possible contributions to donor-acceptor interactions and unusual affinities for small molecules. In this regard, a variety of homobimetallic systems has been synthesized. It has been shown that very simple monometallic macrocyclic counterparts itself facilitate the electrochemical reduction of small molecules like CO_2.[4,7, 17]

Further, binuclear macrocyclic complexes also represent an important class of compounds, since mixed-valence species with less common oxidation states can be stabilized.[21] Redox behavior in such complexes is controlled by the nature of donor atoms, the ability of the ligand to adapt to coordination geometry changes, and the distance between metal centers. Many binuclear macrocyclic complexes have been synthesized in which these parameters are varied systematically, and the influence of these parameters on electron transfer and electronic and magnetic properties has been demonstrated.[1,5, 22] The relative orientation of the metal centers in binuclear complexes also plays a role in determining magnetic and electron transfer properties. Solvent molecules and counter ions can play a significant role during such processes, particularly when the metal centers are coordinatively unsaturated and are prone to undergo geometrical changes. Therefore the 4 or 5 coordinated macrocyclic complexes may show anion/small molecule binding properties. Stabilities of the complexes may be dependent on the central metal ion, its oxidation state and the ligand environment. Therefore metal center of some complexes can be substituted by other metals. The understanding of the metal-metal, metal-ligand interactions of transition metal complexes has important implications for a range of chemical and biochemical areas.[1] A major thrust of many of these determinations has been to identify the unusual properties frequently associated with bimetallic complexes compared to those of the relevant monomer since the metal

properties can be significantly affected by the metal-metal interaction of bimetallic systems in contrast to the monometallic systems. Therefore, the determination of spectral, electrochemical, structural, photochemical, photophysical, kinetic and thermodynamic as well as catalytic properties of these complexes have received considerable attention. In this regard, a very large number of synthetic, as well as natural, bimetallic complexes have now been studied in considerable depth.[1-24] On the other hand, the importance of such systems, for example to the mechanism of photosynthesis, or to the transport of oxygen in mammalian and other respiratory systems, has provided a motivation for investigation of the metal-ion chemistry of macrocyclic as well as many other metal systems in general. Transition metal macrocyclic complexes provide the necessary site for the coordination of guest molecules/ions. In addition, they can act as catalysts for either activation/utilization and electro catalytic reduction of molecules like CO_2 and conversion of small molecules like CO_2 in to useful species/energy.

Among number of transition metal complexes, metalloporphyrins have been demonstrated to be very effective for CO_2 reduction because they,

- can activate small molecules through binding,
- absorb a significant portion of the solar spectrum,
- have long lived excited states,
- can promote multi electron transfer.

The metal-ion chemistry of macrocyclic ligands has now become a major subdivision of inorganic chemistry and undoubtedly great interest in this area will continue in future.

ii. Scientific scope of the project (overall and specific objectives)

The main objective of this research project was to synthesis novel macrocyclic metal complexes capable of trapping/coordinating small hazardous molecules (like CO, SO_2, N_2O, NO, H_2S, CO_2, CH_4 , etc) present as environmental pollutants and converting them into non hazardous and useful entity.

Investigation of trapping hazardous metals ions present in water such as Pb^{2+} , Hg^{2+}, Ag^{+}, Cd^{2+}, Cr^{3+} and Ni^{2+} by these macrocyclic complexes was another aim of this research project. Therefore, in the proposed research, we expected to synthesize several monometallic complexes and the corresponding covalently linked transition metal macrocyclic complexes which are very much useful as photochemical energy converters by decomposing and/or trapping small hazardous molecules present in our environment and reducing water to get H_2 (energy). Therefore the outcome of the reported research is of great interest to a country like Sri Lanka not only for solving environmental pollution issue caused by small hazardous molecules but also for the aspects of energy conversion/conservations. After studying the behaviour of similar model systems, the major aim was to extend the investigation towards similar natural systems such as transition metal prophyrin.

Therefore, in the reported research, we expected to synthesize several simple monometallic complexes as the model systems to investigate the complicated behavior of macrocyclic complexes synthesized by prophyrin system isolated from natural plants.

Natural starting materials were introduced for a more economical approach at the end of the project.

iii. **Materials and methods**

Reagents

The reagents (Organic Trading, Analtica) used in the synthesis were of analytical reagent grade and were used with further purification wherever necessary. Methanol used for the synthesis was distilled before using. All the metal salts (Sigma chemicals, Hemsons Sigma, Analytica, Aldrich, Mark, LOBA and BDH CHEMICALS) for the synthesis were used without further purification. Dithiooxamide (Rubeanic acid) was used after the recrystallisation in methanol. Doubly distilled water was used through out the research. All the reactions were performed under low light conditions and in a N_2 atmosphere as much as possible. Nitrogen (N_2) and Carbon Dioxide (CO_2) were taken from CEYLON OXYGEN LIMITED. Tithonia diversifolia leaves were used for extracting chlorophyll.

Instrumentation

All the compounds were characterized by following Cyclic Voltametric (CV) and UV-Visible, H^1NMR spectroscopic, FT/IR, XRD, AAS and X-ray techniques. Infrared (IR) spectra were determined from FT/IR model 400 and NICOLET 6700 FT/IR spectrometers for dry KBr pellets which were made by fusing KBr and solid samples of the complexes using a 12 ton laboratory press. Those pellets were kept in a desiccator for over night and IR spectra were taken. XRD data for dry powdered solid samples were taken from the SIEMENS D-5000 X-ray diffractometer. The powdered solid samples of complexes were used for the XRD analysis. Single crystal X-ray crystallographic analysis was done by sending few recrystallized crystalline samples to Wayne State University, USA. N,N- ethylenebis(acetylacetoneiminato)Ni(II) Samples synthesized in method *b* were sent to the X-ray lab of Tokyo Institute of University of Japan for getting X-ray measurements. Atomic absorption spectroscopic (AAS) data were recorded from BUCK 200A model atomic absorption/emission spectrophotometer. The cyclic voltammetric (CV) data were collected from the OUTOLAB PGSTAT 12 potentiostat/galvanostat with three electrode system comprised of glassy carbon electrode, saturated calomel electrode and platinum auxiliary electrode in 0.1 M KCl and 0.1 M (tetraethylammoniumhexaflourophosphate)TEAH as the electrolyte. UV-Visible spectra were recorded using a SHIMADZU UV mini – 1240(220-240), SHIMADZU UV-1800 and UV-1601 UV-Visible spectrophotometers for the methanolic and aqeous solutions of the complexes. ^{1}H and ^{13}C NMR for the complexes synthesized in $CDCl_3$ were recorded from Varian YH 300 NMR and Varian Mercury 3000 spectrometers. Xenon lamp (AMKO LAMPHOUSING A1000 series, 75 W), Mechanical stirrers, Nitrogen glove box, Thermometer, pH meter were used for studying the photochemical activities of iron complexes.

CO_2 trapping was monitored with a Vernier Labpro Interface (Fig 13 a) and CO_2 Gas Sensor which measures gaseous carbon dioxide levels by monitoring the amount of infrared radiation absorbed by transmitted carbon dioxide molecules.

Measurement of carbon dioxide gas binding properties

Two methods were used for the creation of CO_2. At the early stages of the research, CO_2 gas was prepared by treating dil. HCl (30 ml) with $CaCO_3$ (5 g of solid) form 0.005-0.01

M samples. In the other method, CO_2 from a CO_2 gas cylinder was passed under known pressure through the known amount of samples. A known amount of CO_2 (in ppm) was passed through either the 1-10 ml portions of the samples or solid sample, over a period of 320 s. The carbon dioxide transmitted through the sample was then passed into a container (5 L) where the gas sensor was set (Fig 13 b). The area under the curve (in the plot given in Fig 13.c) is proportional to the CO_2 concentration. The transmitted CO_2 with time (in *s*) was recorded as ppm*s.

(a) CO_2- Gas sensor

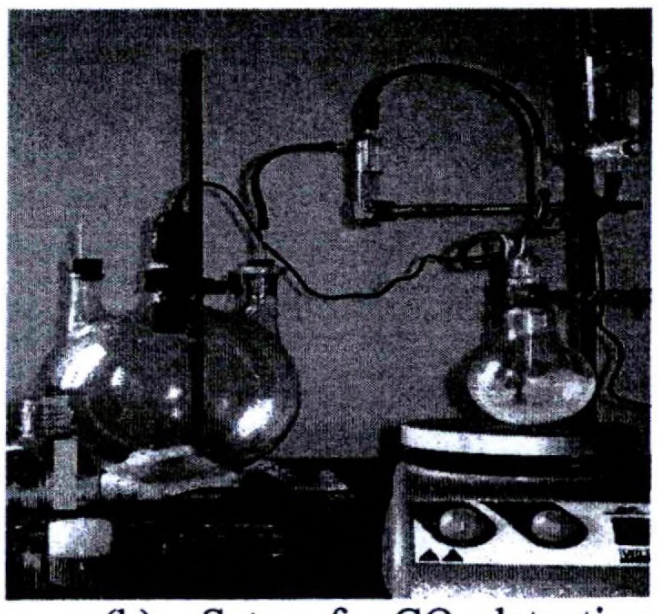

(b) Set up for CO_2 detection

	Latest		
	Time (s)	Temp (°C)	CO2 (ppm)
1	0	46	584
2	4	46	578
3	8	46	560
4	12	46	561
5	16	43	560
6	20	43	561
7	24	42	560
8	28	40	583
9	32	39	584
10	36	38	582
11	40	37	583
12	44	36	605

Temperature
°C

CO2 ppm

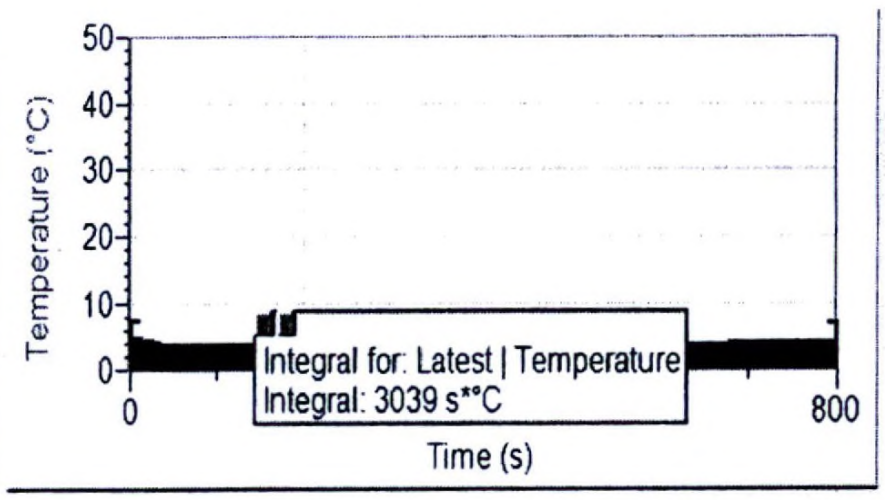

(c) Recording of CO_2 concentration with time in the computer interface

Fig 13

Experimental

1. Copper (II) complex with Dithiooxamide (Rubeanic acid) and acac.

$Cu(CH_3COO)_2.H_2O$ (0.831 g, 0.0042 mol) was dissolved in distilled water (70 ml) in a quick fitted round bottomed flask while stirring the solution magnetically. Recrystallized dithiooxamide (1.000 g, 0.0084 mol) was dissolved in methanol (140 ml) and the solution was slowly added into the blue coloured $Cu(CH_3COO)_2.H_2O$ solution. A portion (50 ml) of the resulting greenish black color mixture was decanted off by using a pipette and the precipitate (**Cu-A**) was filtered, washed (from methanol and distilled water) and dried in a desiccator. Acetylacetone (acac) (5 ml) was added into the remaining mixture and refluxed for two hours. After refluxing it was kept at room temperature for 30 min. Then the resulting black color precipitate (**Cu-B**) was filtered under suction on a Buckner funnel and the precipitate was washed with methanol and distilled water and dried in a desiccator.

1.1 Purification and Characterization

The synthesized complexes were washed with distilled water and methanol several times and then washed with acetone and dried in desiccators. The solubility of those two complexes was tested for many organic solvents, mineral acids and distilled water. The soluble parts were collected and used for UV-visible spectroscopic measurements. Recrystallisation was not successful due to the insolubility of the complex. FT/IR spectroscopic determination and XRD analysis were carried out for solid samples of the two complexes. As the complexes were hard their Mohs hardness was determined using the facilities in the department of Geology. Melting point was determined for the powdered sample of the complex.

1.2 Ion Exchange Study

As the solubility of the complex was very low its solution chemistry was difficult to investigate. Therefore the capability of trapping cations and the ability of ion exchange properties were studied. A column with a 0.5 cm diameter and a 15 cm height was packed by powdered Cu-B complex (4.0 g). (Fig. 2.5) An aqueous Ag (I) ion solution (0.01 M, 3 mL at a time) was passed through the column and the effluent was tested with aqueous NaCl (1.0 M) and Conc. Ammonia solution for Ag (I) and Cu (II). Similarly for aqueous Pb (II), Cd (II), Ni (II) and Zn (II) ion solutions were passed through separate columns packed by the Cu-B and precipitated with suitable precipitating agents. AAS measurements were taken for the effluents after passing very dilute solutions of above cationic solutions (5 ppm to 100 ppm). Similarly CV measurements were recorded between +0.7 V to -0.7 V for the effluent collected after passing Ag (I) aqueous solution through a column packed by the Cu-B at a scan rate of 50 mV/S.

1.3 Ag(I) binding properties; XRF analysis

A column of the Cu-B complex was prepared and 0.1 M $AgNO_3$ solution was passed through the column, and effluents were collected and tested with dil NH_3 and 1.0 m NaCl. The elusion was carried out until the colour of the effluent became blue with dil. Ammonia first and the formation of white precipitate with 1.0 M NaCl second. Then the

complex in the column was collected in to a watch glass and dried in an oven at 60 ^{0}C for two hours and kept in a desiccator. XRF analysis was done for the resultant solid sample.

2. N,N- ethylenebis(acetylacetoneiminato)Ni(II) complex.

This complex was synthesized by two approaches **a** and **b**.

a. $Ni(CH_3COO)_2.4H_2O$ (2.000 g, 0.008 mol) was dissolved in methanol (50 ml) in a quick fitted round bottomed flask on a magnetic stirrer. While stirring the mixture ethylene diamine (**en**, 2.0 ml) was added. Next this mixture was stirred few minutes and acetyl acetone (**acac**, 2.0 ml) was added and the mixture was refluxed for two hours. Then it was kept (30 min) at room temperature. Next the resulting precipitate was concentrated using a rotary evaporator. Finally resulted red colour precipitate was filtered under suction on a Buchnor funnel.

b. $Ni(CH_3COO)_2.4H_2O$ (4.98 g, ~0.02 mol), ethylene diamine (2.7 ml, 0.04 mol), acetyl acetone (4.1 ml, 0.04 mol) were mixed in a quick fitted round bottomed flask. Methanol (20 ml) was added and stirred well. The reaction mixture was refluxed for 2 hours. A dark red crystals formed upon cooling was filtered under suction, washed with methanol and dried in a desiccator.

2.1 Purification and Characterization

The synthesized complex (N,N- ethylenebis(acetylacetoneiminato)Ni(II) complex) was washed with distilled water several times and dried in a desiccator. The solubility of the complex was tested for many organic solvents, mineral acids and distilled water. The complex was purified by recrystallization in ethanol and used for other characterization tests. UV-visible spectrum was recorded for the methanolic solution of the complex. FT/IR spectroscopic determination and XRD analysis were carried out for solid samples of the complexes. . ^{1}H and ^{13}C NMR spectra were recorded with respect to $CDCl_3$. Melting point was determined for the powdered sample of the complex. Recrystallized crystals were sent to Wayne State University, USA for getting X-ray Structure of the complex.

2.2 Acid-base properties of N,N- ethylenebis(acetylacetoneiminato)Ni(II) complex

N,N- ethylenebis(acetylacetoneiminato)Ni(II) complex (0.015 g) was dissolved in methanol (20 ml). UV spectra were recorded with the stepwise addition (micro drop at a time) of 0.1 M HCl to that methanolic solution. After that 0.1 M NaOH was added to the same solution mixture drop wise from a micro syringe and UV spectra were recorded. The colour changes of the solution were also recorded.

2.3 **CO_2 trapping capacity of the N,N'- ethylenebis(acetylacetoniminato) Nickel(II) complex**

Two methods were used for the creation of CO_2. In one method CO_2 from a CO_2 gas cylinder was passed under known pressure. In the other method CO_2 gas was prepared by treating dil. HCl (30 ml) with $CaCO_3$ (5 g of solid). In each case, CO_2 (known amount in ppm) was passed through the 10 ml portions of the complex having different concentrations, over a period of 300 s at known temperatures. The CO_2 transmitted from

the sample was then passed into a container (5 L) where the gas sensor was set and the amount transmitted was recorded as ppms (amount in *ppm* × time.in *s*). IR spectra were recorded from NICOLET 6700 FT/IR spectrometer for dry pellets of the complexes before and after passing CO_2.

The N,N- ethylenebis(acetylacetoneiminato)Ni(II) complex after and before passing CO_2 were recrystalized and sent to Tokyo Institute of Technology in Japan to get X-ray analysis done. Further electrochemical and IR spectroscopic studies were carried out to determine the fate of CO_2 trapped by these systems. IR spectra for solid N,N-ethylenebis(acetylacetoneiminato)Ni(II) complex isolated before and after passing CO_2 were recorded. CO_2 addition experiments were carried out in both solid and solution states.

Crystals of Ni(II) complex was dissolved in methanol in order to get a saturated liquid. Sodium perchlorate crystals were dissolved in distilled water and made a saturated prerchlorate solution. Saturated perchlorate was added dropwise to the saturated Ni(II) complex. Dark red tiny crystals formed were seperated under suction filtration.CO_2 was passed through the recrystallized samples for 5 hrs and XRD analysis was performed using these crystals.

A concentration series of N,N- ethylenebis(acetylacetoneiminato)Ni(II) complex and Ni(II) acetate was prepared in methanolic medium and their CO_2 binding capability were tested with CO_2 gas sensor. Another same concentration series was prepared and the samples were kept in an ice bath in order to maintain in ~4 °C. CO_2 binding capability was tested with CO_2 gas sensor at 5 °C.

3. N,N- ethylenebis(acetylacetoneiminato)Cu(II) complex.

This complex was synthesized by following two procedures **a** and **b** given below.

a. $Cu(CH_3COO)_2.H_2O$ (2.000 g, 0.01 mol) was dissolved in distilled water (40 ml) in a quick fitted round bottomed flask on a magnetic stirrer. While stirring the mixture **en** (2.0 ml) was added. After stirring the mixture (5 min), **acac** (2.1 ml) was added and refluxed for 40 minutes. Next the mixture was kept (30 min) at room temperature and the resulting precipitate was filtered (Filtrate was purple) under suction and washed with distilled water dried in a desiccator.

b. $Cu(CH_3COO)_2.H_2O$ (4.00 g, ~0.02 mol), ethylene diamine (2.7 ml, 0.04 mol), acetyl acetone (4.1 ml, 0.04 mol) were mixed in a quick fitted round bottomed flask. Water (20 ml) was added and stirred well. The reaction mixture was refluxed for 40 min. Purple crystals formed upon cooling was filtered under suction, washed with methanol and dried in a desiccator.

3.1 Purification and Characterization

The synthesized complex (N,N- ethylenebis(acetylacetoneiminato)Cu(II)) was washed with distilled water several times and dried in a desiccator. The complex was purified by recrystallization in ethanol and used for other characterization tests. The solubility of the complex was tested for many organic solvents mineral acids and distilled water. UV-visible spectrum was recorded for the methanolic solution of the complex. FT/IR

spectroscopic determination and XRD analysis were carried out for solid samples of the complexes. ^{1}H and ^{13}C NMR spectra were recorded with respect to $CDCl_3$. Melting point was determined for the powdered sample of the complex. Recrystallized crystals were sent to Wayne State University, USA for getting X-ray Structure of the complex.

3.2 Acid-base Chemistry of N,N- ethylenebis(acetylacetoneiminato)Cu(II)

N,N- ethylenebis(acetylacetoneiminato)Cu(II) (0.015 g) was dissolved in ethanol (20 ml). UV-visible spectra were recorded with the stepwise addition of 0.1 M HCl to that ethanolic solution from a micro syringe. Next 0.1 M NaOH was added micro drop wise to the same solution mixture and the UV-visible spectra were recorded. This experiment was also performed with a large weight (0.050 g) in 30.0 ml of methanol and pH were measured while adding H+ and OH- ions.

3.3 Anion binding capability of N,N- ethylenebis(acetylacetoneiminato)Cu(II)

Cu-en-acac (0.0100 g) was dissolved in Ethanol (10 ml) and 3.5 ml was collected into a UV cell and acidified by adding few micro drops of 1.0 M HCl and UV visible spectra were recorded while adding 1.0 M Cl^- solution drop wise. This experiment was repeated replacing the Cl^- solution with Br^-, I^-, SCN^- solutions seperately.

3.4 Testing the capability of trapping CO_2

CO_2 was created from the reaction between $CaCO_3$ and HCl. CO_2 produced was passed through a series of methanolic solutions of the N,N- ethylenebis(acetylacetoneiminato) Cu(II) having different concentrations at different known temperatures. The amount of the emitted CO_2 was detected by using CO_2 sensor. The IR spectra were recorded for dry KBr pellets of the complex before and after passing CO_2. Controller experiments were carried out for each sample by using $Cu(CH_3COO)_2$.

4. N,N- ethylenebis(acetylacetoneiminato)Fe(II) complex.

Ethylenediamine (2.7 ml, 0.04 mol) and acac (4.2 mL, 0.04 mol) were mixed in methanol (20 mL) in a quick fitted round bottomed flask. Then $Fe(NO_3)_3.9H_2O$ (8.000g, 0.02 mol) which was dissolved in methanol (50 mL) was added and refluxed for two hours. The resulting mixture of red and yellow precipitates formed upon cooling were filtered under suction and washed with cold methanol. The two components were isolated separately by using the differences in their solubility. The red colour complex was dissolved in hot methanol and transferred into the filtrate while yellow colour precipitate (Fe-en-acac-Y) was remained on the filter paper. The reddish filtrate was concentrated using a rotary evaporator and the reddish crystalline precipitate, (Fe-en-acac-R), formed was filtered, washed with water and dried in a desiccator.

4.1 Characterization of Fe-en-acac-R and Fe-en-acac-Y

The synthesized red colour complex, (Fe-en-acac-R), was washed with distilled water several times and dried in a desiccator. The complex was purified by recrystallization in ethanol. The synthesized yellow complex was washed with methanol several times and dried in a desiccator for few hours and used for further analysis. The solubility of the two complexes was tested for many organic solvents, mineral acids and distilled water. UV-visible spectrum in methanol for Fe-en-acac-R complex was recorded. For the Fe-en-

acac-Y complex, UV-visible spectrum was recorded in water. FT/IR spectroscopic determination and XRD analysis were carried out for solid samples of the complexes. ^1H NMR spectrum of the red complex was recorded with respect to $CDCl_3$ while the yellow complex with respect to D_2O.

4.2 Acid-base Chemistry of Fe-en-acac-R

Fe-en-acac-R (0.015 g) was dissolved in methanol (20 ml). UV spectra were recorded with the stepwise addition of 0.1 M HCl to that methanolic solution from a micro syringe. Next 0.1 M NaOH was added drop wise to the same solution mixture and UV spectra were recorded.

4.3 Anion binding capability of Fe-en-acac-R

Fe-en-acac-R (0.0100 g) was dissolved in Ethanol (10 ml) and acidified by adding few micro drops of 1.0 M HCl and UV visible spectra were recorded while adding 1.0 M X^- solution ($X^- = Cl^-, Br^-, I^-, SCN^-$) drop wise.

5. Conversion of Chlorophyll in to an M (II) Complex similar to Hemoglobin

Extraction of Chlorophyll a

Extraction of Chlorophyll *a* was done according to the lmodified iterature procedure[11] and characterized by UV visible spectroscopy.

Fresh leaves of *Tithonia Diversifolia* plant (50.00 g) were carefully washed with distilled water and dried with a paper towel. Dried leaves were cut into small pieces and placed in acetone in a dark reagent bottle fixed with a N_2 filled balloon. Next, the reagent bottle was kept in a dark box for 24 hours. The resultant dark green acetone extract was filtered through a cotton pad and transferred into a separating funnel (30 ml). Then, Petroleum ether (40 ml) was added to it and the solvent system was shaken gently. After that, distilled water (about 120 ml) was added and allowed to separate. Next, polar water-acetone layer was discarded and to the remaining less polar petroleum ether fraction an equal volume (about 40 ml) of 92% methanol solution was added and the solvent system was shaken gently. Then again, distilled water (about 100 ml) was added and it was allowed to separate. Petroleum ether fraction was concentrated using a water bath. The residue isolated was a mixture of pigments containing a large amount of Chlorophyll a and other accessory pigments such as carotenoids.

A TLC analysis on this was done by changing the ratios of acetone and hexane to separate the pigments and found the ideal acetone: hexane composition should be 1:4. Chlorophyll a was isolated using column chromatography by using an 8 cm column of silica gel (60, 0.063 mm, 15 g) as the absorbent, acetone/hexane(1:4 v/v) as the mobile phase. Each fractions were characterized by UV-Visible spectroscopy.

5.1. Preparation of the iron (II) complex and study of CO_2 trapping

Method A.

Chlorophyll *a* separated by the gravity column was evapourated and then dissolved in acetone (5 ml). Then 0.1 M methanolic solution of Fe(111) (5 ml , prepared by dissolving 1.62 g of $FeCl_3$ in 100 ml of distilled methanol) and 1-methyl-2-pyrrolydinone (4 ml)

were added to it and stirred for 3 hours at 30 ^{0}C. The resultant brownish green solution (Fe (III) complex) was acidified with two drops of dilute sulfuric acid and Zn /Hg (10 g) was added to it. The reaction mixture was kept anaerobic for 24 hours by passing nitrogen gas through it. The reduced form of the product, the Fe(II)complex, was isolated as a dark green solution after the evaporation of the solvent on a rotary evaporator at 30 ^{0}C and characterized by following CV ,UV-Visible, H^1NMR spectroscopic techniques. CV data were recorded from OUTOLAB PGSTAT 12 potentiostat/galvanostat with three electrode system comprised of glassy carbon electrode, saturated calomel electrode and platinum auxiliary electrode in 0.1 M KCl as the electrolyte. UV-Visible spectra were recorded using a SHIMADZU UV mini – 1240 (220-240) spectrophotometer. H^1NMR spectra in d_3-$CDCl_3$ and d_6-DMSO were taken by using Varian Mercury 3000 spectrometer.

CO_2 trapping was monitored with a Vernier CO_2 Gas Sensor. CO_2 gas was prepared by treating dil. HCl (30 ml) with $CaCO_3$ (5 g of solid). Carbon dioxide (0.05 mol) was passed through the 1 ml portions of the samples over a period of 320 s. The CO_2 transmitted through the sample was then passed into a container (5 L) where the gas sensor was set.

Method B.

Solvent of the identified Chlorophyll a fraction was evaporated off using a water bath and the residue obtained was dissolved in acetone (10 ml)

Indirect method

To chlorophyll (10 ml) extract, 0.1 mol dm^{-3} HCl (1.0 ml) was added (pH=3) and it was heated in a water bath to accelerate the reaction. A color change from dark green to brownish-green indicated the formation of Pheophytin, which was then confirmed with UV-Vis spectrophotometer. Next, to the Pheophytin solution, a concentrated solution Fe (III) Chloride (1 ml, 0.00 g dissolved in 5 ml of acetone) was added and heat was heated for 2 min in water bath. A color change from brownish-green to dark green was observed.

Direct method

To chlorophyll extract (10 ml), the concentrated solution of Fe(III) Chloride (1 ml) was added and the mixture was heated in a water bath for 2 min.

A. Analysis of the Iron(III)-Porphyrin complex

Complexes obtained from both direct and indirect methods were analyzed as follows.

I. Using UV-Vis spectrophotometer: wavelength 190-1100 nm

II. Using Cyclic Voltammetry : Electrolyte 0.1 M KCl
Potential range -1.5-1.5 V

B. Preparation of iron(III)-Porphyrin complex coordinated with N-methyl-2-pyyrolidinone

To the iron(III)-Porphyrin complex (10 ml) a Nitrogen base, N-methyl-2-pyyrolidinone (4 ml) was added and it was stirred for 3 hours at the 30°c.a brownish green solution results.

C. Preparation of Iron(II)-Porphyrin complex

To reduce the resulting brownish green solution in to Fe^{+2} state, it was acidified with two drops of dilute H_2SO_4 and then Zn-Hg amalgam was added. The reaction mixture was kept inside a N_2 filled glove box for 24 hours, providing low light conditions. The product was isolated as a dark green solution after the evaporation of the solvent on a rotary evaporator for 5 hrs at 30°c.

D. Analysis of the Iron(II)-Porphyrin complex

The product was analyzed as follows.

I. Using UV-Vis spectrophotometer: wavelength 190-1100 nm

II. Using Cyclic Voltammetry : Eectrolyte 0.1 M KCl
Potential range -1.5-1.5 V

E. Isolation of the product as solid

Iron(III)-Porphyrin (5 ml),and Iron(II)-porphyrin (5 ml) were taken separately and dilute Glacial acetic acid (5 ml) was added and a formation of a bright yellow precipitate from Fe^{3+} state and a pale green precipitate from Fe^{2+} state were observed. Precipitate were filtered out washed thoroughly with dilute glacial acetic and let it to dry inside a desiccator.

F. Characterization of the products.

Both solids and the filtrate were analyzed as follows.

Analysis of the solid products

I. Solubility was tested in various solvents (Hexane, Ethyl acetate, Methanol, Acetone, Distilled water, DMSO)

II. Substitution of the metal center with Cu^{+2}
Possibility of a different metal ion to substitute the Fe^{+3}/Fe^{+2} center of the Fe-Porphyrin complex was studied. The substitution was confirmed by testing the eluted solutions with $K[Fe(CN)_4]$and $K_2[Fe(CN)_4]$.

G.CO_2 reduction analysis

a. Conventional CO_2 reduction

A Conventional method for CO_2 reduction was applied for the complex Fe(II)-Porphyrin (liquid), (where Fe in +2 oxidation state). CO_2 (g) was passed through a sample of Fe(II)-Porphyrin over a particular time period and the amount of CO_2 transmitted was determined by passing it into a flask where a CO_2 gas sensor was set. Therefore, lower transmitted of CO_2 indicates higher absorbance by the sample hence a higher absorption of CO_2. After passing CO_2, UV-Visible and CV data were recorded. Same procedure was repeated for two controllers; a chlorophyll solution and acetone (10 ml) containing N-methylpyrolidinone (8 ml) and $FeCl_3$ (10 ml)

b. Photochemical CO_2 reduction

Photochemical CO_2 reduction was done by irradiating Visible light on a sample of Fe (III)-Porphyrin (liquid). Fe(III)-Porphyrin complex was dissolved in a solution containing acetone (10 ml), 5% TEA (Triethyl amine) and saturated with CO_2.The CO_2 concentration inside the setup was measured using Vernier CO_2 detector. The probe was fixed in to one neck of the two necked flask using two quick-fit connectors, one with special mechanism to prevent any liquid vapor reach the probe. Before the irradiation

CO_2 concentration inside the setup was brought into a higher but to a constant value by continuously monitoring CO_2 concentration using the Vernier interface to the computer. Then the setup was air sealed using quick fit glassware applying grease. Next, irradiation was done using a 75 W-xenon lamp, placing the sample container on a water bath to control temperature at a constant value (35^0-40^0C). Other radiation (UV and IR) were avoided as much as possible. IR radiation was avoided by passing radiation through the water filled container and avoided the UV radiation by irradiating through two Pyrex glass walls (Glass wall of the sample container, glass wall of the water bath). With the irradiation, the CO_2 concentration was continuously monitored and recorded for a period of one hour. Same procedure was repeated for two controllers; a chlorophyll solution and a solution containng acetone(10 ml), N-methylpyrolidinone (8 ml), $FeCl_3$(10 ml) and TEA (5%).

5.2 Preparation and isolation of Co(II) complex similar to heamoglobin and study of CO_2 trapping

Chlorophyll *a* residue was dissolved in acetone (5 ml).Then 1 drop of HCl was added to it (pH 6.2). Then 0.1 M methanolic solution of cobalt (II) chloride (5 ml, prepared by dissolving 0.25 g of $CoCl_2.6H_2O$ in 5 ml of distilled methanol) was added and stirred for 3 hours at room temperature. Then cobalt (II) complex was isolated using column chromatography with silica gel (silica gel 60, 0.063 mm, 5.00 g) as the adsorbent and ethyl acetate/hexane (1:4 v/v) as the eluent. Then the isolated Co (II) complex was characterized by following spectroscopic techniques. CV data were taken in acetonitrle containing 0.1 M TEAH as the electrolyte. To isolate the solid product, Triethylammine (1 ml) was added to the Co (II) complex (5 ml). Light green colour solid was obtained. Then IR spectra were recorded from NICOLET 6700 FT/IR spectrometer for dry KBr pellets of the complexes before and after passing CO_2. XRF spectra of the solid were also obtained. CO_2 trapping was monitored with a Vernier LabPro CO_2 gas sensor as mentioned before.

5.3 Preparation of the Ni (II) complex similar to heamoglobin and study of CO_2 trapping

Chlorophyll *a* separated by a gravity column was evaporated and dissolved in acetone (5 ml). Then 0.1 M Methanolic solution of Ni (II) (5 ml prepared by dissolving 2.48 g of Ni $(CH_3COO)_2$ in 100 ml of distilled methanol), one drop of dil. HCl were added to it and stirred for 3 hours at room temperature. The resultant brownish green solution of Ni (II) complex was treated with Zn/Hg (10 g). The reaction mixture was kept under anaerobic conditions in glove box for 24 hours by passing N_2 gas through it. The product was isolated as a dark green solution and characterized by UV visible spectroscopy

6. Attempted synthesis of binuclear complexes:

N,N- ethylenebis(acetylacetoneiminato)Ni(II) complex (0.725 g, 0.0025 mol) was treated with dibromoorthoxylene (0.33 g, 0.00125 mol) in MeOH (30 mL) refluxing for 4 hrs. Yellowish dark red solution was obtained and the attempts made to remove solvent and isolate the solid product became unsuccessful.

(iv).Results/outputs and Discussion

1. Copper (II) complex with Rubeanic acid and acetylacetone

1.1 Physical Properties of Cu-A and Cu-B

Both complexes Cu-A and Cu-B were isolated as hard, shiny, black solids. The Cu-A is the copper (II) dithiooxamado complex and Cu-B is formed by reacting Cu (II) with dithiooxamide and acetylaceton in 1:2:2 stoichiometric ratios respectively.

Both complexes Cu-A and Cu-B are insoluble in almost all the solvents except concentrated Nitric and Hydrochloric acids. The hardness of the complexes are in between 2.5 (finger nail) and 3 (calcite) according to the Mohr's hardness scale. The streak test shows a dark gray color streak on a porcelain plate. Melting points of the complexes are above 280 °C. Due to the high insolubility of these compounds in almost all the solvents, further studies could not be carried out as expected and the methodology was deviated to study the solid state chemistry/behavior of the complex.

1.2 Characterization - IR data

The predicted structures are given below (Fig. 14).

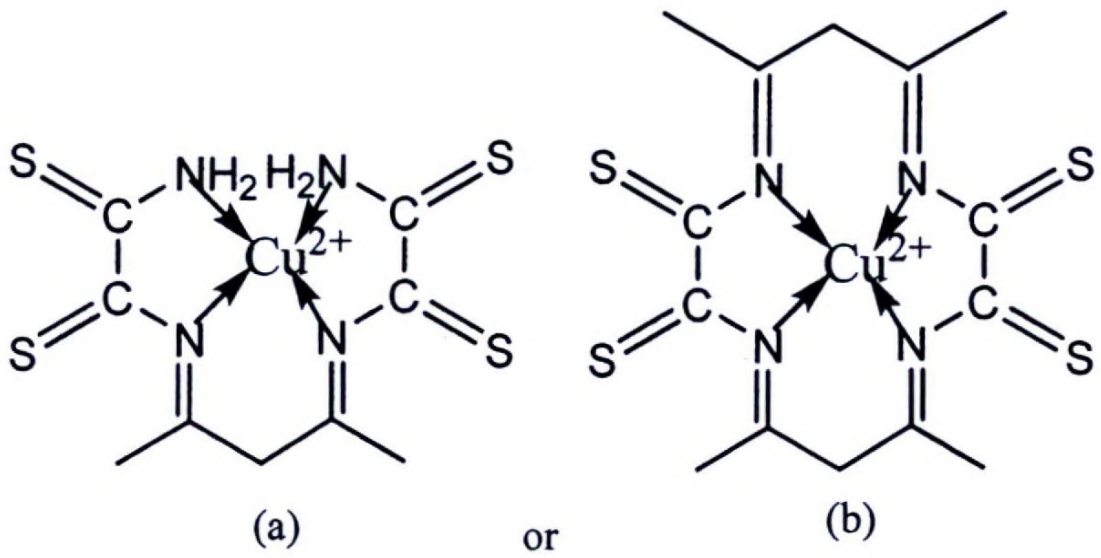

Fig. 14 The predicted structures for Cu-B complex

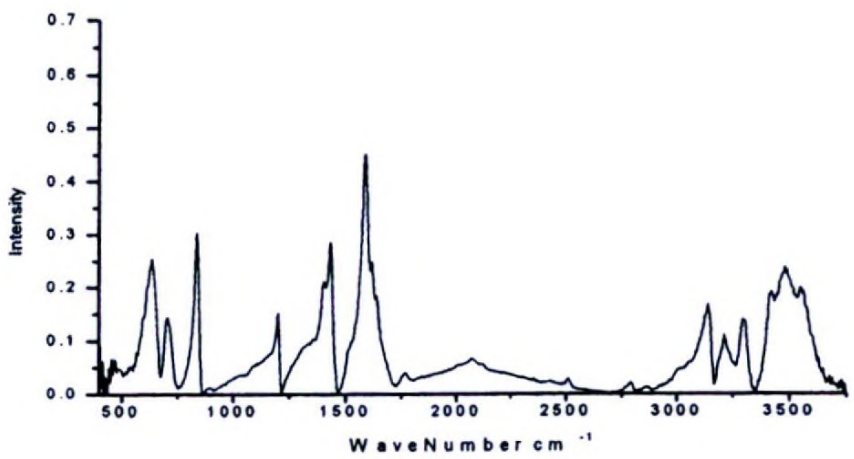

Fig. 14.1 IR Spectrum of Rubeanic acid

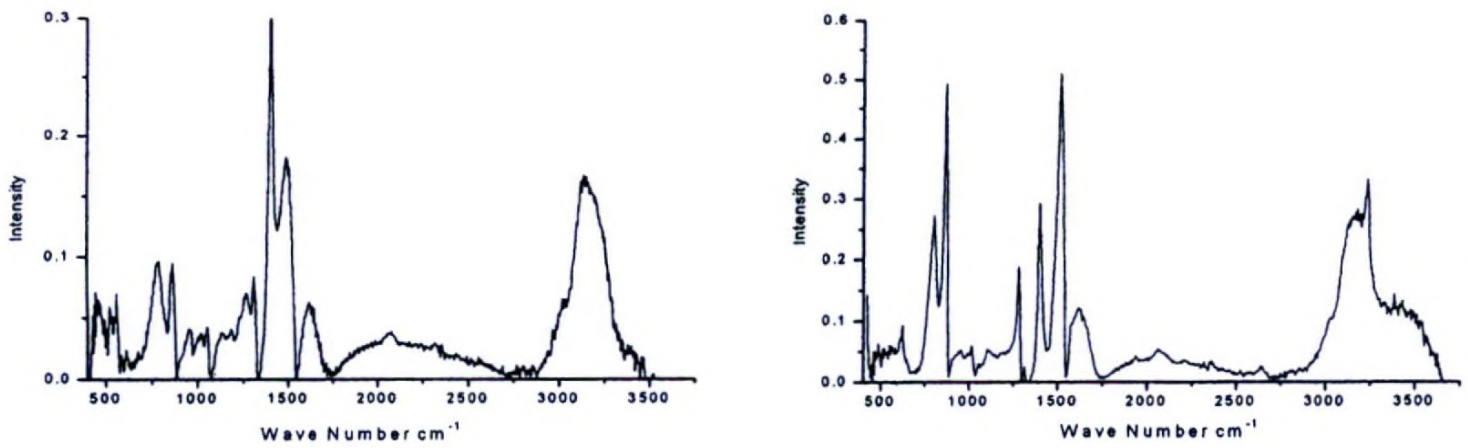

(a). (Cu-B) **(b) (Cu-A)**

Fig. 14.2 IR spectra for Cu(II) complex with Rubeanic acid and acetylacetone

IR data of the two complexes show significant differences in spectra of free dithiooxamide and metallo derivatives in the region of N-H absorptions (Fig.14.2 (a) and (b)). This observation is consistent with the reported data for a similar complex. The band at 3137 cm^{-1} attributed to N-H stretching frequency is sharper and higher in frequency in metallo derivatives compared to the free dithiooxamide. However, IR data for copper (II) dithiooxamido complex (Cu-A) and the new complex (Cu-B) are very much similar to each other except for the two additional strong bands at 872 $cm^{-1}$and 1518 cm^{-1} corresponding to C=C stretching and bending modes of $Cu(acac)_2$ fragment of the complex .The absence of a strong band at 1577 cm^{-1} corresponding to C=O stretching frequency of $Cu(acac)_2$ fragment supports the formation of a cyclic complex.

1.3 Characterization - XRD data

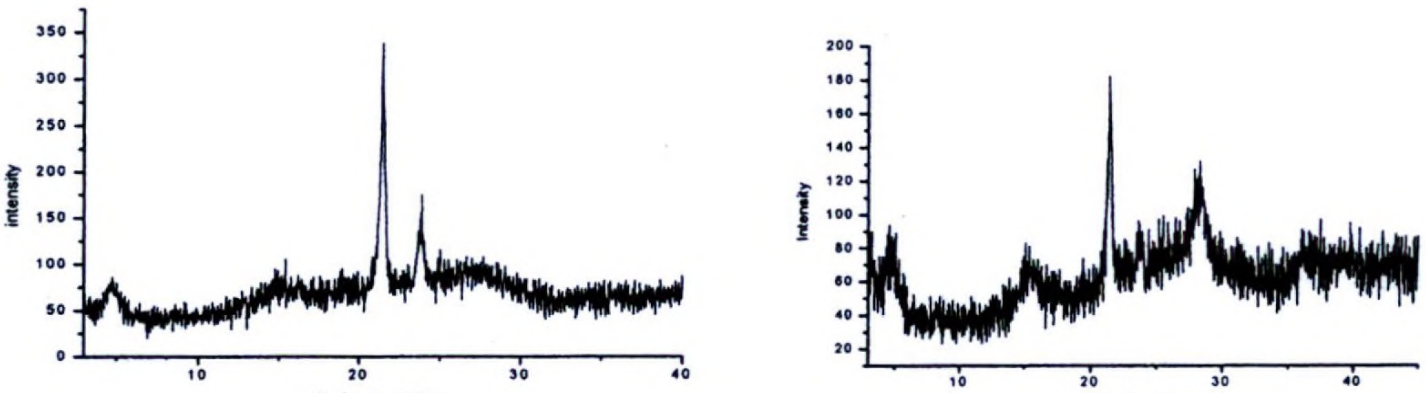

(a). Cu-A **(b). Cu-B**

Fig. 15 XRD spectra

According to the XRD data the two complexes (Cu-A and Cu-B) show an identical peak but with different intensities at the same 2-theta value (21.4) and also the noises in the baseline indicates that the complexes are in amorphous phase or in semi crystalline phase (Fig. 15 (a) and (b)). The structure corresponded to the major band is not listed in the data base (PCPDFWIN *2004*). However, the 2 θ values at 23.899 (with d space 3.7202) and 21.528 (with d space 4.1243) are common to dithiooxamide also. The major peak of the

two complexes is also present in the XRD pattern of dithiooxamide though it is not its major band. However the intensities and the number of bands of the two spectra show some differences. The resultant decrease in the intensity of the major band for Cu-B may be due to the loss of intensity by scattering the radiation between the pores present in the particles. This observation is consistent with the reported data for Fe_3O_4 nanoparticals. The calculated particle sizes using XRD data and the Debye-Scherrer formula (3.1) [57, 58]

$$\mathbf{D = k\lambda/\beta\cos\phi} \qquad (3.1)$$

Where D = Median diameter of the particle, λ = Wavelength of X-ray, β= FWHM of the peak, ϕ = Position of the peak, k= 0.9, are shown in the Table 3.2.

Table 1. Particle sizes inferred from XRD data

Complex	Particle Size (nm)
Cu-A	16.55
Cu-B	13.24

Interestingly, a reduction in size of the new complex by ~3 nm together with the reduction in intensity of the XRD peaks compared to copper (II) dithiooxamido complex may be also indicative of the packing of the molecule to form a macrocyclic configuration.

1.4 Ion Exchange capacity inferred from qualitative tests, AAS and CV data

Table 2. Ion exchanging ability of the Cu-B complex

0.01 M Aqueous solution passed through the column	Precipitating agent	Precipitate formation with effluent	Effluent with Conc. ammonia
Ag (I)	1M NaCl	-	Blue solution
Pb (II)	1M NaCl	White	No color change
Cd (II)	5M NaOH	White	No color change
Ni (II)	DMG	Red	No color change
Zn (II)	5M K_2CO_3	White	No color change

Table 3. Testing for Ag(I) ions using ASS

Concentration of the Ag(I) solution passed through the column(3 ml)	Absorption for Ag(I)	Absorption for Cu(II)
5 ppm	-	-
5 ppm	-	-
5 ppm	-	-
10 ppm	-	-
10 ppm	-	-
10 ppm	-	-
20 ppm	-	0.002
20 ppm	-	0.004
20 ppm	-	0.005
100 ppm	-	0.029
100 ppm	-	0.046
100 ppm	-	0.065
1079 ppm (0.001 M)	-	0.092
1079 ppm (0.001 M)	-	0.122
1079 ppm (0.001 M)	-	0.141
2158 ppm (0.002 M)	-	0.172
2158 ppm (0.002 M)	-	0.233
2158 ppm (0.002 M)	-	0.254
10790 ppm (0.010 M)	-	0.614

Table: 4 Summery of AAS analyzing

Metal ions	Whether the metal ion present in the effluent	Whether the Cu(II) ion released in to the effluent
Ag (I)	No	Yes (when [Ag(I)] >20 ppm)
Pb (II)	Yes	No
Cd (II)	Yes	No
Ni (II)	Yes	No
Zn (II)	Yes	No

Analysis of the data obtained in Tables 2, 3 and 4 implies an interesting affinity of the complex towards Ag(I) ions. According to the data in the Table 2, the effluent collected after passing Ag(I) solution became blue with Conc. ammonia confirming that the effluent contains Cu(II) ions. The effluent tested with NaCl has not shown any precipitate formation indicating the absence of Ag(I) ions in the effluent. This result indicates trapping of Ag(I) into the copper complex when passing aqueous solutions of Ag(I) through a column packed with Cu-B complex while releasing Cu(II) ions. The test results shown in Table 3 implies neither such a trapping of those ions nor release of Cu(II) ions occur with Pb(II), Cd(II), Zn(II) and Ni(II). According to the AAS data shown in Table 4, the copper complex used has trapped Ag(I) up to 20 ppm solutions without releasing Cu(II) ions.

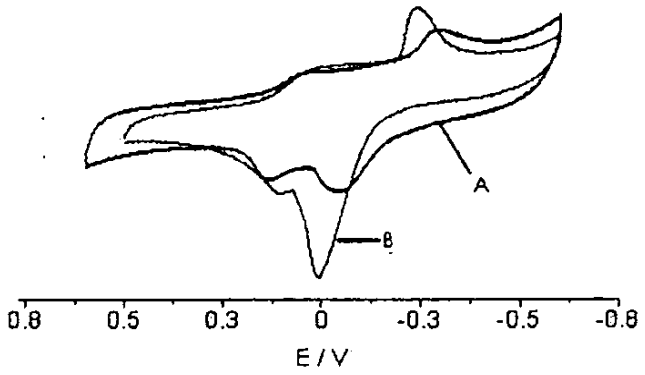

Fig.16 Cyclic Voltammogram for the effluent after passing 0.001M $AgNO_3$ solution through the column of Cu-B (A- effluent after passing Ag (I) , B- Copper acetate solution)

The CV data (Fig.16) for the effluent collected after passing Ag(I) ions through the column also confirm that the effluent contains Cu(II) ions and not Ag(I) ions. When the concentration of the Ag(I) ions exceeds 20 ppm it starts to release Cu(II) ions from the complex while trapping Ag(I) ions in to the complex. The specific affinity of the complex towards the Ag (I) ions may be due to the poor solvation associated with small charge and size factors of Ag (I) ions.

1.5 Ag (I) ion trapping capacity inferred from XRF analysis

Ag (I) ion trapping capacity of the Cu-B complex was confirmed by the XRF analysis. The Cu-B complex in the column after passing Ag (I) ions was collected, washed with water and dried in an oven at 60 ^{0}C. The XRF analysis was done for this dried samples. According to the XRF spectrum after passing Ag (I) ions, it is given that the complex contain 69.06 % of Ag and 30.94 % of Cu. (Fig. 18).According to the XRF data, before passing Ag (I) ions there was 99.92 % copper in the complex with respect to other metals and no any silver (I) ions present (Fig. 17). Therefore the trapping Ag (I) ions while removing Cu (II) from the system can be confirmed from the XRF analysis.

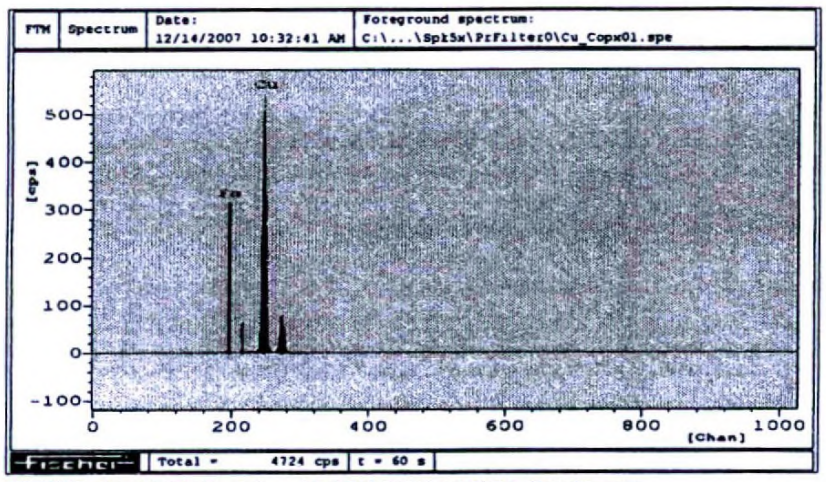

Fig. 17 XRF spectrum before passing Ag (I) through Cu-B

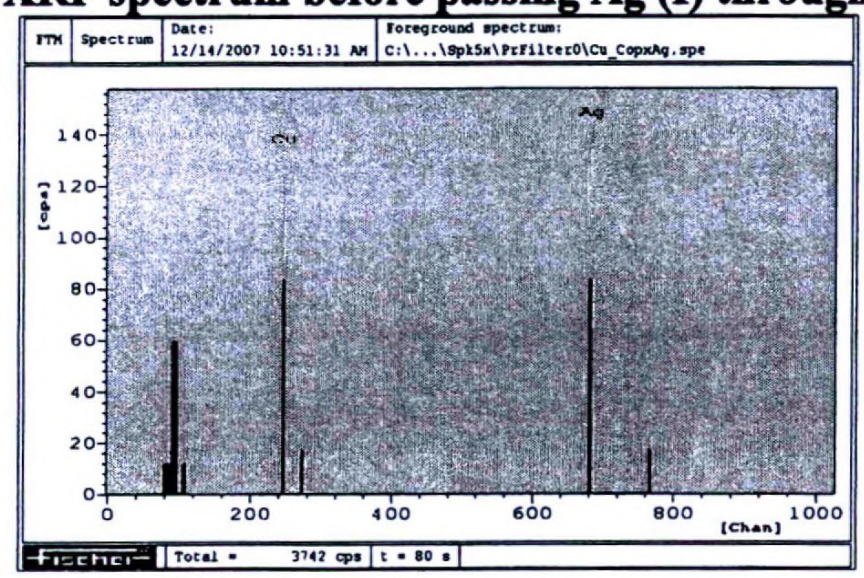

Fig.18 XRF spectrum after passing Ag (I) through Cu-B

2. N,N- ethylenebis(acetylacetoneiminato)Ni(II) complex.

2.1 Physical Properties

The Ni-en-acac complex was isolated as a shiny, brownish red colour, crystalline solid after concentrating the mixture of Ni (II), en and acac in a rotory evaporator. The complex is highly soluble in organic solvents and mineral acids and forms a yellow colour solution. However the solubility in water is poor.

2.2. Characterization –IR Spectra

In the IR spectrum (Fig. 19) the bands at 615 $cm^{-1}$and 767 cm^{-1} can be assigned to M-N vibrations and the bands at 460 $cm^{-1}$and 486 cm^{-1} can be assigned to M-O vibrations.

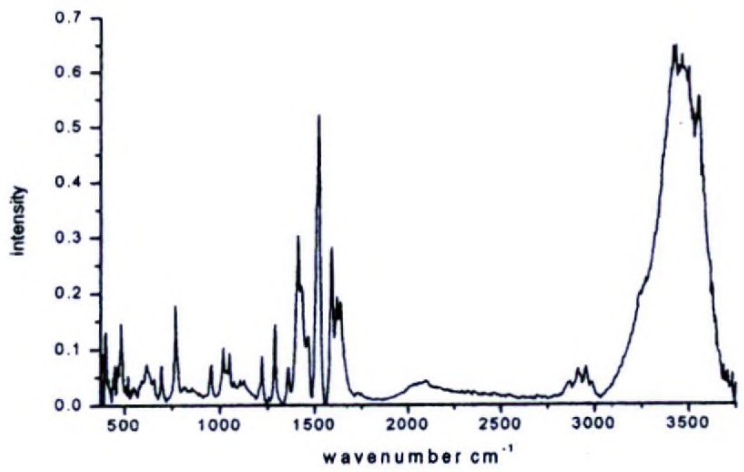

Fig. 19. IR Spectrum of N,N- ethylenebis(acetylacetoneiminato)Ni(II) complex

Therefore Ni^{2+} - N and Ni^{2+} - O bond formations are confirmed from the IR data. The band at 1637 cm^{-1} can be attributed to C=N vibrations. These observations support the coordination of en and acac to Nickel (II) center as predicted. [25,26]

The analysis of single crystal X-Ray crystallographic data revealed the structure of the N,N- ethylenebis(acetylacetoneiminato)Ni(II) complex is same as the structure (fig. 20) obtained by the similar work of S.K.Gupta, etal in 2002.[14]

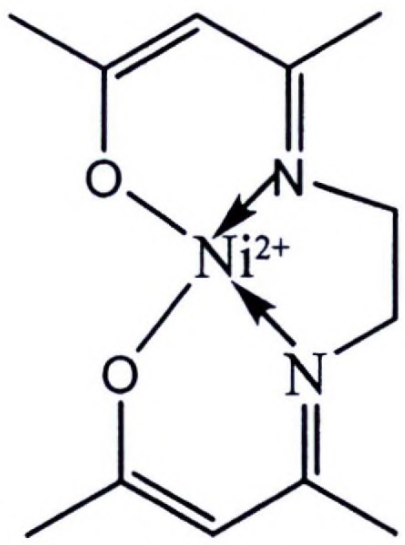

Fig. 20. The X-Ray crystal structure of the Ni-en-acac complex

2.3 The acid-base properties of the Ni-en-acac complex

When the complex is dissolved in aqueous methanol the solution turns to yellow and the pH of the solution is 7.6. When adding HCl (0.1 M) into the yellow solution, the colour turned gradually to colourless at about pH~1.8. When adding NaOH (0.1 M) into the same solution, the colour turned back to dark yellow. The UV- visible spectra with the addition of H^+ and OH^- to the methanolic solution of the complex, were also supportive for the above observation. (Fig. 21) The intensity of the peak at 565 nm due to the d-d transition of the Ni(II) complex decreased with the addition of HCl (0.1 M). The colour of the solution also decreased and finally became colourless.

(a) UV-Visible spectra with the addition of 0.1M HCl (a) micro drop wise into a methanolic solution of the N,N- ethylenebis(acetylacetoneiminato)Ni(II) complex
(b) **UV-Visible spectra with the addition of 0.1 M NaOH micro drop wise into the same (acidified) solution of N,N- ethylenebis(acetylacetoneiminato)Ni(II) complex**

Fig. 21

2.4. CO_2 binding capacity

At room temperature, the complex shows ~ 35% more CO_2 absorption than nickel acetate, and the absorption capacity is unusually insensitive to the amount of complex present.

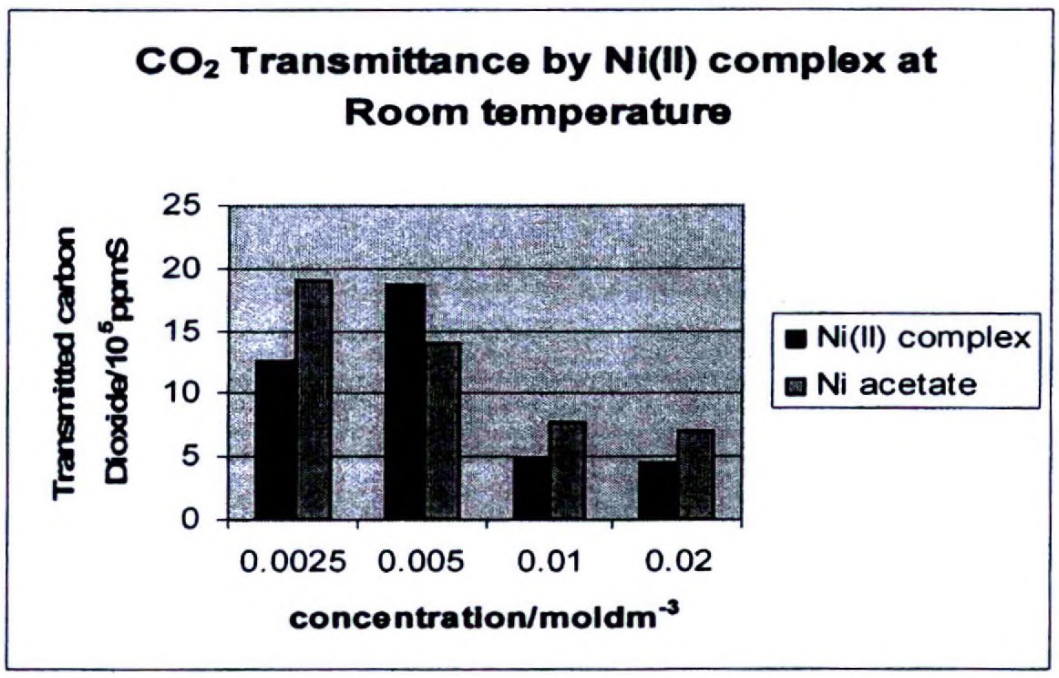

Fig 22: CO_2 transmittance by the various concentrations of N,N-ethylenebis(acetylacetoneiminato)Ni(II) complex at RT for 300 s.

At room temperature, the complex shows ~ 35% more CO_2 absorption than the starting material, nickel acetate. When the temperature goes down to 4-5 °C the CO_2 absorption depends on the amount of complex present in the medium showing about 50% more CO_2 absorption than nickel acetate of same concentration.

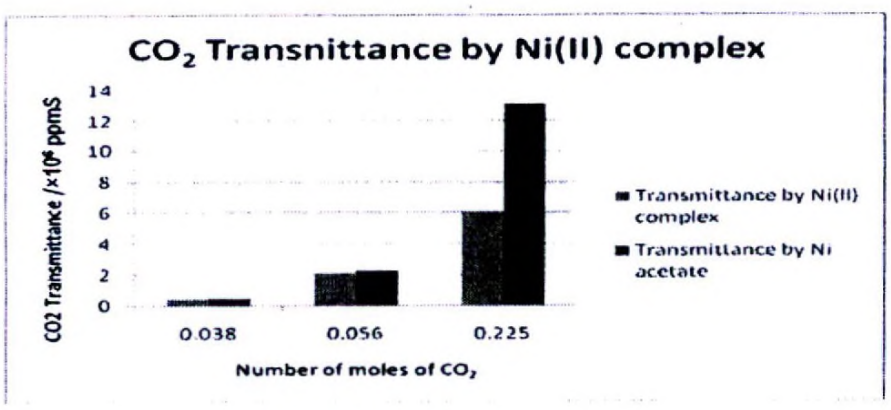

Fig 23: The amount of CO_2 Transmitted by 0.005 mol dm^{-3} of Ni(II) complex and Ni(II) acetate with increasing amounts of CO_2 gas at room temperature for 300 s.

At relatively higher CO_2 concentrations the Ni(II) complex shows more than 50% CO_2 absorbance than the starting material Ni(II) acetate.

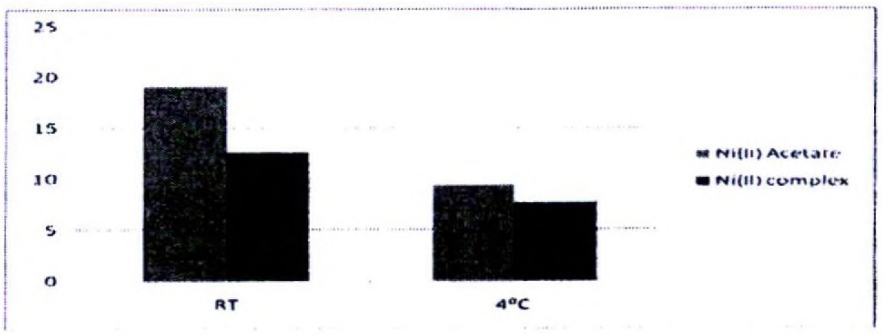

Fig 24: CO_2 transmittance for 0.0025 M concentrations of Ni(II) complex at RT and 4 °C

When the temperature goes down to 4-5 °C the CO_2 absorption depends on the amount of complex present in the medium showing about 50% more CO_2 absorption than nickel acetate of same concentration.

The presence of asymmetric stretching bands around 2900 cm^{-1} in The FTIR spectra of solid samples of the complex after passing CO_2 supports for trapping of CO_2 by the Ni(II) complex (Fig 25a, Fig 25.b,Fig 25.c,Fig.25.d)).

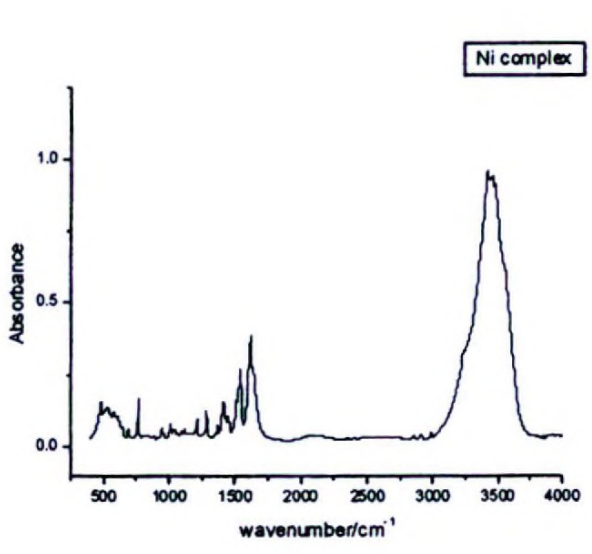

Fig.25.a: FTIR spectrum of Ni (II)complex

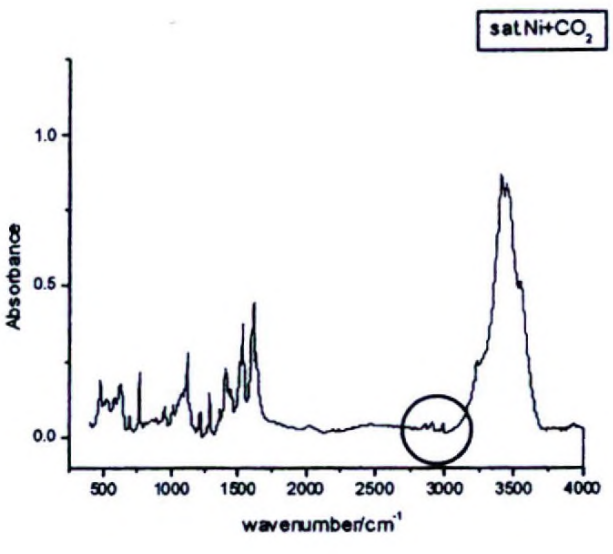

Fig.25.b: FTIR spectrum of saturated Ni (II) complex after passing CO_2 gas

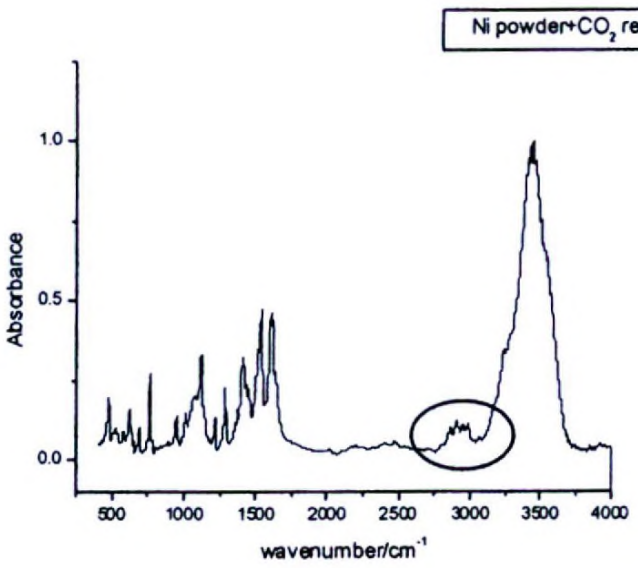

Fig.25. c: FTIR spectrum of Ni (II) complex (Recrystalized solid) after passing CO_2 gas

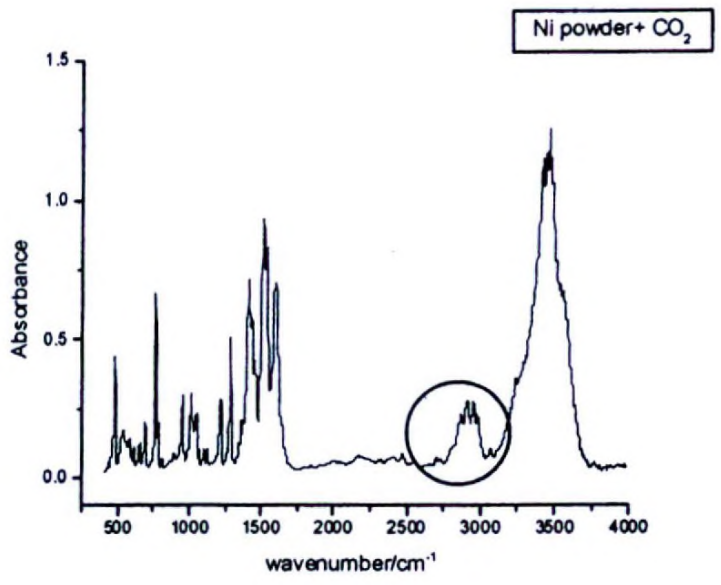

Fig.25.d FTIR spectrum of Ni(II) complex (original solid) after passing CO_2 gas

Comparison of CO_2 trapping capacity

Extracted natural chlorophyll a shows ~20% more CO_2 absorbance than Ni(II) incoorparated chlorophyll a system. However, Reduced Ni Chlorophyll a system shows ~70 % more CO_2 absorption than unreduced Ni(II) chlorophyll a system. It is about ~60% more CO_2 absorption compared with natural chlorophyll a. (Fig.26)

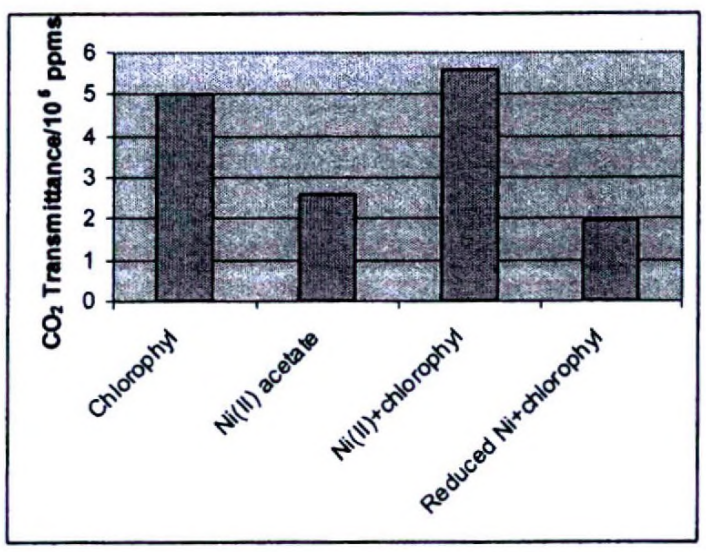

Fig.26: CO_2 Transmittance by natural and modified chlorophyll asystems.

3. N,N- ethylenebis(acetylacetoneiminato)Cu(II) complex

3.1 Physical Properties

The complex synthesized is a pinkish purple shiny crystalline solid which is soluble in organic solvents and mineral acids and gives a purple colour solution. However, it is insoluble in water.

3.1 Characterization of N,N- ethylenebis(acetylacetoneiminato)Cu(II) complex

The single crystal x-ray crystallographic structure of the complex is shown in Fig.27

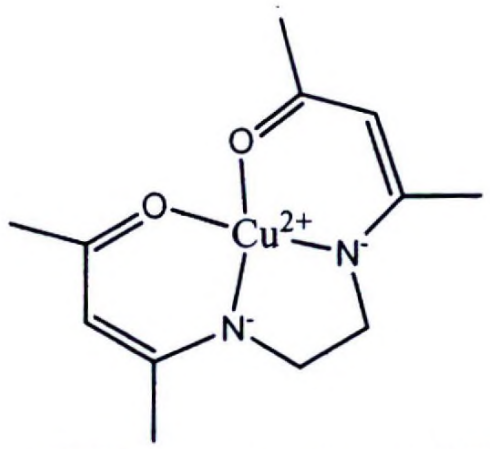

Fig.27 The single crystal X-ray structure of N,N- ethylenebis(acetylacetoneiminato) Cu(II) complex

3.2 Acid-base properties of N,N- ethylenebis(acetylacetoneiminato)Cu(II) complex

The band at 540 nm in the UV-visible spectrum of the complex (Fig.28 and 29) may be due to the d-d transition of the copper complex. This band disappears and a new band appears around 820 nm giving an isobestic point at 680 nm with the addition of H^+ ions into an ethanolic solution of the compound. With the addition of H^+ proceeds, the colour of the solution gradually turns to colourless. Interestingly, the band around 540 nm reappears and the solution colour turns to purple again with the addition of OH^- ions into the same solution. According to the above observation, the possibility of using this complex as an indicator for non aqueous titrations can be further studied.

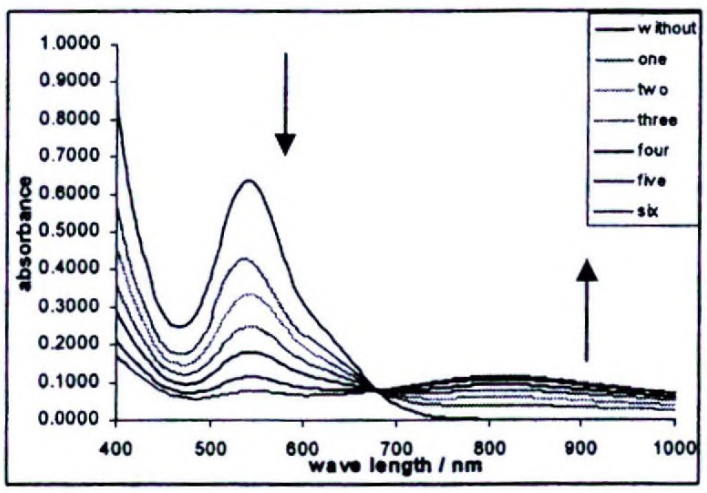

Fig. 28. UV-Visible spectra with the addition of 0.1 M HCl micro drop wise into an ethanolic solution of N,N- ethylenebis(acetylacetoneiminato)Cu(II) complex

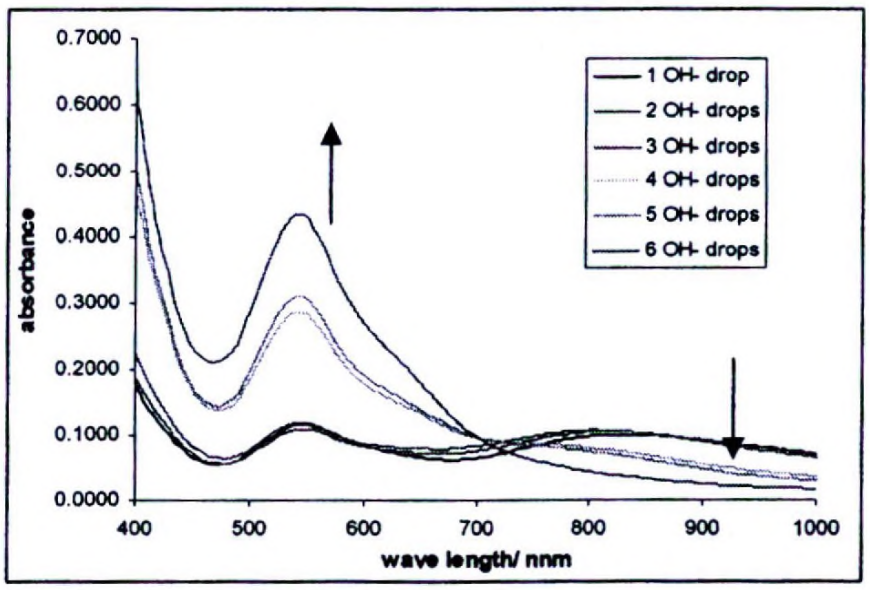

Fig. 29. UV-Visible spectra with the addition of 0.1 M NaOH micro drop wise into the same N,N- ethylenebis(acetylacetoneiminato)Cu(II) complex solution mixture

Table 5. Colour of the N,N- ethylenebis(acetylacetoneiminato)Cu(II) complex in different pH values

pH value	Colour
9.0	purple
8.5	Purple
7.0	Light Purple
6.0	Light purple
4.0	Light purple
2.0	Colourless
1.0	Colourless

The CV of the compound shows an anodic peak at 0.87 V for the complex in acetonitrile when TEAH is used as the electrolyte. With the addition of H^+ ions into this solution, a new peak appears at -0.30 V (anodic peak) and at -0.59 V (cathodic peak). However, this peak disappears with the addition of OH^- ions giving a CV similar to the CV of the original compound (Fig.30, 31). These results are also consistent with the reversibility of the acid-base chemistry of the copper complex.

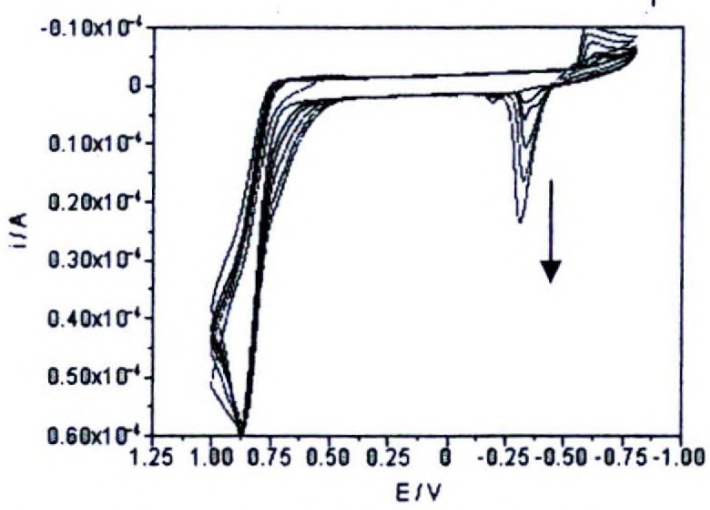

Fig. 30. CV with the addition of 1.0 M HCl to an ethanolic solution of N,N-ethylenebis(acetylacetoneiminato)Cu(II) complex

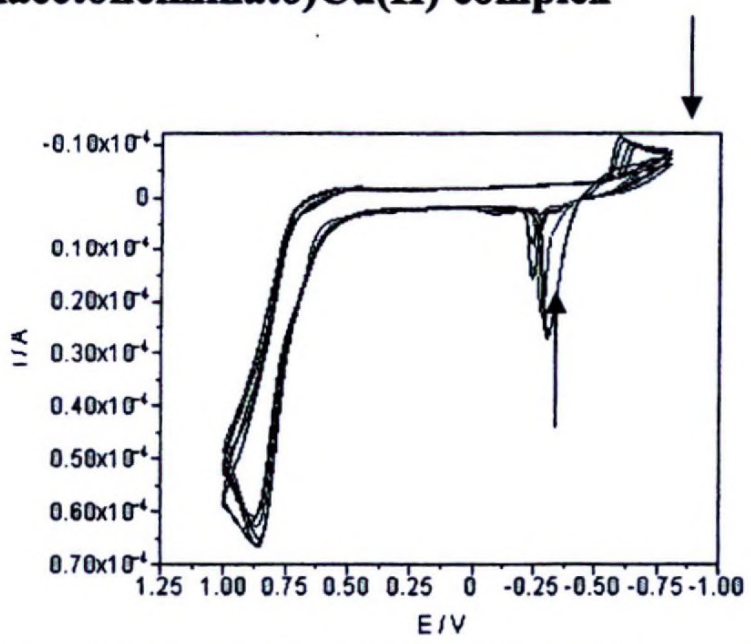

Fig. 31 CV with the addition of 1.0 M NaOH to the same ethanolic solution of N,N-ethylenebis(acetylacetoneiminato)Cu(II) complex

3.3.2.. Proposed mechanism for acid-base reaction

With the addition of H^+ ions

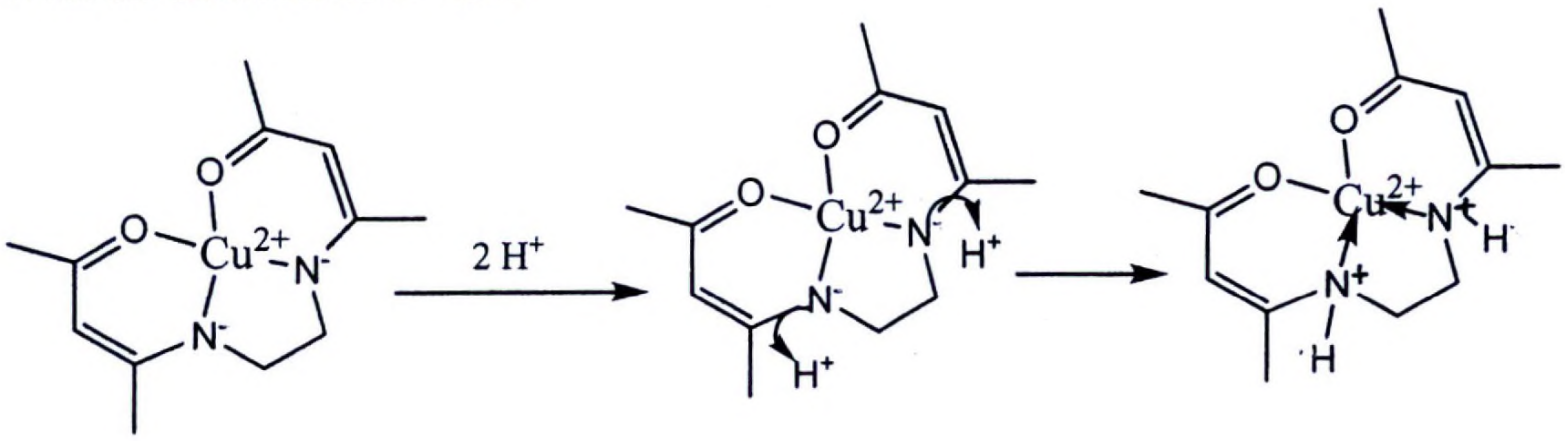

With the addition of OH^- ions

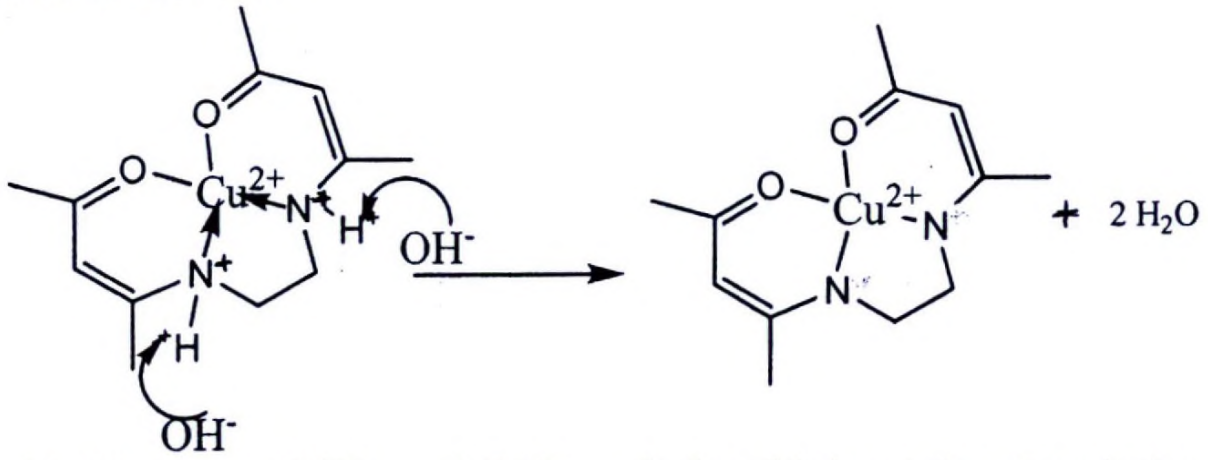

3.3.3 Anion binding capability of N,N- ethylenebis(acetylacetoneiminato)Cu(II) complex

Stepwise addition of SCN^- and Br^- to the solution separately at pH < 2 shows an appearance of a new band at 795 nm and 790 nm respectively with the disappearance of the band at 540 nm (Fig. 32 and 33). This red shift of the d-d band together with the intensity decrease may be due to the protonation of the ligand environment bonded to the Cu^{2+} center by decreasing the crystal field stabilization energy (CFSE) of the complex and increasing the symmetry of the system. Addition of Cl^-, Br^-, SCN^- and I^- to the complex at pH< 2 turns the colour of the solutions to yellow with the intensity order Cl^- <Br^-<SCN^-<I^-. The UV-Visible spectral changes with successive addition of SCN^- and Br^- are shown in Fig.32 and Fig.33 respectively.

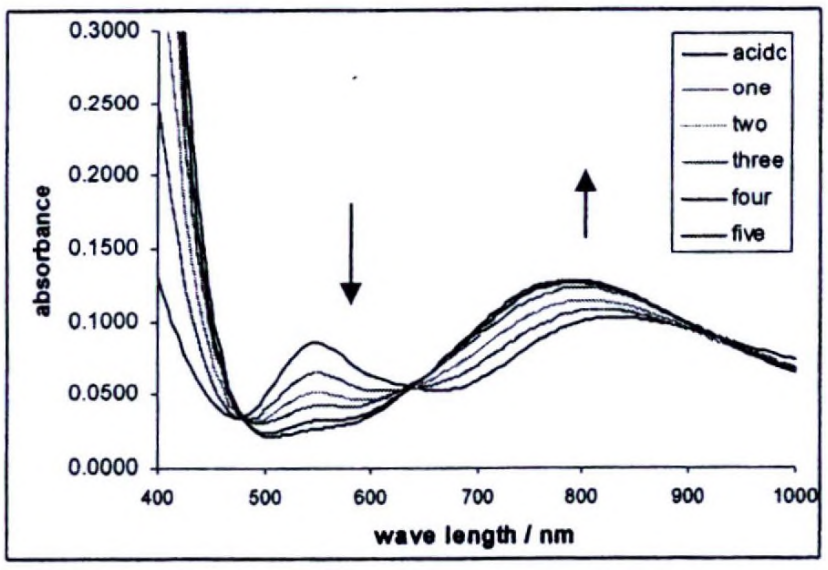

Fig. 32 UV-visible spectra with the stepwise addition of 1.0 M SCN^- to acidic ethanolic solution of N,N- ethylenebis(acetylacetoneiminato)Cu(II) complex

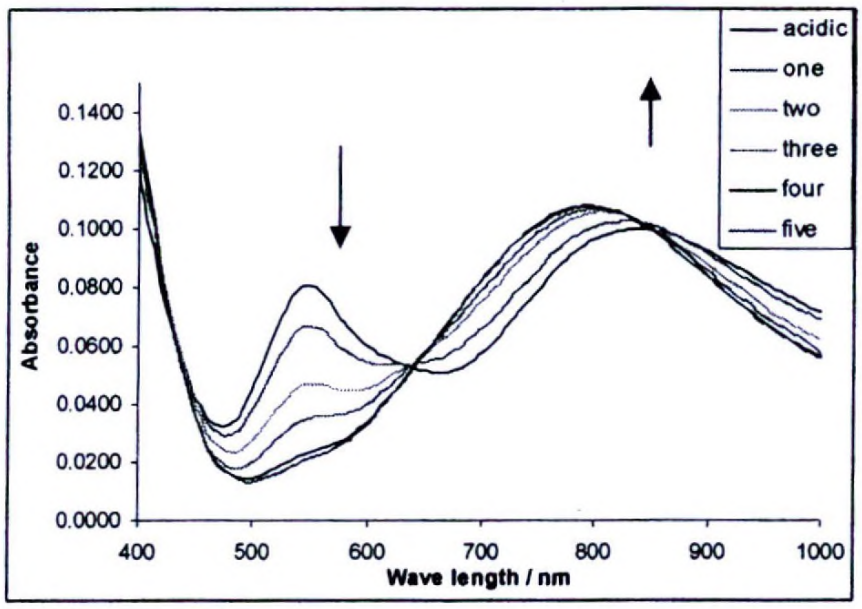

Fig. 33 UV-visible spectra with the stepwise addition of 1.0 M Br^- to acidic ethanolic solution of N,N- ethylenebis(acetylacetoneiminato)Cu(II) complex

3.3.4 Proposed reaction mechanism for anion binding

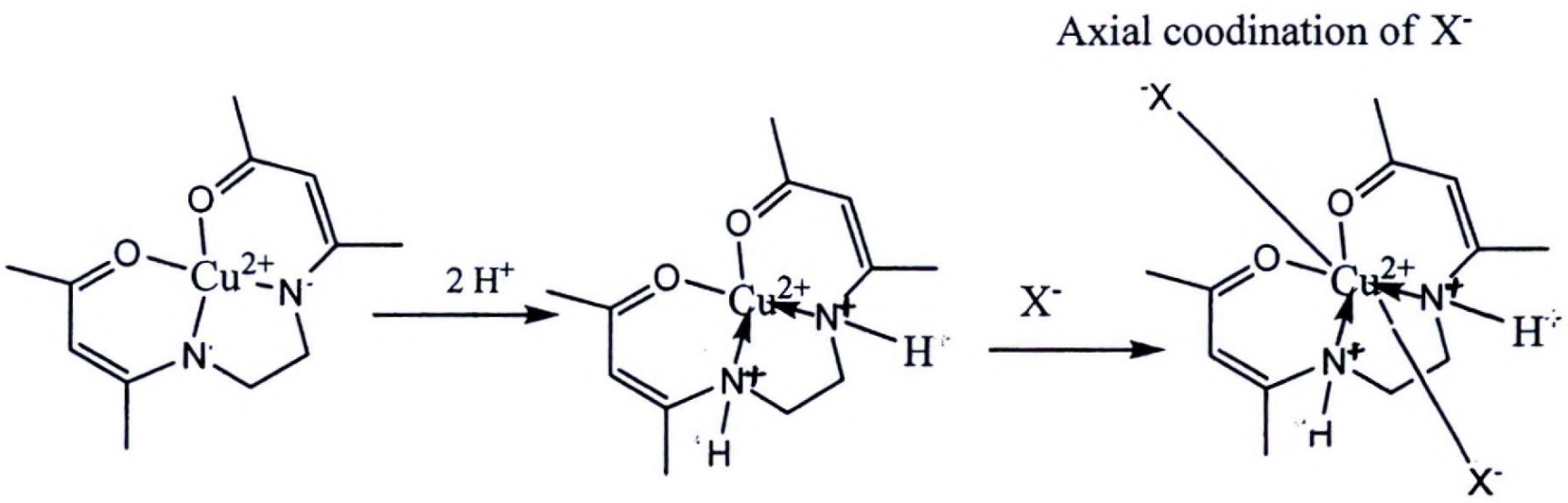

Where X^- =Cl^-, Br^-, I^-, SCN^-

3.4 Carbon dioxide trapping capability of N,N- ethylenebis(acetylacetoneiminato) Cu(II) complex

The decrease in the CO_2 concentration of the N,N- ethylenebis(acetylacetoneiminato) Cu(II) complex is about two times higher than the simple salt of Copper ($Cu(CH_3COO)_2$). (Fig.34). This observation indicates comparatively higher absorption of CO_2 by Cu-complex. This association may be due to the significant axial coordination or trapping of CO_2 into the Cu-en-acac complex. This affinity is higher at low temperatures indicating the higher affinity of binding CO_2 at lower temperatures. (Fig.35). The intensity gain in the bands at 2095 cm^{-1} and 2900 $cm^{-1}$of the IR spectrum (Fig.36) after passing CO_2 may be due to stretching of coordinated/bound CO_2 to the Cu(II) complex.

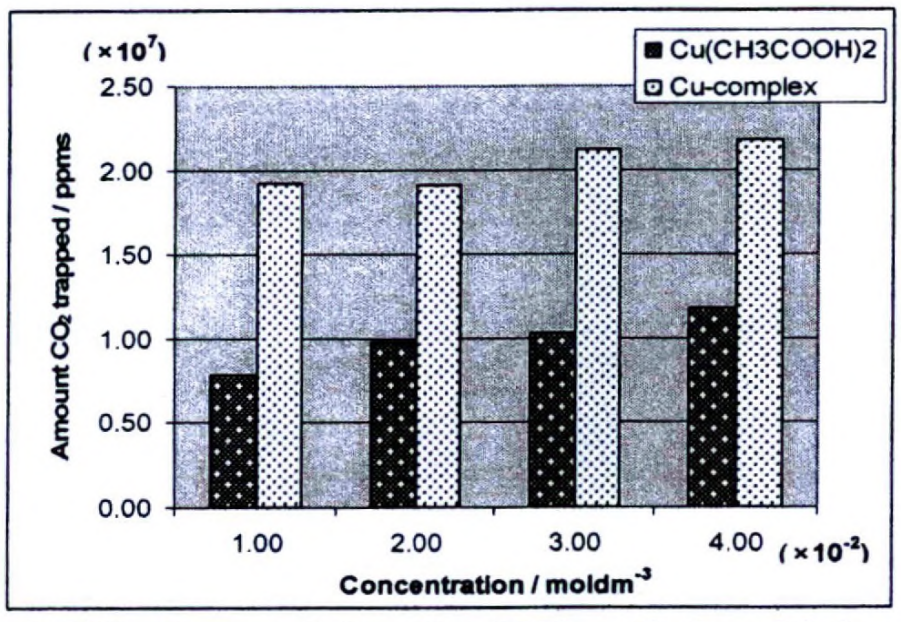

Fig. 34. Amount of CO_2 trapped by the N,N- ethylenebis(acetylacetoneiminato) Cu(II) complex complex and $Cu(CH_3COO)_2$ at RT

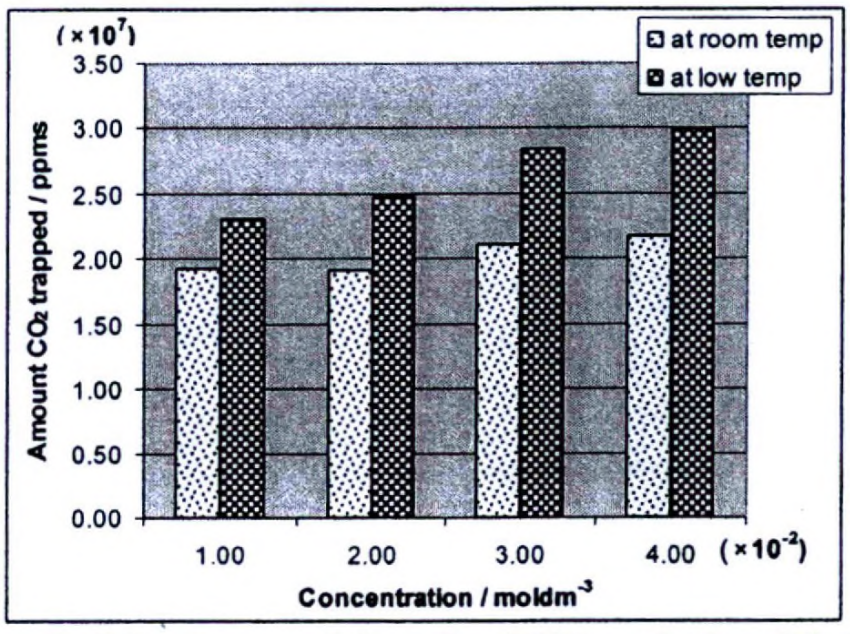

Fig. 35. Amount of CO_2 trapped by the N,N- ethylenebis(acetylacetoneiminato) Cu(II) complex at different temp.

Table 6. The CO_2 amount trapped by the N,N- ethylenebis(acetylacetoneiminato) Cu(II) complex and $Cu(CH_3COO)_2$

(Total amount of CO_2 Passed = 5.518×10^7 ppms)

Concentration / moldm^{-3} (in methanol)	**Amount CO_2 trapped at RT, Into $Cu(CH_3COO)_2$ in ppms ($\times 10^7$)**	**Amount CO_2 trapped at RT. Into Cu-complex in ppms ($\times 10^7$)**	**Amount CO_2 trapped at low temp. (< 4 ^{0}C) into Cu-en-acac in ppms ($\times 10^7$)**
0.01	0.791	1.924	2.313
0.02	0.978	1.917	2.472
0.03	1.034	2.121	2.850
0.04	1.177	2.181	2.991

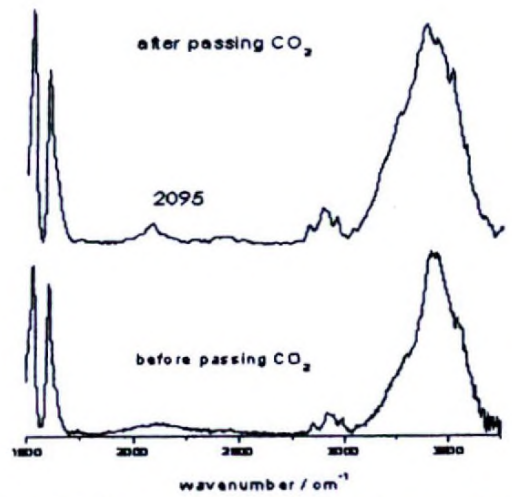

Fig. 36. IR spectra of the N,N- ethylenebis(acetylacetoneiminato)Cu(II) complex before and after passing CO_2 through a solid sample of the complex

The CO_2 absorption by the Cu (II) complex is ~60% greater than that of Cu (II) acetate of 0.1 mol/dm^{-3}.

3.4.1 Proposed mechanism for CO_2 binding

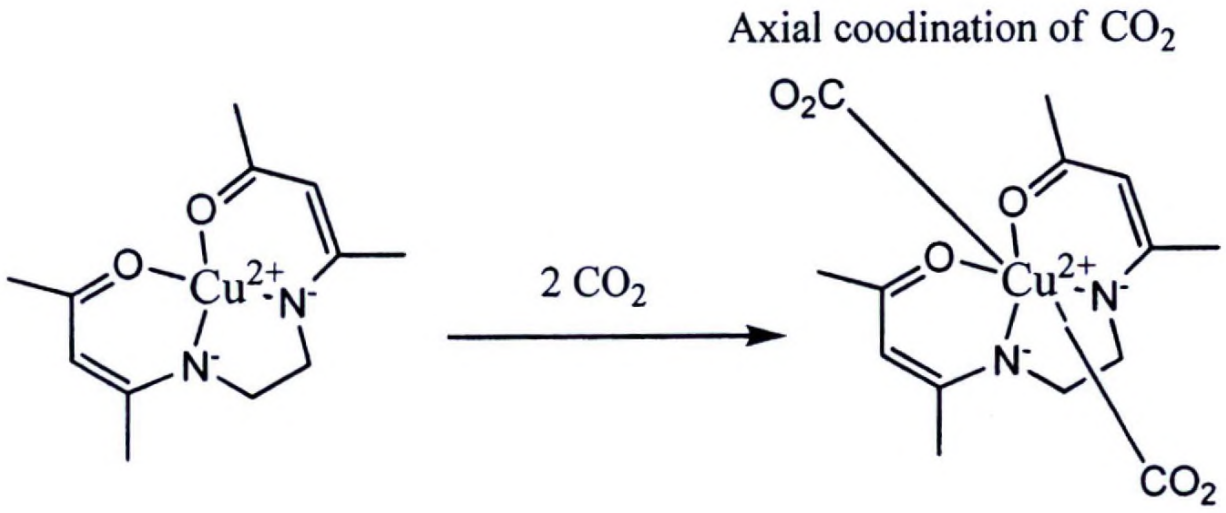

The N,N- ethylenebis(acetylacetoneiminato) Cu(II) complex (0.04 moldm^{-3} in methanol) shows the capability of trapping ~34% of CO_2 passed at room temperature. The trapping capacity increases upto~54% at 3^0C.
Therefore the N,N- ethylenebis(acetylacetoneiminato) Cu(II) complex may be used for the utilization of CO_2.

4. N,N- ethylenebis(acetylacetoneiminato)Fe(III) complex

The reddish crystalline complex (Fe-en-acac-R) formed is insoluble in water and soluble in mineral acids and in common organic solvents while the yellow complex (Fe-en-acac-Y) is soluble in water and insoluble in organic solvents.

4.1 Characterization of Fe-en-acac-R and Fe-en-acac-Y

The IR spectra of the Fe-en-acac-R and Fe-en-acac-Y complexes are shown in Fig.37 and 38 respectively.

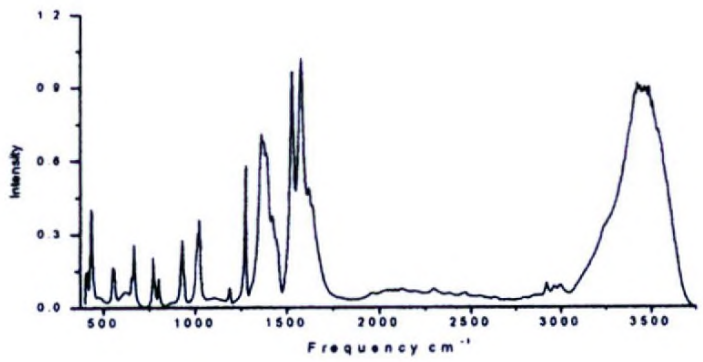

Fig. 37. IR spectrum of Fe-en-acac-R

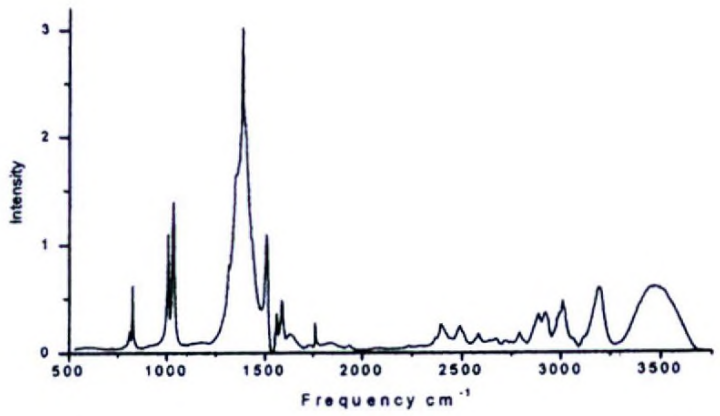

Fig. 38 IR spectrum of Fe-en-acac-Y

According to the IR spectrum of Fe-en-acac-R, the bands at 3420 cm^{-1}, 1574 cm^{-1}, 920 cm^{-1} and 772 cm^{-1} are attributable to O-H / N-H, C=O / C=N and C-H vibrations respectively. The bands at 667 $cm^{-1}$and 772 cm^{-1} can be assigned to Fe-N vibrations and the bands at 433 $cm^{-1}$and 549 cm^{-1} can be assigned to Fe-O vibrations. Therefore Fe-N and Fe-O bond formations are confirmed from the IR data (Fig.37). According to the IR spectrum of Fe-en-acac-Y, (Fig. 38) there is no band in the finger print region. That is no bands in between 400 cm^{-1} to 800 cm^{-1} region. This means there is no bond between the metal center and the ligands. However there are some bands which are similar to the bands in the spectrum of Fe-en-acac-R complex too. The bands at 3460 cm^{-1}, 1564 cm^{-1} are attributable to O-H / N-H, C=O / C=N vibrations respectively.

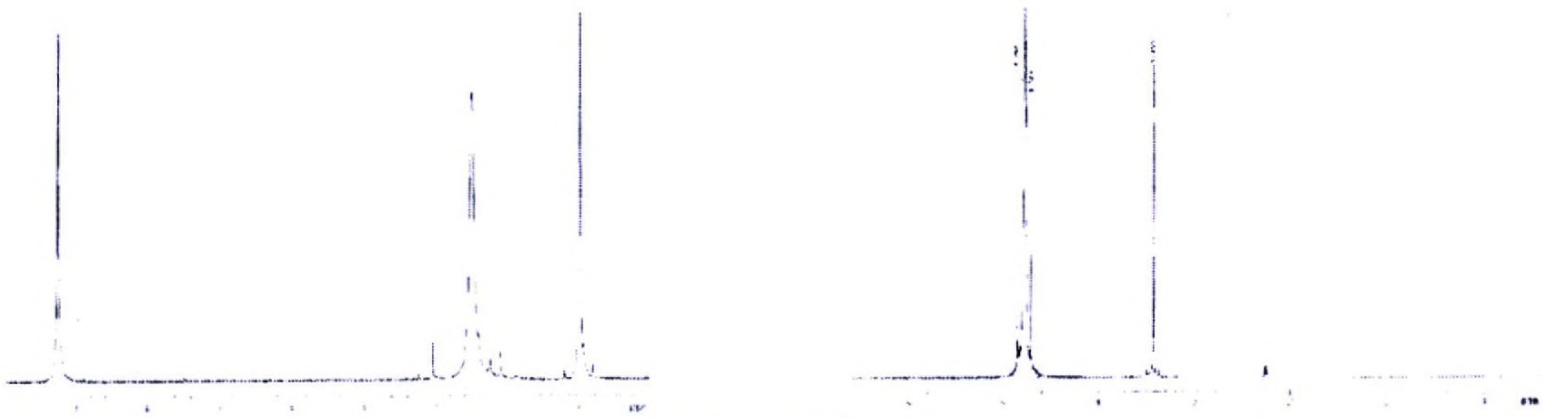

(a)^{1}H NMR spectrum of Fe-en-acac-Y ; (b) **^{1}H NMR spectrum of Fe-en-acac-Y**
Fig. 39

There is no unusual line broadening in the ^{1}H NMR spectrum of the Fe-en-acac-Y complex (Fig.39(b)) unlike in the Fe-en-acac-R complex. This is confirming that there is no metal ion in the yellow complex.

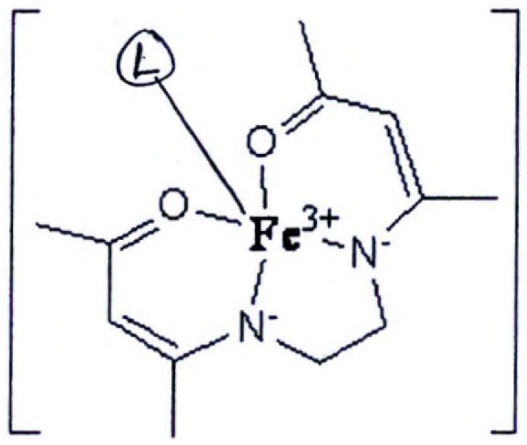

Fig. 40 Predicted structure of Fe-en-acac-R complex

4.2 Acid-base properties of Fe-en-acac-R

UV spectrum of Fe-en-acac-R in aqueous methanol shows two bands at 350 nm and 428 nm. The band at 350 nm disappears and the band at 428 nm shifts towards higher λ (red shift) with the addition of H^+, changing the colour of the solution from yellow to reddish orange (Fig.41). However the reverse can be seen with the reappearance of the band at 350 nm and a blue shift of the band at 428 nm while turning the colour back to yellow with the addition of OH^- into the same solution (Fig.42).

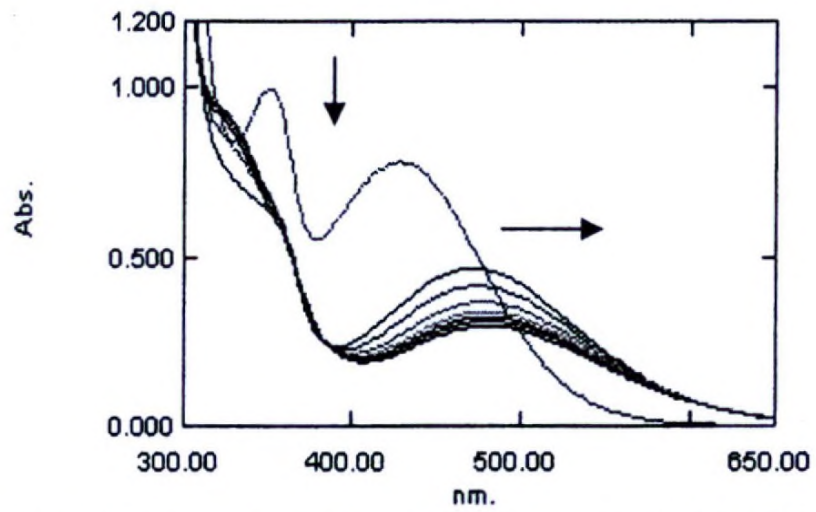

Fig. 41 UV-visible spectra with the stepwise addition of 0.1 M HCl into ethanolic Fe-en-acac-R

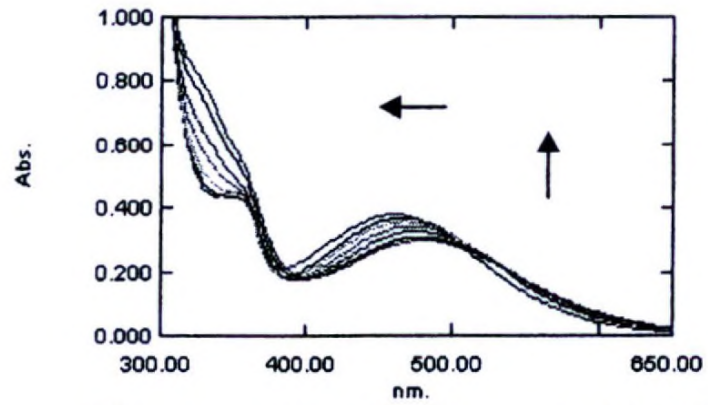

Fig. 42. UV-visible spectra with stepwise addition of 0.1 M NaOH into same solution of Fe-en-acac-R

4.3 Anion binding capability of Fe-en-acac-R complex

With the stepwise addition of SCN^- into an aqueous methanolic solution of the complex at pH~2 the band at 350 nm disappears while gaining the intensity and the blue shift of

the band at 460 nm with an isobestic point at 364 nm (Fig.43). A similar behavior observed with Cl^- and Br^- addition. However I^- addition indicated a decrease in the intensity of the band at 460 nm together with an intensity gain of the band at 350 nm.

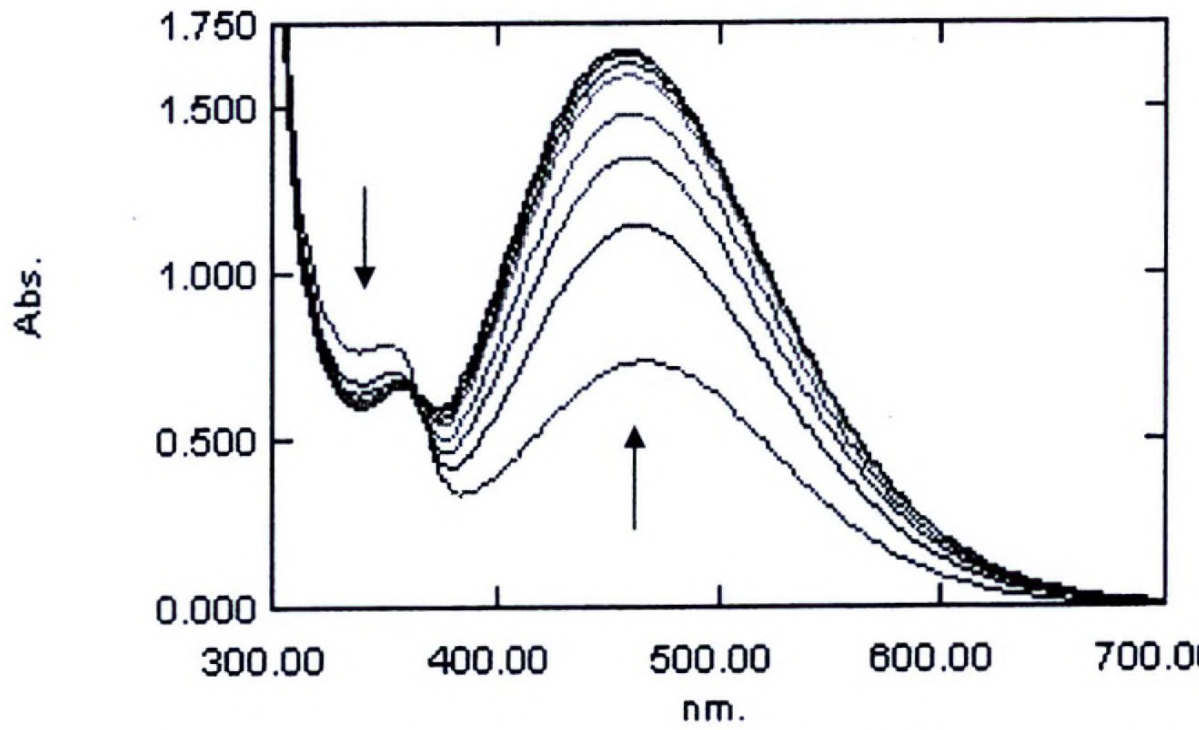

Fig. 43. UV-visible spectra with the stepwise addition of 1.0 moldm^{-3} SCN^- into acidified ethanolic solution of Fe-en-acac-R

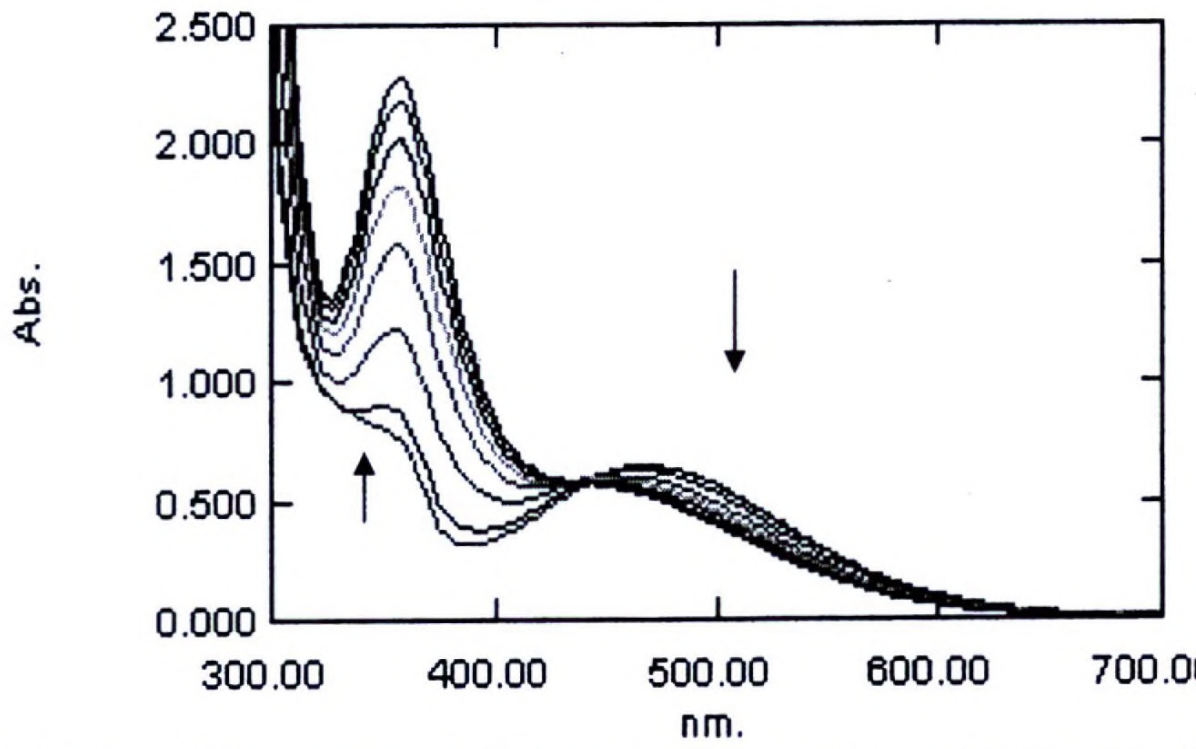

Fig. 44. UV-visible spectra with the stepwise addition of 1.0 moldm^{-3} I^- into acidified ethanolic solution of Fe-en-acac-R

The UV visible band at 350 nm may be due to MLCT and the bands ~420-460 nm may be due to the d-d transition of the complex under different ligand fields created by anion added. The intensity gain and the blue shift of the band at ~420-460 nm observed with anion (X) addition where X= OH^-, SCN^-, Cl^-, Br^- are indicative of anion binding into the Fe^{3+} center of the complex (Fig.43). This observation qualitatively implies a higher affinity of the complex for complexation with OH^-, SCN^-, Br^- and Cl^- ions. The reversible spectral and colour changes of the complex in the presence of H^+ and OH^- may be related with the acid base properties of the complex. However, the intensity gain at the 350 nm

together with the disappearance of the band at 428 nm (Fig.44) with the addition of I^- proceeds is indicative of the reduction of Fe^{3+} into Fe^{2+} by I^- and binding of I_2/I_3^- to Fe^{2+} center. The complexation of the complex can be given as in the equation as follows.

$$X^- + [LFe]^{3+} \rightleftharpoons [LFeX]^{2+} \quad \text{when } X=I^-,\ I_2 \text{ may be formed}$$

$$[LFeI]^{3+} + I^- \rightleftharpoons I_2 + [LFe]^{2+} \quad \text{or}$$

$$[LFe]^{3+} + 2I^- \rightleftharpoons I_2 + [LFe]^{2+}$$

$$[LFe]^{2+} + I_2 + \text{ex } I^- \rightleftharpoons [\mathbf{LFeI_3}]^+ \quad \text{where } X^- = Cl^-, Br^-, I^-, SCN^-$$

Though the intensity of CT band at 350 nm is dependent on the nature of X, its energy is independent on the nature of X. It seems likely that this band is a MMCT band (Fe^{3+}/Fe^{2+}) originally from the coupling of two Fe^{3+} and Fe^{2+} centers through halide or SCN^- bridge.[27,28]

5. Fe(II)-porphyrin Complex similar to Hemoglobin

The exchange of central Mg (II) ion in isolated chlorophyll-a, for other metal ions governs by soft and hard of acid base properties depending on the ionic radius and the charge of metal ions. Coordination of the metal center to the ligand was confirmed with the shift in absorption maxima to shorter values (blue shift) which is consistent with metallochlorophylls and with the corresponding color changes.

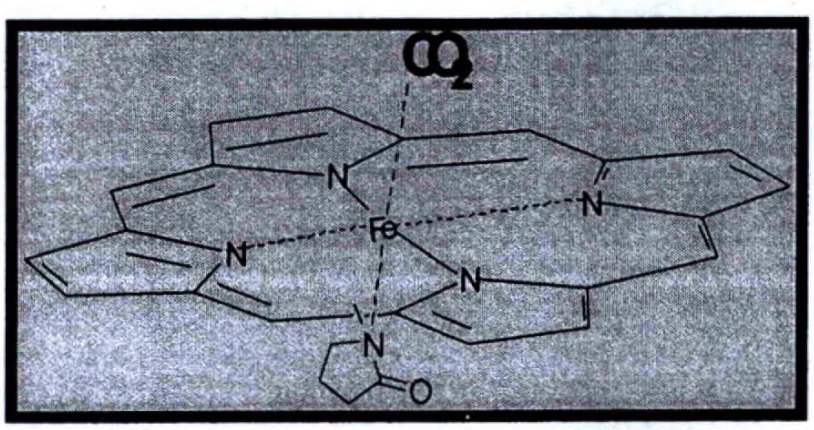

Fig.45

After the coordination of the metal center, Fe (III) center was reduced to Fe (II) using Zn/Hg. Reduction was visible by the color change from brownish green to dark green. Introduction of bulky N-methyl-2-pyridinone base was expected to provide necessary steric hindrance to restrict the formation of a dimer required for the aerial oxidation of Fe (II) (fig. 45).

The Fe (III) complex, first comes as a brownish green liquid that turns to dark green on reduction with Zn/Hg to Fe(II) complex. The Fe (II) complex is stable up to 48 hrs in air and for months under anaerobic conditions. The Fe (II) Chlorophyll solid product was first characterized using FT-IR. The observed peaks can be assigned to following vibrations/stretching modes.

Table 7. IR data for Fe(II)-porphyrin Complex

Observed band, cm^{-1}	vibrations
619	Fe-chlorin (Macrocyclic ligand, MCL)
1110	=C-C, C-O and C-N of the MCL
1633	C=C and C=O of MCL
3506	O-H

The presence of Fe center was confirmed by the appearance of a relatively higher Fe peak (275 cps) in XRF spectrum.

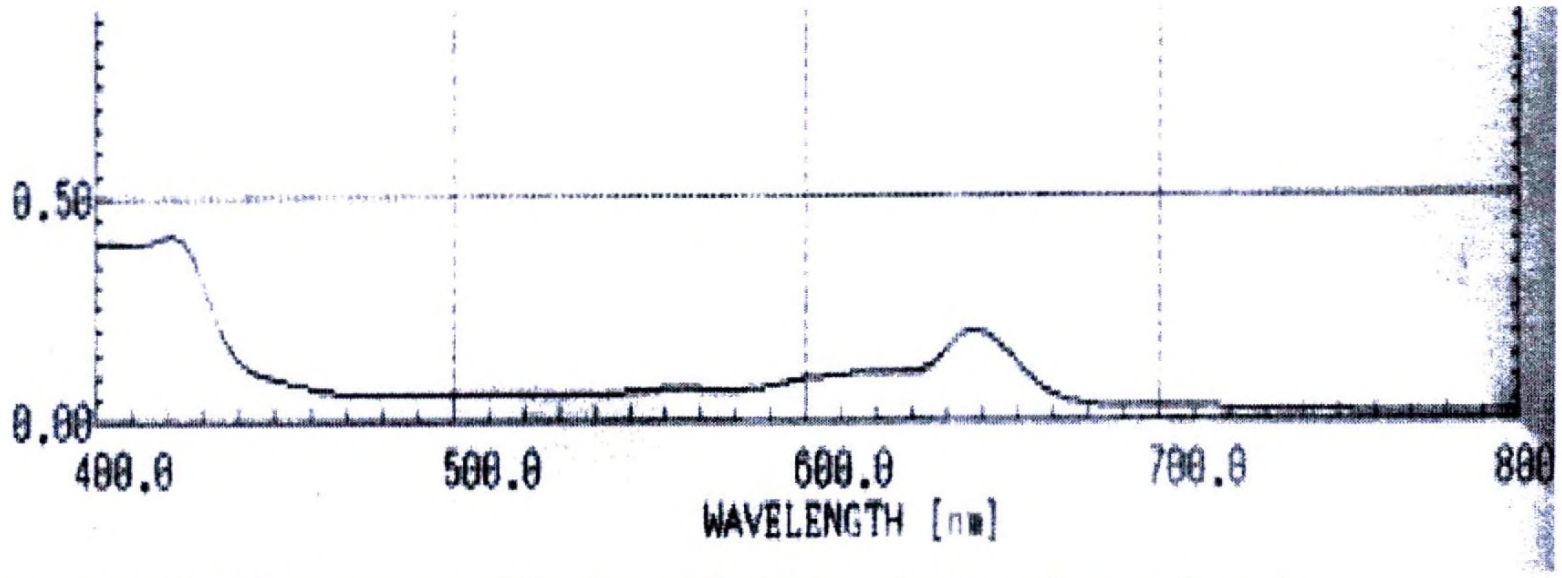

Fig. 46 UV-VIS spectrum of the liquid Fe(ii) Porphyrin using methanol

The UV-Visible spectrum of the Fe(II) porphyrin complex in methanol/acetone mixture (1:1 *v/v*) shows similarities to that of Fe(III) complex except the presence of several new bands between 500-600 nm. The presence of a strong band at ~360 nm in the UV-visible spectrum of the Fe(III) porphyrin complex and simple salts of Fe(III) and not in the spectrum of Fe(II) complex may be due to the LMCT from any ligand, L to Fe(III). Such a band is absent in Fe(II) analogue because it has filled dπ orbitals (for d^6).In Fe(II) complex, there is a significant metal dπ to porphyrin π*orbital interaction (metal to ligand π-back bonding). This results in an increased porphyrin to energy separation causing the electronic absorption to undergo hypsochromic (blue) shifts as depicted by the Fe(II) porphyrin complex. Though the appearance of the two bands (Soret & Q bands) are similar to both Fe(III) porphyrin and chlorophyll, the blue shift in both bands supports to metallation of porphyrin ring by Fe(II) center. The d-d band of Fe(II) complex may be concealed under the blue(Soret) band due to MLCT band at ~429 nm. Parallel to this observation, there is a significant difference in the electrode potentials of Fe(III) and Fe(II) complexes. The electrode potential of Fe(II) complex shifts to a higher value than the relevant Fe(III) analogue indicating the higher stability (Lower or –ve ΔG) for the Fe(II) complex. This observation is consistent with the reported observation on CO binding to Fe(II) porphyrin system

Table 8. Absorption maxima of Chlorophyll and Iron-substituted chlorophyll in acetone.

	Chlorophyll-a (Mg^{2+} center)	**Fe(II) Chlorophyll**
Blue / Soret band	429.0 nm	421.0 nm
Red / Q band	661.0 nm	650.0 nm

The CO_2 absorption by the Fe(III) complex is ~50% greater than that of Fe(III) nitrate at all concentrations.

Table 9. Comparison of CO_2 binding capacity of Fe(III)/(II) complexes studied under method b of 5.

Studied system	**Transmitted CO_2 / 10^5 (ppm* Second)**
Fe(II)Chlorophyll with N-base	5.03
Fe(III)Chlorophyll	19.32
Fe(II)Chlorophyll	11.29
$FeCl_3$	19.27
Chlorophyll-a	11.6

The amount of CO_2 transmitted from the Fe(II) complex was 0 ppm during the first 50 s.(Fig. 47). Gradual increase in the CO_2 transmittance can be seen after 150 s of passing. Deduction in CO_2 transmittance is significantly higher (4-5 times greater) for the Fe(II)complex than the chlorophyll and Fe (III) complex (Fig. 48). Steady decrease in the amount of CO_2 transmittance can be seen with increasing the concentration of the Fe (II) complex by keeping the total volume constant (Fig.49). This observation implies the higher capacity for Fe(II)complex for CO_2 binding. There are literature evidence for binding CO strongly to Fe(II)porphyrin complexes but not to Fe(III)porphyrins.

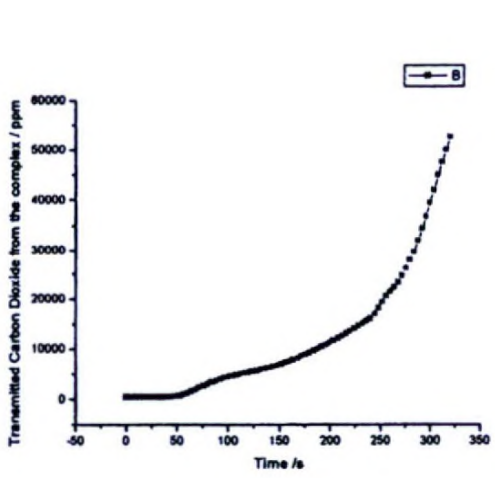

Fig.47CO_2 transmittance from Fe(II)complex with time

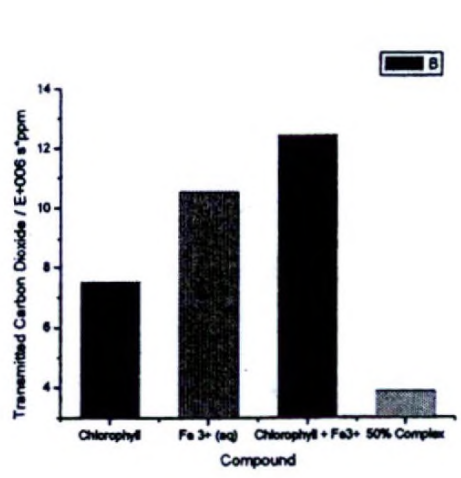

Fig.48 CO_2 transmittance for complexes

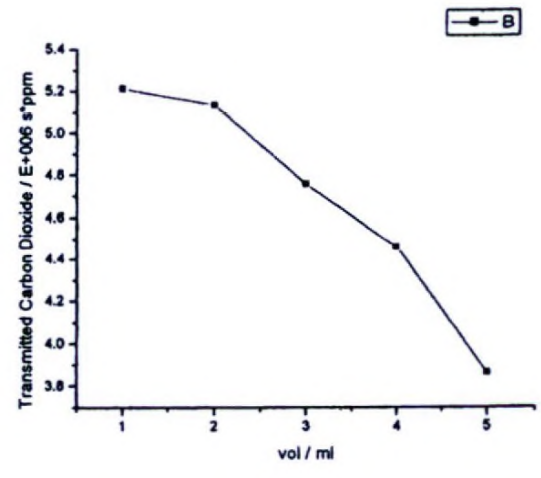

Fig.49 CO_2 transmittance with increasing [Fe(II)complex]

This has been due to strong backbonding interaction strengthening the Fe-C bond in Fe(II)porphyrin complex compared to the Fe(III)analogue. The behavior in the present

Fe(II) complex compared to Fe(III) may also be due to the similar backbonding strengthening of Fe(II) complex. The Fe(II) center at Fe(II) complex is sterically more hindered compared to Fe(III) complex due to the axial coordination of 1-methyl-2-pyrrolydinone fragment. The steric hindrance of the bulky 1-methyl-2-pyrolydinone causes it to be further below the porphyrin plane. This pulls Fe(II) down in to the plane, making it unable to bind a second 1-methyl-2-pyrrolydinone on top of it. Further it prevents the oxidation of Fe(II) in to Fe(III) because the required dimerization of two Fe(II) units through a O_2 bridge is sterically unfavorable. However, this arrangement may facilitate the binding of CO_2 from the opposite side to which 1-methyl-2-pyrrolydinone coordinated. On the other hand there may be a possibility to incorporate CO_2 with the 1-methyl-2-pyrrolydinone fragment of the Fe(II) complex. Further experiments to determine the actual mechanism are currently underway.

Substitution of Fe(II) center by Cu(II)

Upon refluxing the solid Fe(II) porphyrin complex with aqueous Cu(II) acetate, a development of a new band around 300 nm was observed after 15 min. of the reaction. The intensity of the band increased with time as shown in fig. 50. This may be due to the MLCT from Cu(II) to Porphyrin Charge transfer.

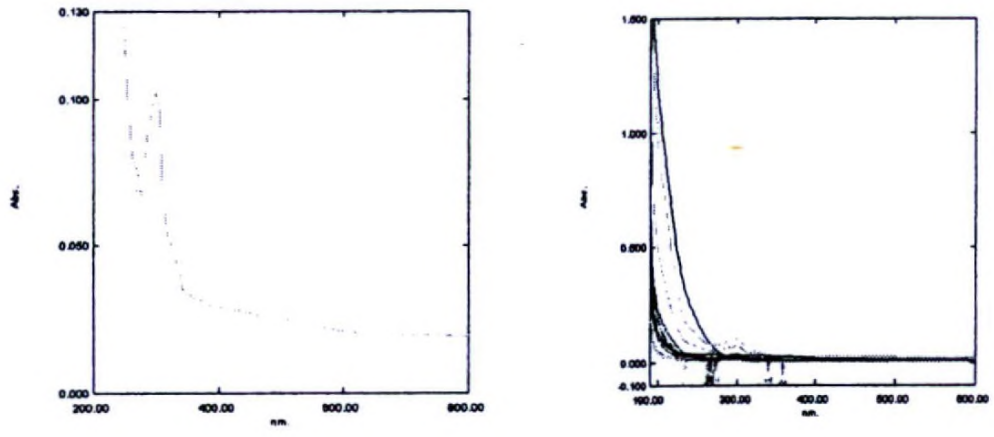

(a) (b)

Fig. 50 UV-VIS spectra of the solution (a) after 165 min of addition of Cu^{2+} (b) after each 15 min. of addition.

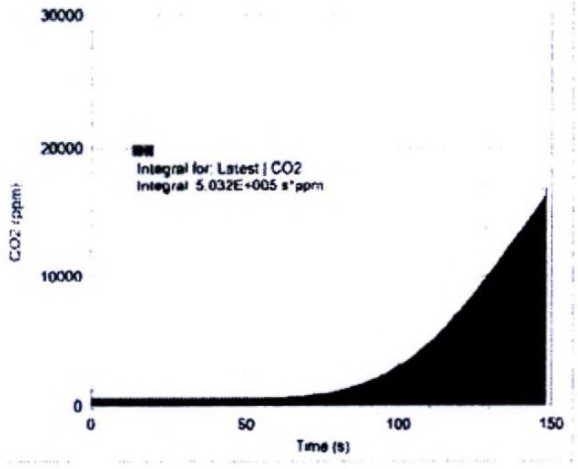

Fig.51 CO_2 transmittance of Fe(II)Chlorophyll complex.

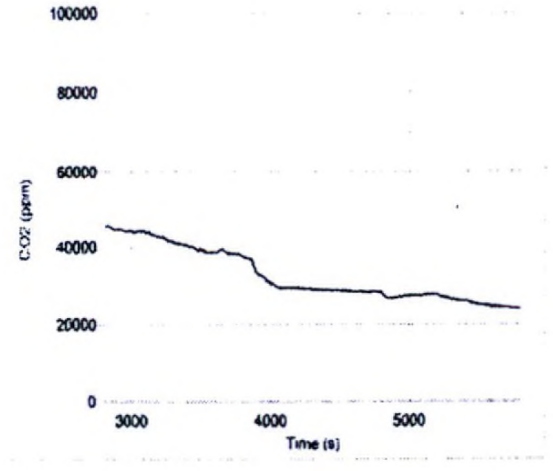

Fig. 52 Change in amount of CO_2 in the flask with the irradiation for Fe(III)Chlorophyll ;(trial1).

Previous studies on CO_2 reduction by J.Grokowski, Pedatsur Neta and Etsuko Fujita illustrate that Iron-Porphyrins do not react with CO_2 until the Fe(III) center is reduced to a lower oxidation state. In the present study, photochemical CO_2 reduction was carried out to test the ability of homogeneous, multi-electron photochemical reduction of Fe-chlorophyll complex, and to identify its role as the both light absorber and the catalyst.

Table 10. Change in amount of CO_2 in the photochemical reduction for studied systems.

System	**$[CO_2]_{initial}$ (ppm)**	**$[CO_2]_{Final}$ (ppm)**	**$[CO_2]_{initial}$-$[CO_2]_{Final}$=Δ (ppm)**	**$\Delta/[CO_2]_{initial}$x100%**
Fe(III)Chlorophyll-*Trial 1*	45510	23967	21543	47.33
Fe(III)Chlorophyll-*Trial 2*	44970	24258	20712	46.06
Chlorophyll-a + $FeCl_3$	45700	36760	8940	19.56

With the Irradiation of the sample over an hour, Fe(III)Chlorophyll system showed 46.70% average reduction in CO_2 concentration inside the flask. Which was nearly 2.3 times reduction in CO_2 concentration than that by isolated chlorophyll-a. The decrease in CO_2 might be due to the multiple electron transfer reduction by the iron center, most probably two electron reduction to yield CO. Fe(III)Porphyrins ,(Fe(III)P), undergo photoreduction to the Fe(II)Porphyrin state by excitation at the ligand-to-metal charge transfer band. It has been found that the process can be greatly accelerated by the addition of triethylamine. Therefore, Fe(III)Porphyrin was dissolved in acetone containing 5% TEA, where it forms several possible complexes Et_3N(Cl)Fe(III)chlorophyll ,(acetone)(Cl)Fe(III)chlorophyll, $(Et_3N)_2$Fe(III) ,(Et_3N)(acetone)Fe(III)chlorophyll. Photoreduction was carried out using a 75 W-xenon lamp and with a glass and a water filter to avoid UV and IR radiation as much as possible. Previous studies indicate that the reduction is most likely an intramolecular electron transfer from the axially bound TEA to the iron center.

$Et_3N(Cl)Fe(III)P \xrightarrow{h\nu} Et_3N^{\cdot+} + Cl^- + Fe(ii)P$

The $Et_3N^{\cdot+}$ radical cation is capable of oxidizing the Fe(II)Porphyrin. This back electron transfer, however is thought to be suppressed by a competing reaction that converts the radical cation into a reducing species, which may reduce another Fe(III)Porphyrin.

$Et_3N^{\cdot+} + Et_3N \longrightarrow Et_3NH^+ + Et_2N\dot{C}HCH_3$

$Et_2N\dot{C}HCH_3 + ClFe(III)P \longrightarrow Et_2N^+{=}CHCH_3 + Fe(II)P + Cl^-$

Further illumination results in the reduction to Fe(I)P, but the process is found to be less efficient. The mechanism is same and it is again the excitation of the ligand to metal charge transfer band.

$Et_3NFe(II)P + h\nu \longrightarrow Et_3N^{\cdot+} + [Fe(I)P]^{-1}$

The concentration of TEA is found to be has a stronger effect here than in the reduction of Fe(III)P. Photolysis of the Fe(III)P in an organic solution containing 5% TEA and

bubbled with CO_2 is found to be lead to stepwise reduction as above and formation of (CO)Fe(II)P as the most stable product. This indicates a reduction of CO_2 to CO. Photolysis of this is known to decompose to CO and Fe(II)P. The yield of CO_2 increased with the prolonged photolysis (> 1.5 hr) and the solution gradually turned into green and then become yellow indicating the destruction of macrocycle. However, by modifying the conditions required to back electron transfer regeneration of Fe(III)P and further decomposition of CO would be possible.

6. Co (II) Complex similar to Hemoglobin

Treatment of chlorophyll with acid substitutes the Mg(II) ion with two hydrogen atoms gives an olive-brown colour pheophytin. Then the addition of cobalt chloride dissolved in methanol turns it to dark green solution.

The Co(II) porphyrin solid product was characterized using FT-IR and XRF.

IR bands at 3439 cm^{-1}, 1645 cm^{-1}, 1390 cm^{-1} , 1041 cm^{-1} are attributed to N-H, C=C ring/ C=N ring stretching , C-O stretching , C-C stretching respectively . The band in the region 522 cm^{-1} may be due to metal-ligand vibtration, suggest that porphyrin nitrogen is coordinating to the metal ions. The bands in the region, 2926 cm^{-1}, 2378 cm^{-1} may reasonably attributed to C-H stretching and C-H bending vibration modes, respectively. The presence of small new band at 2677 cm^{-1} of the IR spectra after passing CO_2 through the solid may be due to the C=O stretching of associated carbon dioxide. Several new bands (1166 cm^{-1} and 1465 cm^{-1}) were appeared in fingerprint region after passing CO_2 through the solid. These bands could be attributed to stretching of metal-C bond of CO_2 coordinated complex. The XRF spectra revealed the presence of relatively higher peaks for Cobalt K_α and K_β indicating the presence of Co center.

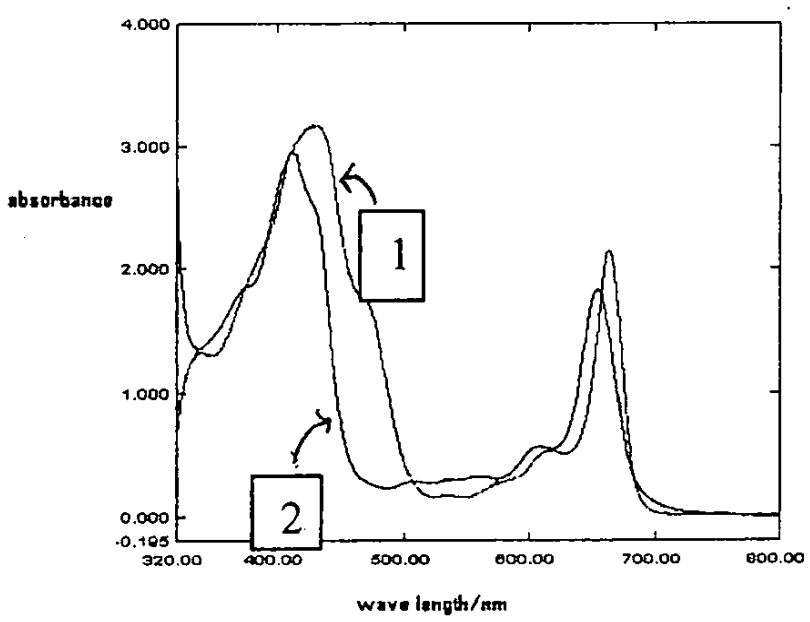

Fig.53.UV-Visible spectra of chlorophyll-a (1) and Co(II) Porphyrin complex (2)

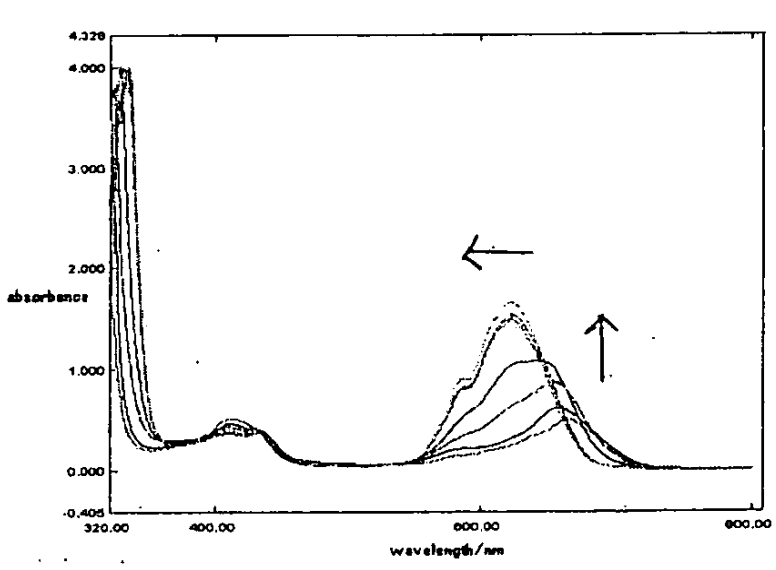

Fig.54.UV-visible spectra Co(II) Porphyrin complex with the addition of SCN^-

In the UV-Visible spectrum of the Co(II)Porphyrin complex, the wave lengths of maximum absorption are shifted to the shorter wavelength (blue shift) in both soret and the Q band on the replacement of Mg (II) in chlorophyll by Co(II). This shift of absorption maxima of the bands indicates Co(II) complex formation. The band around

655 nm-665 nm which is common to both chlorophyll and Co(II) complex may be due to the intra ligand electronic transition of porphyrin. The band at 560.0 nm may be due to Charge transfer transitions (MLCT) of the Co(II) complex by dπ of d^7-Co(II) and π* of porphyrin interaction. The d-d band of Co(II) may be concealed by huge CT bands.
With the stepwise addition of SCN^- in to Co(II) complex band around 655 nm- 665 nm shifts toward lower λ (blue shift)while gaining the intensity, the intensity of the band at 413 nm decreases. The intensity gain and the red shift of the band at 320 nm-380 nm observed with SCN^- addition which implies substitution of axially coordinated Cl^- with SCN^- anion (fig 54). There is a significant difference in the electrode potential of $CoCl_2$ and Co(II) complex. The oxidation potential of Co(II) complex have shifted by 0.213V compared to $CoCl_2$ indicating the higher stability (Lower or –ve ΔG) for the Co(II) complex.

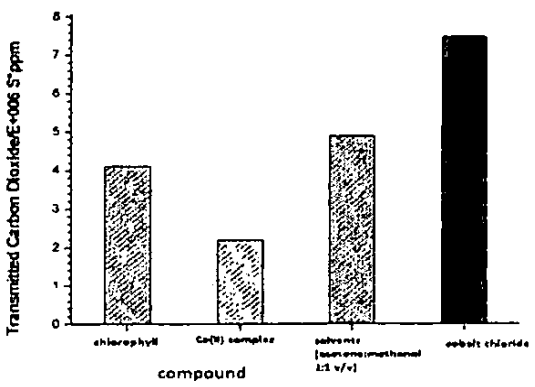

Fig.55. CO_2 transmittance for different solutions

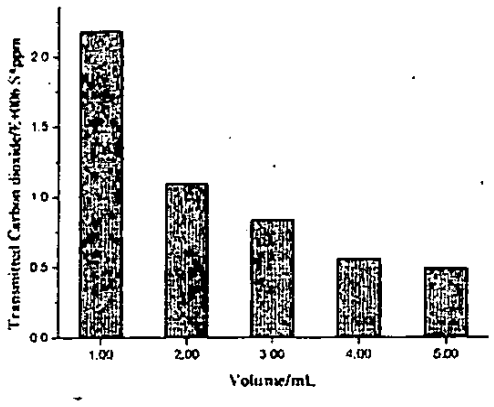

Fig.56. CO_2 Transmittance with increasing [Co(II) complex]

The decrease in the CO_2 transmittance in Co(II)porphyrin complex is about two times higher than the chlorophyll. Steady decrease in the amount of CO_2 transmittance can be seen with increasing the concentration of the Co (II)porphyrin complex by keeping the total volume constant (fig 56). This observation indicates that association may be due to the significant axial coordination or trapping of CO_2 in to the Co (II) complex.

(v).Conclusions

Copper (II) complex with Dithiooxamide (Rubeanic acid) and acac is different from both copper (II)dithiooxamido and copper(II) acetylacetonato complexes though the real structure is not confirmed. The remarkable affinity of the trapping of Ag (I) ions to the complex at concentrations below 20 ppm without releasing any Cu (II) may be due to the presence of tiny pores with compatible sizes of solvated Ag(I) ions. However, substitution of Cu(II) ions of the complex only with Ag (I) ions and not with other ions like Pb (II), Cd (II), Ni (II), Zn (II), at concentrations above 20 ppm is specific and unusual. The unusual behavior of the new complex may be used for the application of this type of systems for specific trapping of some other noble ions like Au (I).

N,N- ethylenebis(acetylacetoneiminato)Cu(II)
The UV-Visible spectroscopic data of the N,N- ethylenebis(acetylacetoneiminato)Cu(II) complex show an interesting acid base behavior of the complex and its capability of trapping anions like SCN^-, Cl^-, $Br^-$and I^-.The complex (0.04 $moldm^{-3}$ in methanol) shows the capability of trapping ~34% of CO_2 passed at room temperature. The trapping capacity increases up to ~54% at 3 ^{0}C.

N,N- ethylenebis(acetylacetoneiminato)Fe(III)

The synthesized Fe(III) complex, may not be structurally similar to the N,N-ethylenebis(acetylacetoneiminato)Cu(II), but shows an interesting acid-base properties and significant affinity towards anions though the net reaction products are different.

N,N- ethylenebis(acetylacetoneiminato)Ni(II)

N,N'-ethylenebis(acetylacetoniminato) Nickel(II) hemihydrates complex shows higher CO_2 trapping capacity than simple nickel salts . The CO_2 binding capacity of the complex is insensitive to the concentration of the complex, but increases at very low temperature for the same complex concentration.

M(II)complexes similar to hemoglobin

M(II) porphyrin type complexes where M=Fe(II), Co(II) and Ni(II) capable of trapping CO_2 has been synthesized by using the chlorophyll extracted from *titonia* species as the starting material. Such a M(II) substituted Chlorophyll complex showed much impressive CO_2 binding ability than initial Chlorophyll. The binding capacity varies inversly with temperature for all the complexes. Future studies can be focused with certain structural modifications in order to achieve better results. Studies on Photochemical CO_2 reduction show that Fe(III)Chlorophyll complex is a much effective photo catalyst, and by providing necessary conditions it may even contribute to obtaining future fuel and chemical needs by converting H_2O to H_2 and by converting CO_2 either to CH_4 or HCOOH.

The Fe(II) , Ni(II) and Co(II) substituted Chlorophyll complexes can be used as catalysts to bind and convert CO_2 and as potential agents for reducing global warming. Photocatalytic reactivity of the complexes needs to be carried out with very sophisticated instruments. The current work has been very impressed by several experts in the field in Australia and USA. Further investigations are planned to carry out with the collaboration of a research team in University of Melborne, Monash in Australia and Trinity University in USA.

Table 11. A Summary of the synthesized complexes

Complex	**Predicted Structure**	**Appearance**	**Special Properties**
Cu (II) complex with Rubeanic acid and acetylaceton Cu-B	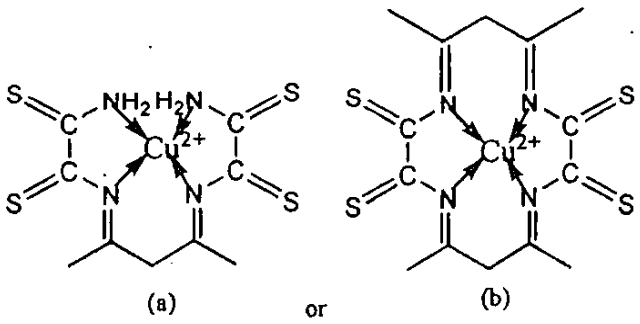	Hard, black colour solid	Remarkable affinity for silver (I) ions
N,N-ethylenebis(acetylacetoneiminato) Ni(II) complex	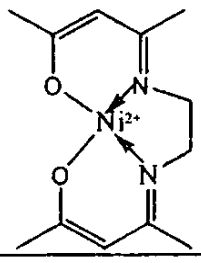	Brownish red colour crystallin	Capable of trapping anions and CO_2

Ni-en-acac		e solid	
N,N-ethylenebisCu (II) complex Cu-en-acac	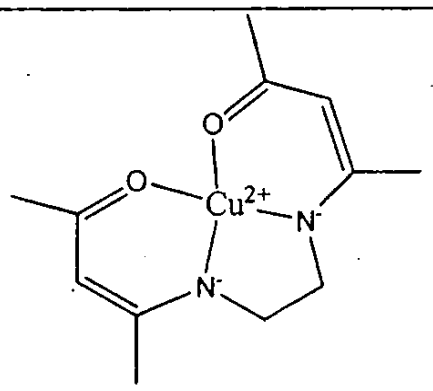	Purple colour crystalline solid	Capable of trapping anions and CO_2
N,N-ethylenebis(acetylacetoneiminato)Fe(III) complex Fe-en-acac-R	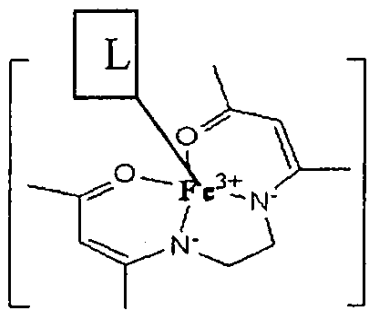	Red colour crystalline solid	Capable of trapping anions
Fe-en-acac-Y	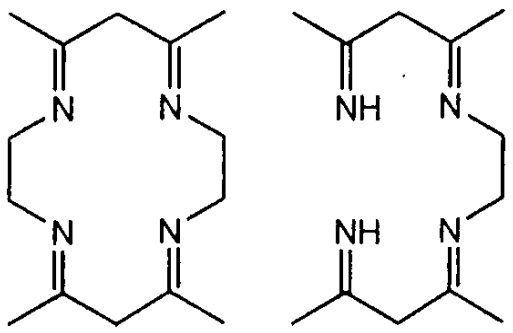 (a) or (b)	Yellow colour crystalline solid	No metal center, Only a ligand complex
M(II) porphyrin type Complex Where M(II) = Fe(II), Co(II), Ni(II)	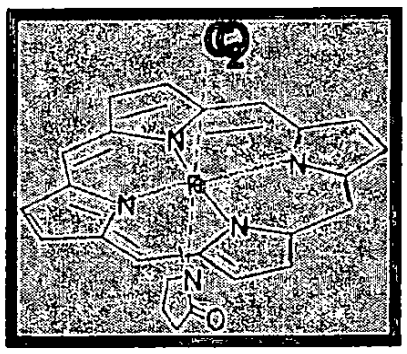	Green liquid, can be solidified	Capable of trapping CO_2

vi) References.

1. Udugala-Ganehenege, M.Y.; Heeg, M.J.;.Hryhorczuk, L.M.; Wenger, L.E; Endicott, J.F. *Inorg. Chem.*, **2001**, 40(7), 1614-1625.
2. Udugala-Ganehenege, M.Y.; Heeg, M.J.;.Hryhorczuk, L.M.; Wenger, L.E; Endicott, J.F. *Inorg. Chem.*, **2005**, 44, 6019-6033.

3. Lindoy,L.F.,*The Chemistry of Macrocyclic Ligand Complexes*, Cambridge University Press, **1989**, 1
4. McAuley, A; Subramanian, S.*Inorg.chem.***1997**,36, 5376.
5. Ciampolini, M.; Fabbrizzi, L; Perotti, A.; Seghi, B.; Zanobini, F.*Inrog.Chem.***1987**, 26, 5376.
6. Buyttafava, A.; Fabbrizzi, L.; Perotii, A; Seghi, B. *J.Chem.Soc., Chem.Commun.*,**1982**, 1166.
7. Szalda, D. J.; Fujita, E.; Scanzenbachev, R.; Paulus, H.; Elias. H. *Inorg.Chem.* **1994**, 33, 5855.
8. a. Fabbrizzi, L. *Comments Inorg. Chem.* **1985**, 4(1), 33 and reference therein.
   b. Amendola, V.; Fabbrizzi, L.; Licchelli, M.; Mangano, C.; Pallavicini, P.; Parodi, L.; Poggi, A. *Coor.Chem.Rev.*, **1999**, (190-192), 649
9. McAuley, A.; xu. C. *Inorg. Chem.* **1992**, 31, 549 and references therein.

9. Balzani, V. (Ed), *Supramolecular photochemistry*, Reidel: Dordrecht, The Netherlands, **1987**, 167
10. Arnout, L. (Ed), *Photochem.Phobiol.A:Chem*, Reidel: Dordrecht, **1994**, 82, 1
11. Khalyfa A., Kermasha S., Extraction, Purification and characterization of chlorophylls from spinac leaves, Macdonald Campus, McGill University, Canada

12.Seleem H.S., El-Shetary B.A. and Khalil S.M., *J. Serb. Chem. Soc.*, 68(10), 2003, 7129-7136
13.Boucher L.J. and Faulker L.R., *Electrochemical Methods,* Wiley Pub., 1980, 6-10
14. Gupta, S.K., Hitchock, P.B., Kushwah, Y.S., (2002), *J.Coord.Chem.*, **55**, 1401
15. Taube H. and Mayer T., J. *Inorg. Chem.*, 1968, 64, 135
16.Endicott J.F., Kumar K., Ramasami T. And Rotzinger F.P., *Inorg. Chem.*, 1983, 30, 141

12. Fox, M. A.; Channon, M. (Eds.), *Photoinduced Electron Transfer*, Parts A-D, Elsevier; Amsterdam, **1988**

13. Beley, M. P.; Sauvage, J. P. *J. Chem. Soc., Chem. Commun.*, **1984**, 1351.
14. Hamada, B. S..; Brunschwig, B. S; Fujita, E.; Korner, M.; Sakaki, S.; Yan, R.; Wishart, J.F.. *J.Phys..Chem.*, **1999**, A103, 5645
15. Fujita, E. Coor. *Chem. Chem. Rev.*, **1999**, 185-186, 373
16. Rawele, S.C.; Moor, P.; Alcock, N. W. J. *Chem.Soc.; Chem. Commun*, **1992**, 684
17. Kimura, E.; Wada, S.; Shjonoya, M; Takahashi, J.; Iitaka, Y. *J.Chem. Soc.Chem. Comun.*, **1990**, 397
18. Richardson, D.E.; Taube, H. *J.Am.Chem.Soc.*, **1983**, 105,409
19. Creutz, C. *Progr. Inorg. Chem.* **1983**, 30, 1
20. Gould, I. R.; Farid, S. *Acc. Chem. Res.* **1996**, 29, 522
21. Crutchley, R. Adv. *Inorg. Chem.*, **1994**, 41, 273
22. Taube, H. *Can. J. Chem.*, **1959**, 37, 129
23. Taube, H.; Meyer, T. *J.Inorg. Chem*, **1968**, 64, 135
24. Endicott, J.F.; Kumar, K.; Ramasami, T..; Rotzinger, F. P.; Progr. *Inorg. Chem.*,

1983, 30, 141
25. Rose E.J., Venkatasubramanian P.N., Swartz J.C., Jones R.D., Basolo F. Hoffman B.M., *Proc. Natl. Acad. Sci. USA,* 1982, Vol. 79, 5742-5745
26. Costisor O. and Linert W., Metal *Mediated Template Synthesis of Ligands,* 2004, 210-300
27. Nakamoto K., *Infrared and Raman Spectra of Inorganic and Coordination Compounds, 1986, 190-342.*
28. Argazzi R., Larramona G., Contado C., Bignozzi C.A., *Journel of Photochemistry and Photobiology A: Chemistry*, 2004; 164

(vi). Problems if any, encountered during the implementation of the project

Chemicals/Equipments were not received on time. It took more than one year to get certain chemicals. The procedure applied for buying chemicals and equipment is very lengthy and cannot be satisfied. By getting the tender board approval for the cheapest one, the quality of certain items received is very poor. E.g. Gas regulators. It was very hard to find reliable dealers for buying certain chemicals.

Carrying out the analysis parts were mainly dependent on the instrumentation such as CV, IR, AAS, XRD, etc, which is not always functioning properly. The UV-Visible Spectrophotometer bought from the grant was the only reliable equipment to carry out the research. Photochemical excitation experiments were carried out with much of the difficulties and minimum facilities available.

The RA registered for the project had faced some personal difficulties to continue his work for more than two and half years so that the assistance from another RA had to be anticipated.

Writing frequent letters to get certain approvals(both in and out), especially for making payments to RA's and certain deviations of the project unforeseen, project reports every 6 months, was a real burden with the other commitments of the university as a Senior Academic member.

Section 4

Impact of Research results:

i) Relevance of results achieved to scientific advancement: The unusual properties found from some of the complexes and the significant CO_2 binding capacities of the complexes synthesized are much relevant to scientific advancement.

ii) Relevance of results achieved to national/socio-economic development

The potential applications in

- CO_2 trapping and conversion in to another useful entity.
- Extraction of gold

iii) Dissemination/application of research output

The research output has been disseminated through the oral and poster presentations of different Seminars, conferences, research sessions (PURSE, SLAAS)

Section 5

Miscellaneous

i) List of major equipment acquired during the project period and their functionality.

Equipment	Functionality
Cyclic Voltameter OUTOLAB PGSTAT 12 potentiostat/galvanostat	Irregular
SHIMADZU UV mini – 1240(220-240), SHIMADZU UV-1800 and UV-1601 UV-Visible spectrophotometers	Good, but tedious because it's a single beam one. Poor Poor
Varian Mercury 3000 and Varian YH 300 NMR spectrometer	Irregular Irregular
Vernier Labpro Interface and CO_2 Gas Sensor	Not sensitive for very high CO_2 concentration
Model 400 and NICOLET 6700 FT/IR spectrometers	Not functioning At IFS
SIEMENS D-5000 X-ray diffractometer	Irregular, Data base is not large enough
BUCK 200A model atomic absorption/emission spectrophotometer.	Irregular, Gives problems due to unavailability of many lamps
Single crystal X-ray crystallographic analysis was done by sending few recrystallized samples to Wayne State University, USA. and X-ray lab of Tokyo Institute of University	Excellent, but expensive and time consuming

ii) List of publications/communications arising from the project and/or presentations made at seminars, workshops etc. (Copies are attached)

Publications

1. Synthesis of Novel Copper (II) Complex capable of trapping hazardous cations present in water. A.M.K.S.P.Adhikari, M.Y.Udugala-Ganehenege * Proceedings of Peradeniya University Research Sessions PURSE 2007, volume12 (part II), 304-306.
2. Synthesis of Novel Copper (II) Complex that shows remarkable affinity for Ag^+ ions. A.M.K.S.P.Adhikari, M.Y.Udugala-Ganehenege *
   Department of Chemistry, Faculty of Science, University of Peradeniya.

National Conference on Advanced Materials for Emerging Technologies (NCAMET)-2007, Ceylon Journal of Physical Sciences, 14, 29-38, **2008**.

3. Determination of anion binding to Iron Ethylenediamine-Acetylacetone complexby spectroscopic methods, A.M.K.S.P.Adhikari, **M.Y.Udugala-Ganehenege** * Department of Chemistry, Faculty of Science, University of Peradeniya, Proceedings of Peradeniya University Research Sessions PURSE, Volume 13-part I, **2008**, 445.

4. Spectroscopic Evidence for the pH Sensitivity and Anion Trapping Capability of N,N-ethylenebis(acetylacetoneiminato)copper(II) Complex, A.M.K.S.P Adhikari, **M.Y.Udugala-Ganehenege *,** Department of Chemistry, Faculty of Science, University of Peradeniya, Sri Lanka Association of the Advancement of Science (SLAAS), proceedings of the 64th Annual session, part I- Abstract, 26 Nov-Dec-**2008**, Colombo.

5. Conversion of chlorophyll into an iron complex similar to heomoglobin, L. Pahalagedara, M.Y.Udugala-Ganehenege*, Dpeartment of chemistry, Faculty of Science, University of Peradeniya, Sri Lanka Association of the Advancement of Science (SLAAS), proceedings of the 65th Annual session, part I- Abstract, Dec-**2009**,Colombo.

6. Investigation of carbondioxide trapping capability of N,N,Ethylenebis (acetylacetoneiminato) copper (II) complex, A.M.K.S.P.Adhikari, **M.Y.Udugala-Ganehenege** * , Department of Chemistry, Faculty of Science, University of Peradeniya, Proceedings of Peradeniya University Research Sessions PURSE, Volume 14, **2009**, 234.

7. Synthesis and CO_2 binding / reduction studies of Iron substituted Chlorophylls Ranil Gurusinghe, M.Y. Udugala-Ganahenege, Department of Chemistry, Faculty of Science, University of Peradeniya. University of Peradeniya, Peradeniya University Research Sessions PURSE, **2010**, (submitted).

8. Synthesis of Co(II) substituted chlorophyll-a and determination of its CO_2 binding properties**,** R.L.C.U Lenora, M.Y.Udugala-Ganehenage* Department of Chemistry, Faculty of Science, University of Peradeniya University of Peradeniya, Peradeniya University Research Sessions PURSE, **2010** (submitted

9. Carbondioxide trapping capacity of N,N'-ethylenebis(acetylacetoniminato) Nickel(II)hemihydrates complex**.** M.Dissanayake, M.Y.Udugala-Ganehenege * Department of Chemistry, Faculty of Science, University of Peradeniya. Sri Lanka Association of the Advancement of Science (SLAAS), (Poster, accepted) 66th Annual session, part I- Abstract, Dec-**2010**, Colombo.

Section 6

Summary Statement of Expenditure (indicate under Personnel, Equipment, Consumables, Travel and Subsistence and Miscellaneous)

		Total expenditure Rs.
Personal	Research Student	9 16 800.00
Equipment- (Items purchased)	Foreign / Local	12 56 860.22
	UV visible Spectrophotometer, Glove box Magnetic Stirrer, Hot plate, Stirring Bars Gas Regulator (General Purpose, High Purity), Gas Cylinders (N_2,CO_2), Interfacing for CO_2 gas Detector probe	
Consumables	Foreign / Local	2 88 833.27
Travel and Subsistence		5 900.00
Miscellaneous Bank Charges		89 945.75 26 513.21
Total		**25 84 852.45**

Note: Final financial statement had already been sent with a balance of Rs. 1631.55/=

Section 7

i) Grantees' signatures

Dr (Mrs.) M.Y.Udugagala-Ganehenege

ii) Comments of the Head of the Department/signature

Progress Satisfactory.

Head
Department of Chemistry
University of Peradeniya
Peradeniya, Sri Lanka.

iii) Head of the Institution's signature

VICE - CHANCELLOR
University of Peradeniya
Peradeniya
Sri Lanka

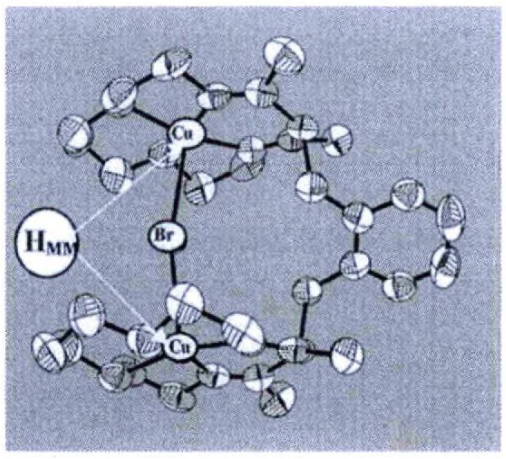

F.g.1. Br^- bridged dimeric Copper complex
Udugala-Ganehenege, etal,
Inorg.Chem., 40(2), 2001, 1614-1625.

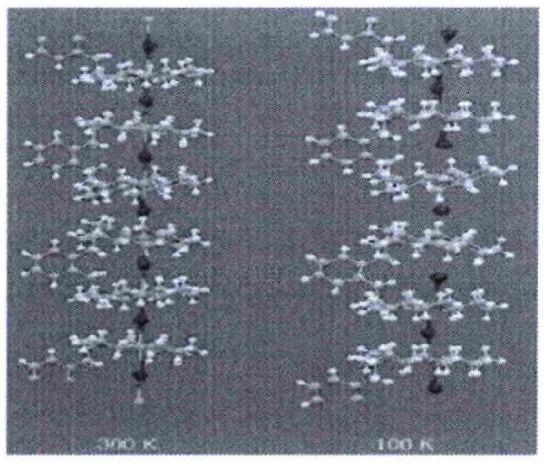

Fig.2. Br^- bridged dimeric Nickel complex
Udugala-Ganehenege, etal,
Inorg.Chem., 44, 2005, 6019-6033.

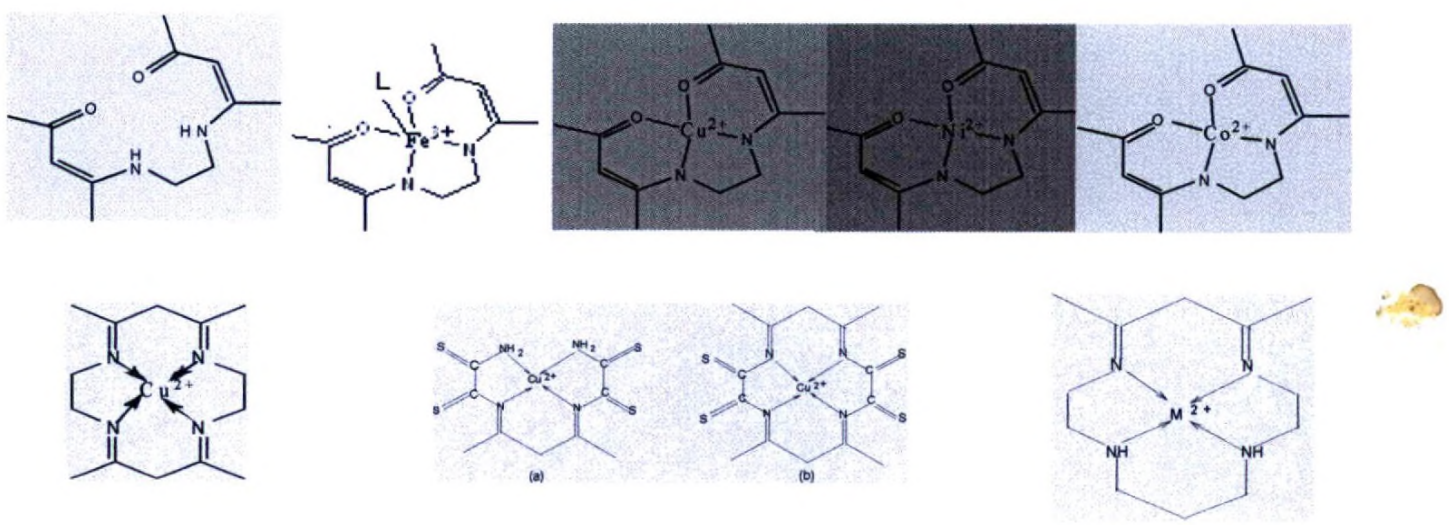

Fig.3

Fig.4

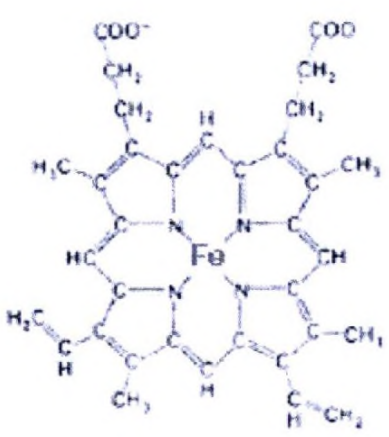

Fig.5

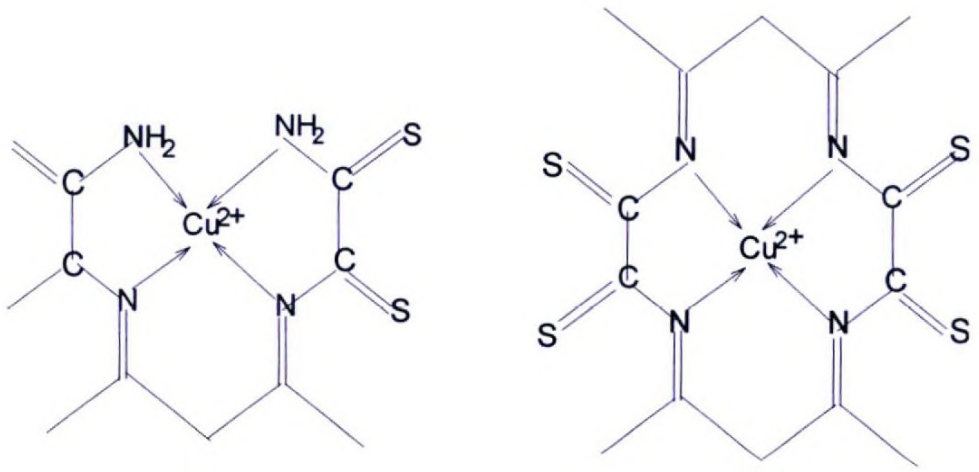

(a) (b)

Fig.6

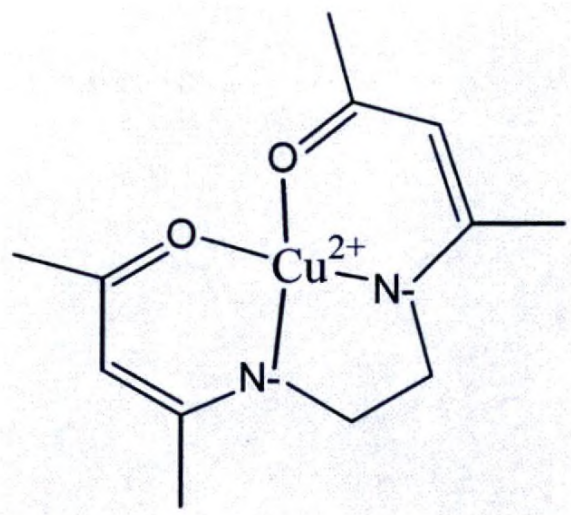

Fig.7. Structure based on X-ray data

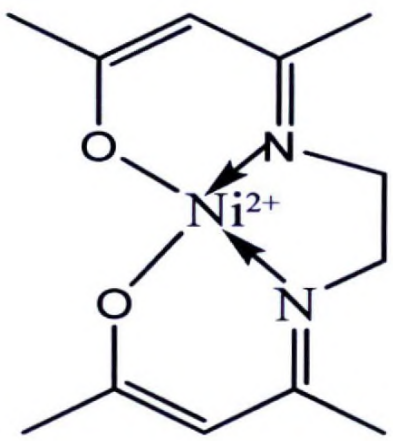

Fig.8. Structure based on X-ray data

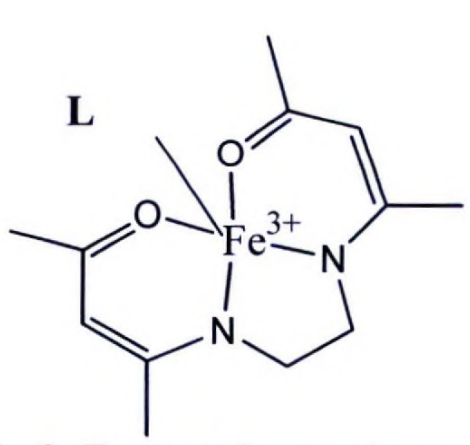

Fig.9. Expected structure

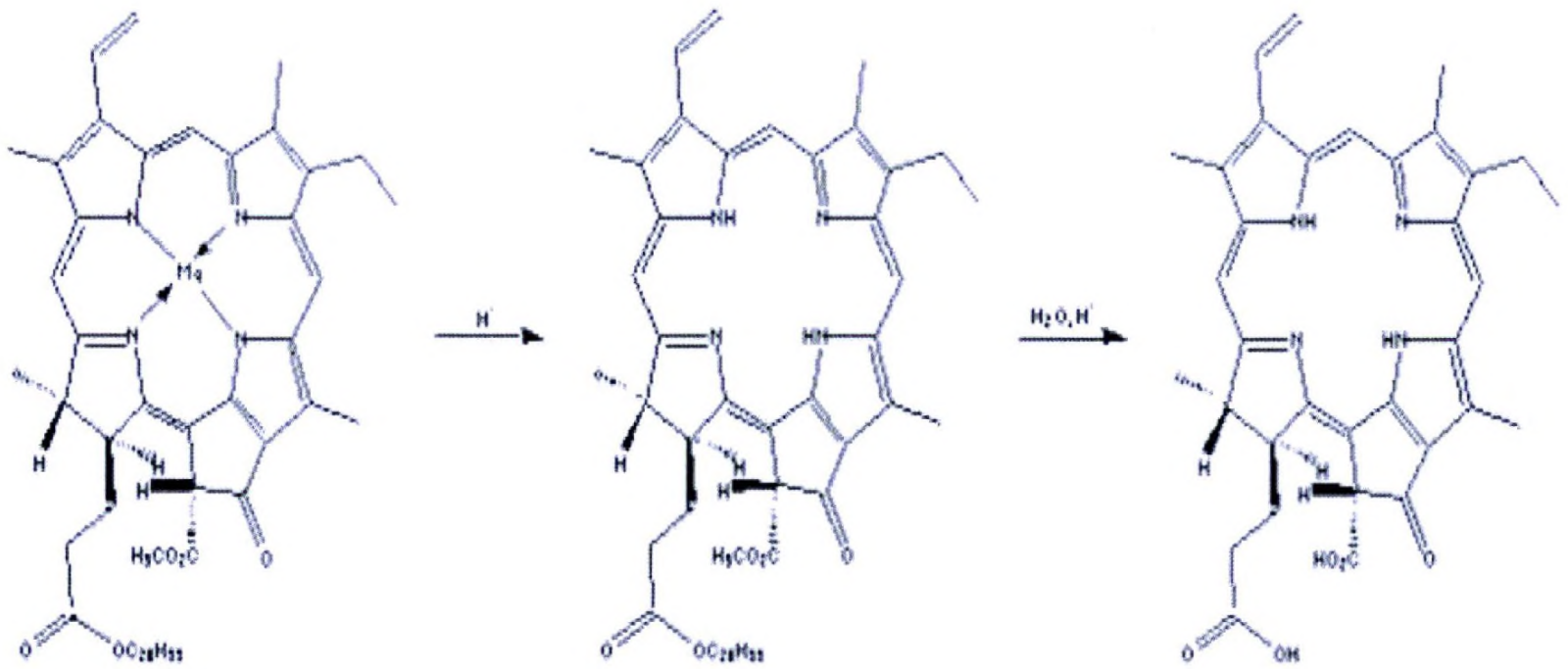

Chlorophyll-*a* Phaeophytin-*a* Phaeophorbide-*a*

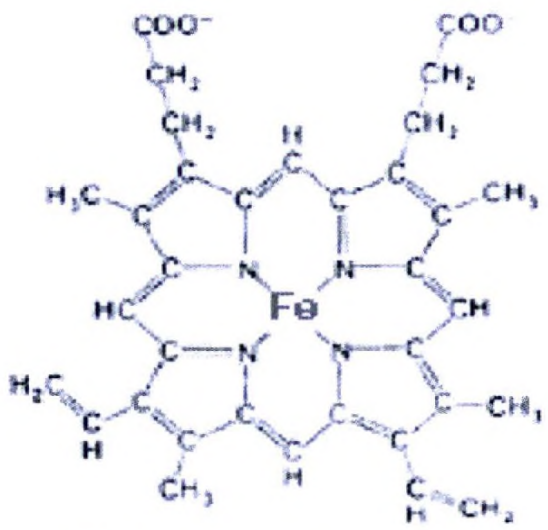

Fig.10. Steps in substituting Mg(II) center by transition metals(Fe, Co, etc)

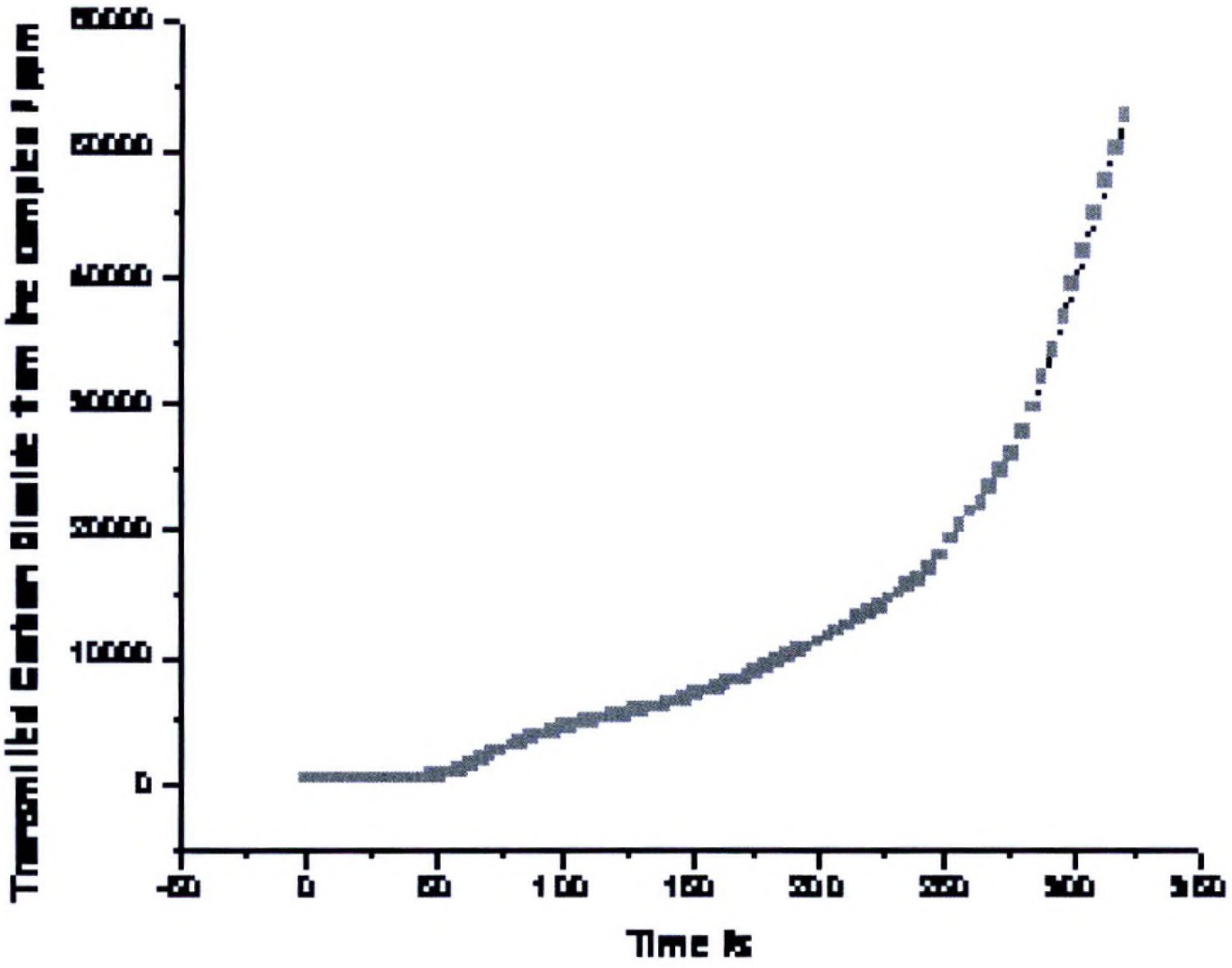

(a) CO_2 transmittance from Fe(II)complex with time

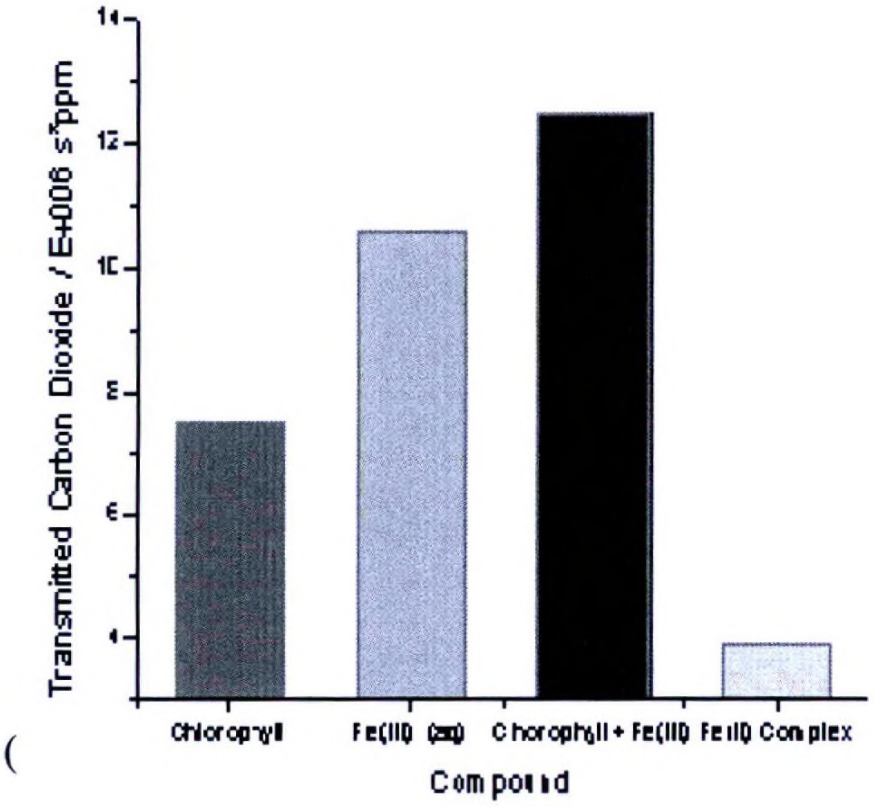

(

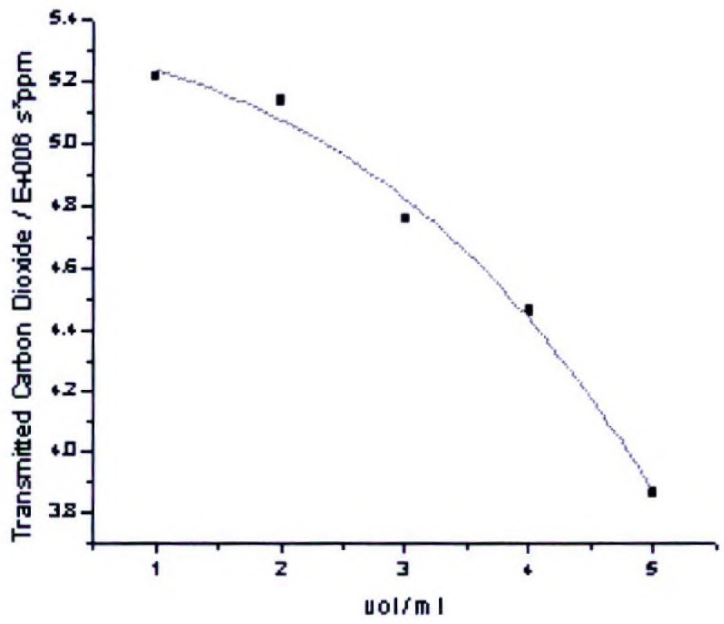

CO_2 transmittance with
ıcreasing [Fe(II)complex]

Fig.11: Chlorophyl, Fe (III), Chlorophyl+ Fe(III), Fe(II) complex

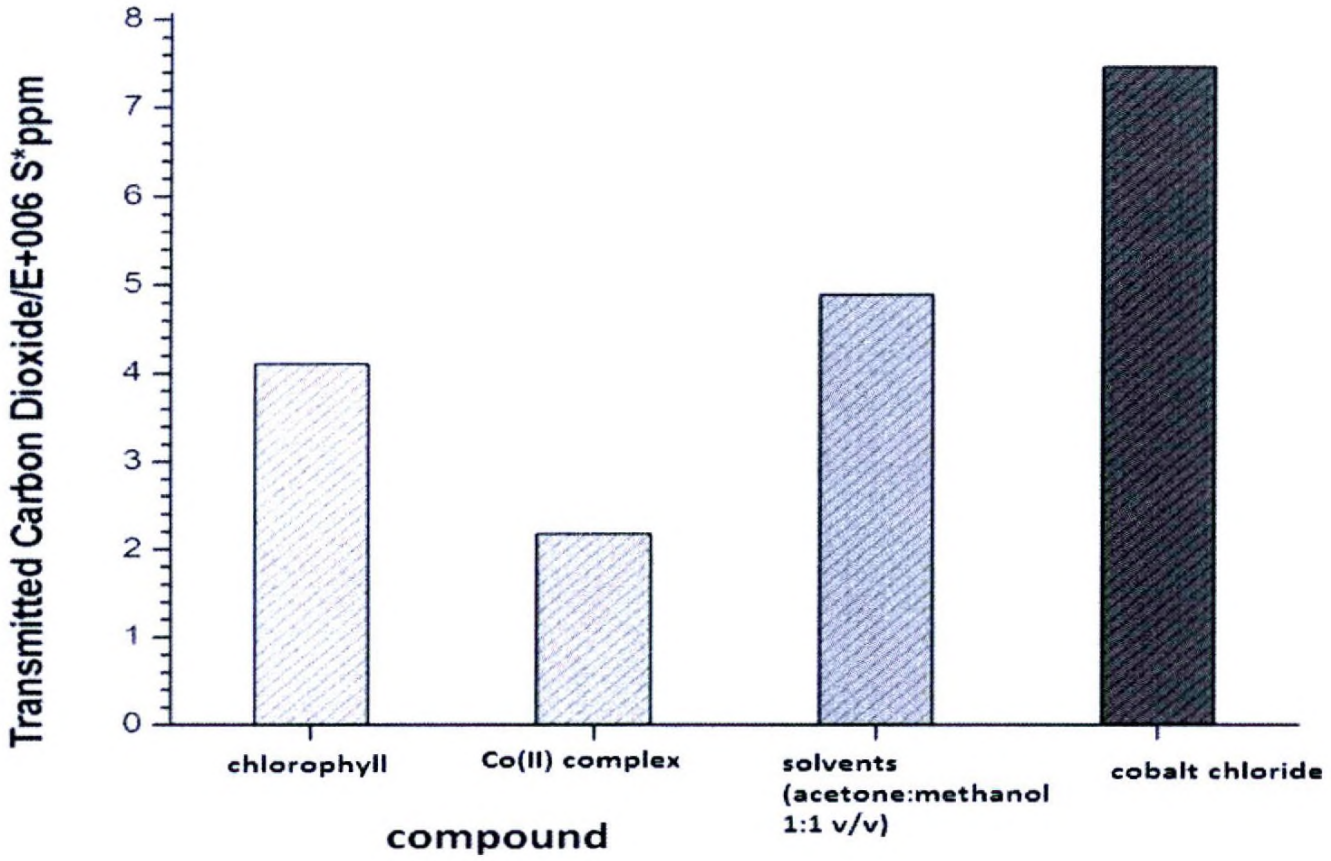

(a). CO2 transmittance for different solutions

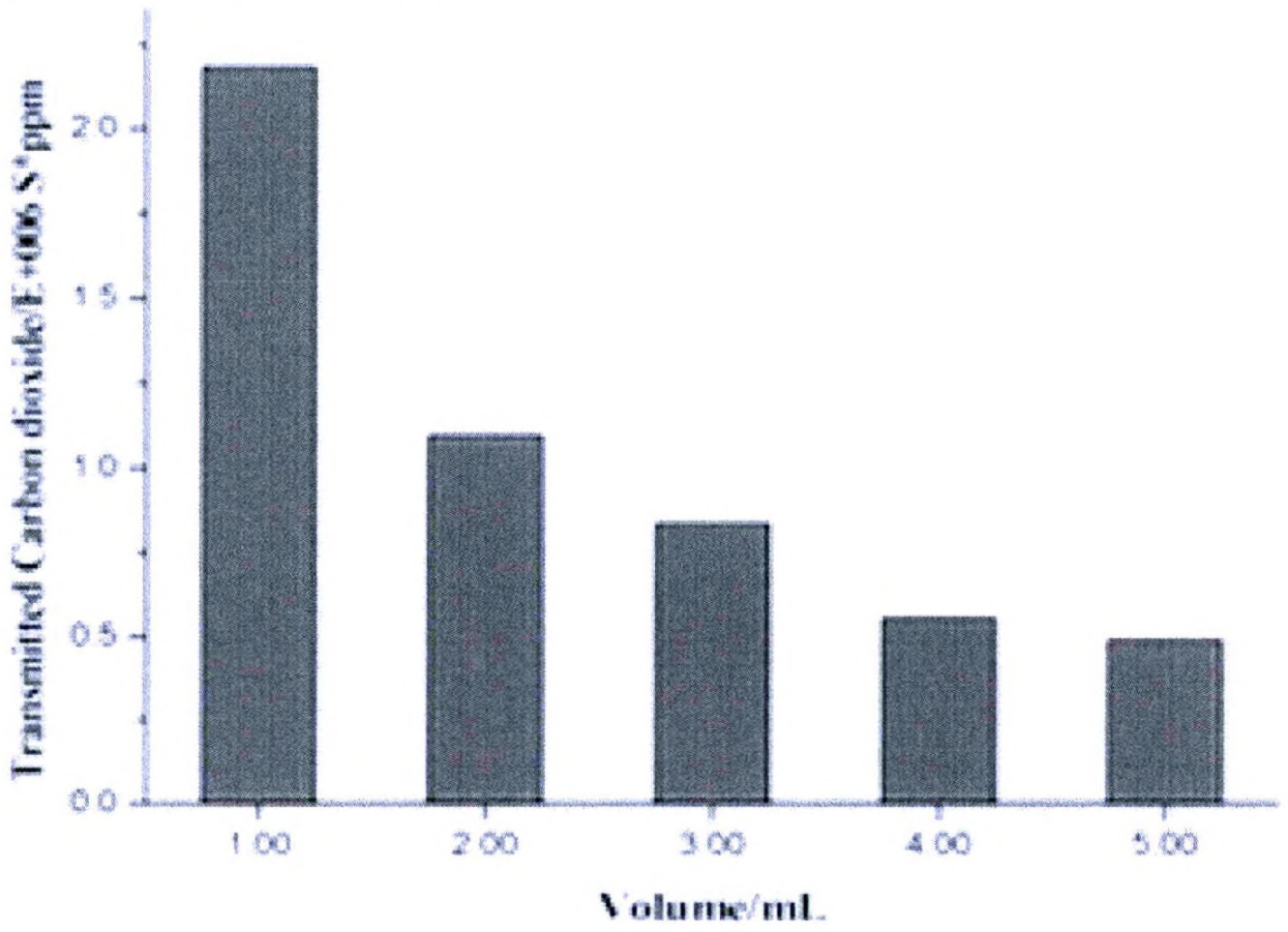

(b). CO_2 Transmittance with increasing [Co(II) complex]

Fig.12.

(a) CO_2- Gas sensor

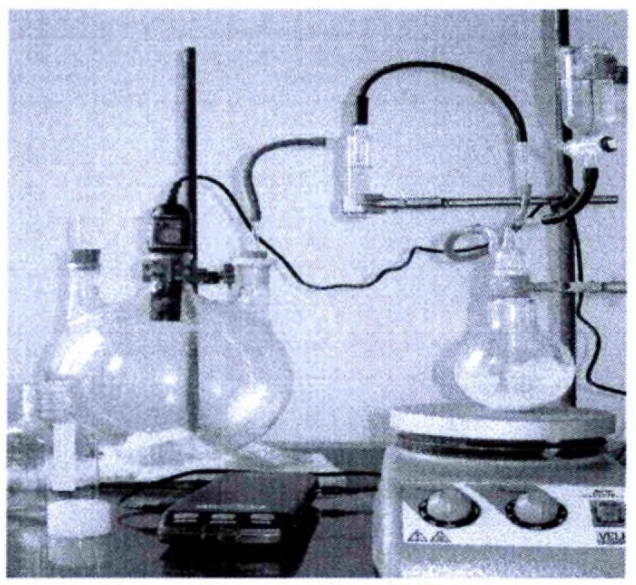

(b) Set up for CO_2 detection

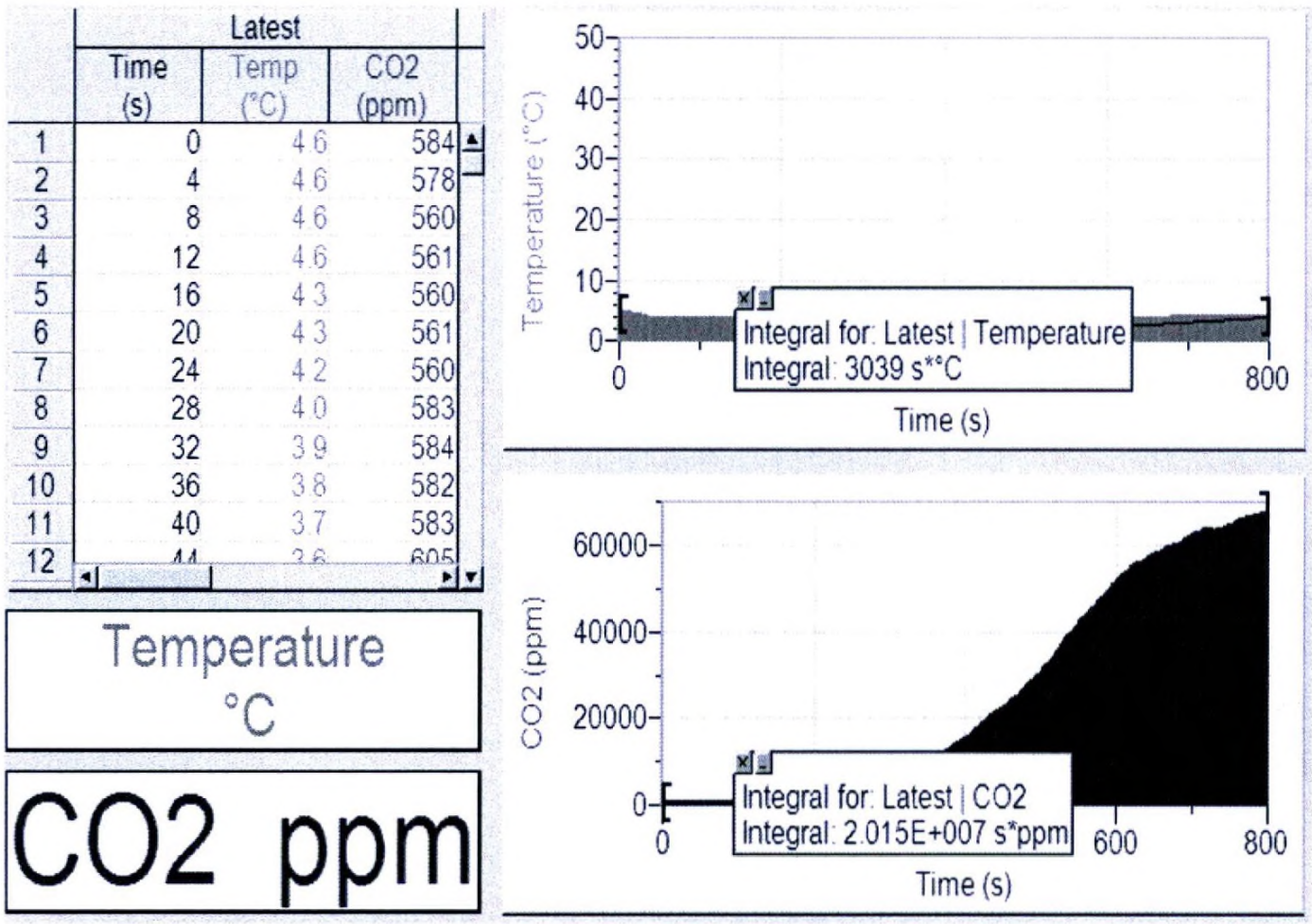

(c) Recording of CO_2 concentration with time in the computer interface

Fig 13

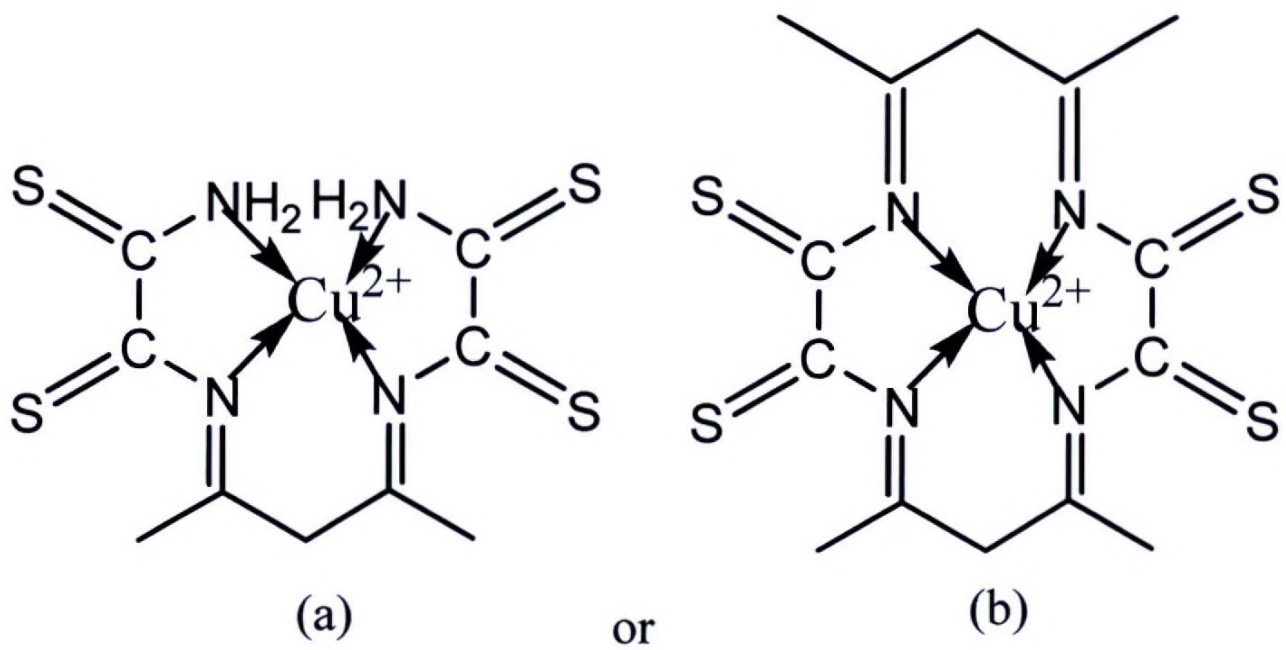

Fig. 14 The predicted structures for Cu-B complex

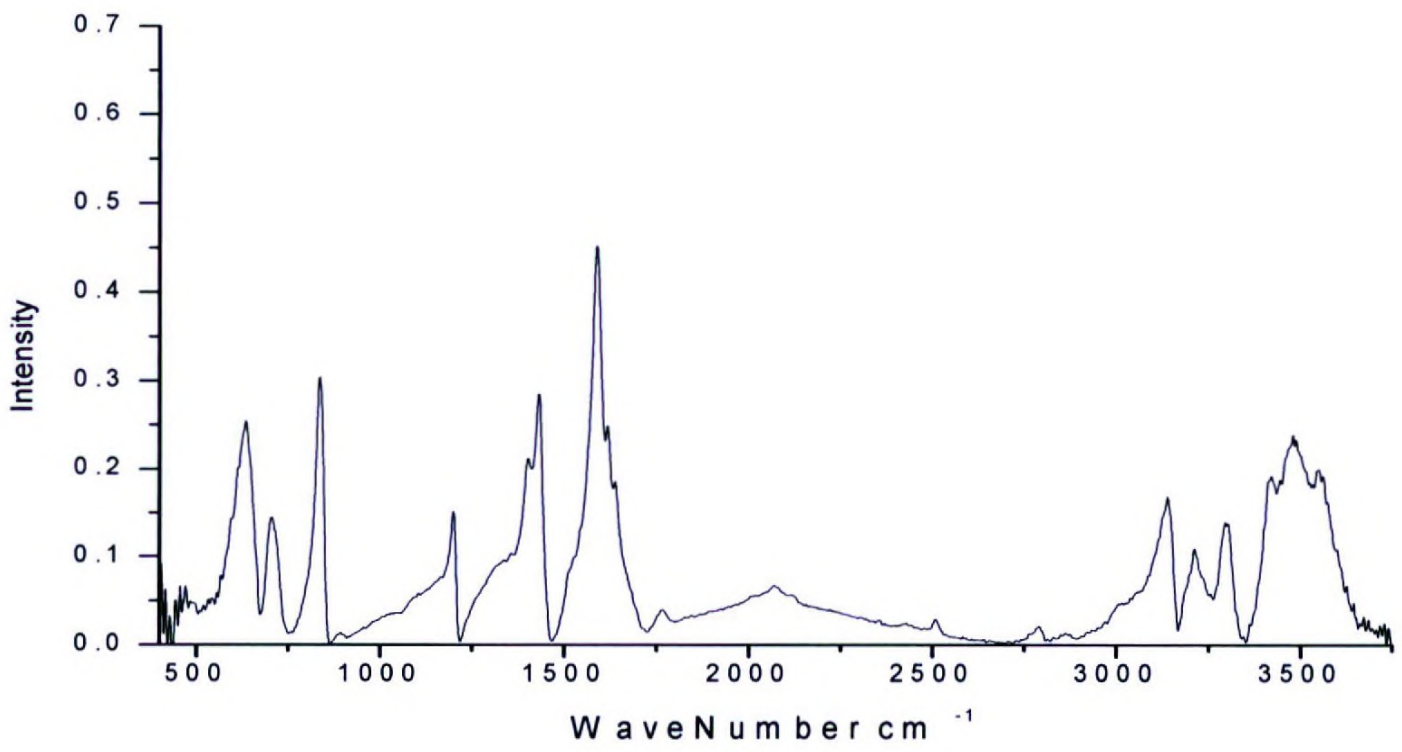

Fig. 14.1 IR Spectrum of Rubeanic acid

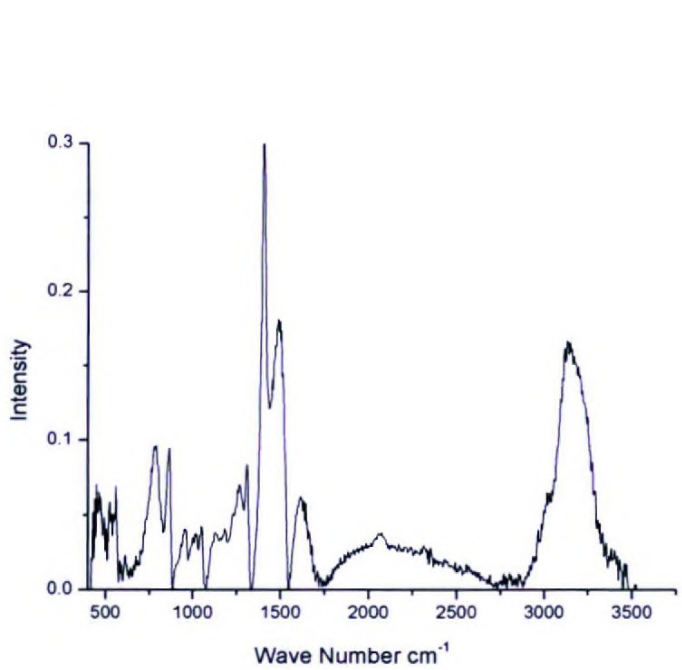

(a). (Cu-B)

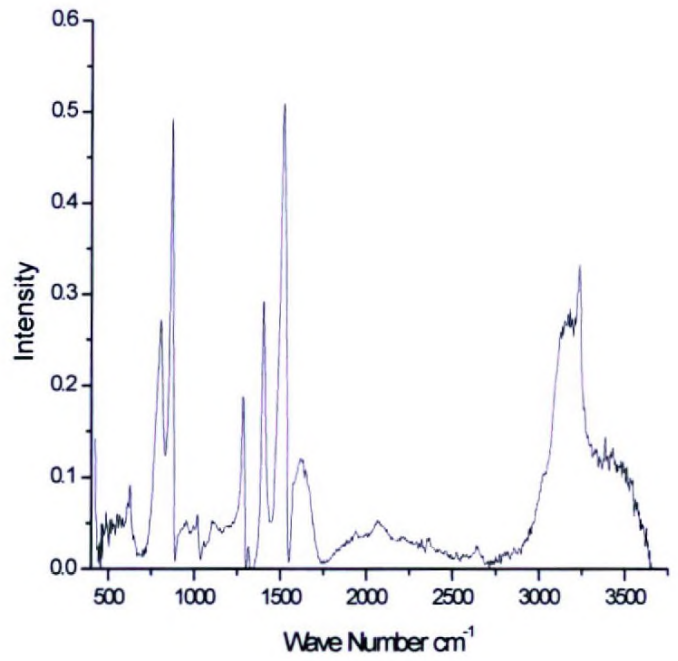

(b) (Cu-A)

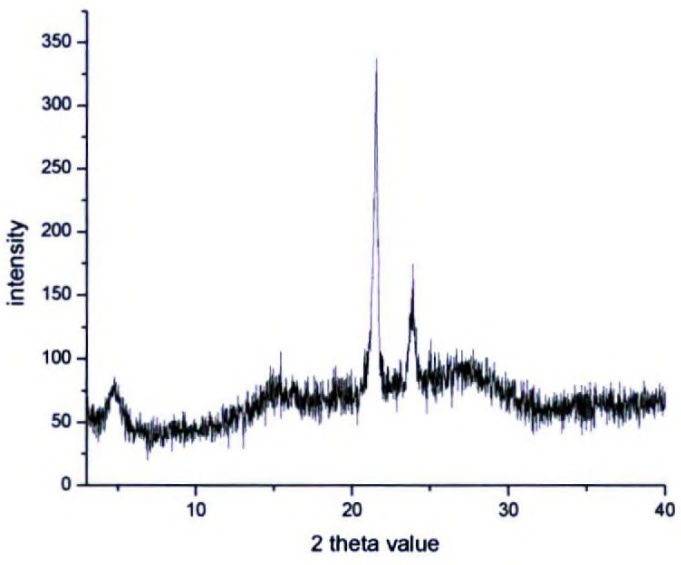

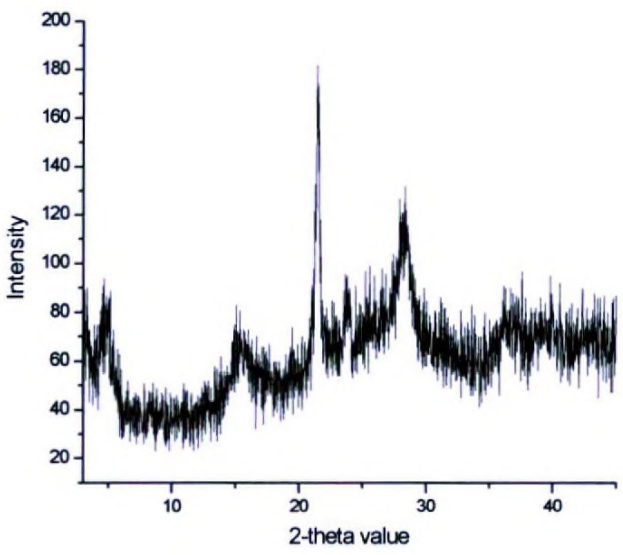

(a). Cu-A (b). Cu-B

Fig. 15 XRD spectra

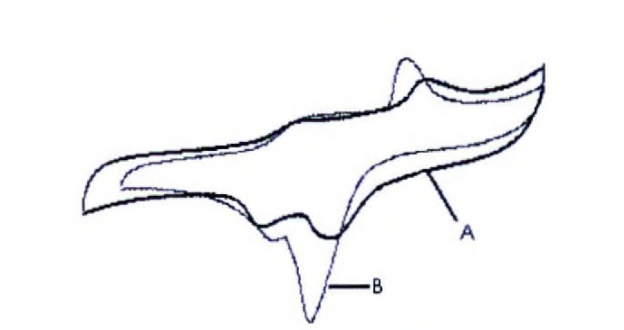

Fig.16 Cyclic Voltammogram for the effluent after passing 0.001M $AgNO_3$ solution through the column of Cu-B (A- effluent after passing Ag (I) , B- Copper acetate solution)

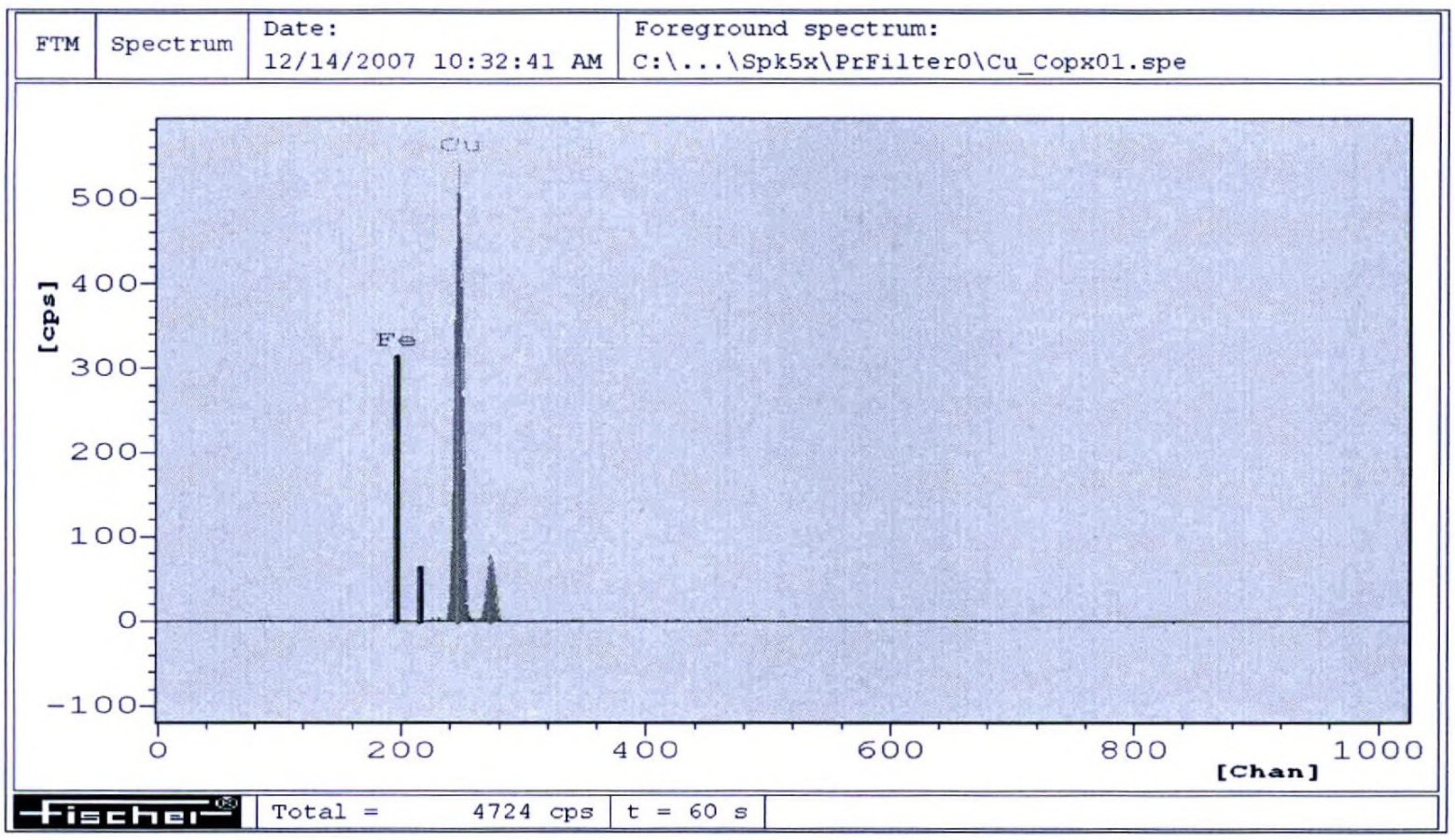

Foreground: C:\...\Spk5x\PrFilter0\Cu_Copx01.spe
Meas. para. (foreground spectrum):
High voltage = 50 kV (875) Prim. Filter = Ni
Collimator 2 = 0.60 Dm. Anode current 900 uA
Meas. distance = 0.87 mm

Notes:
Cu 99.92
Fe 0.08

Results of analysis: (%)
29 Cu = 99.92
26 Fe = 0.08

Fig. 17 XRF spectrum before passing Ag (I) through Cu-B

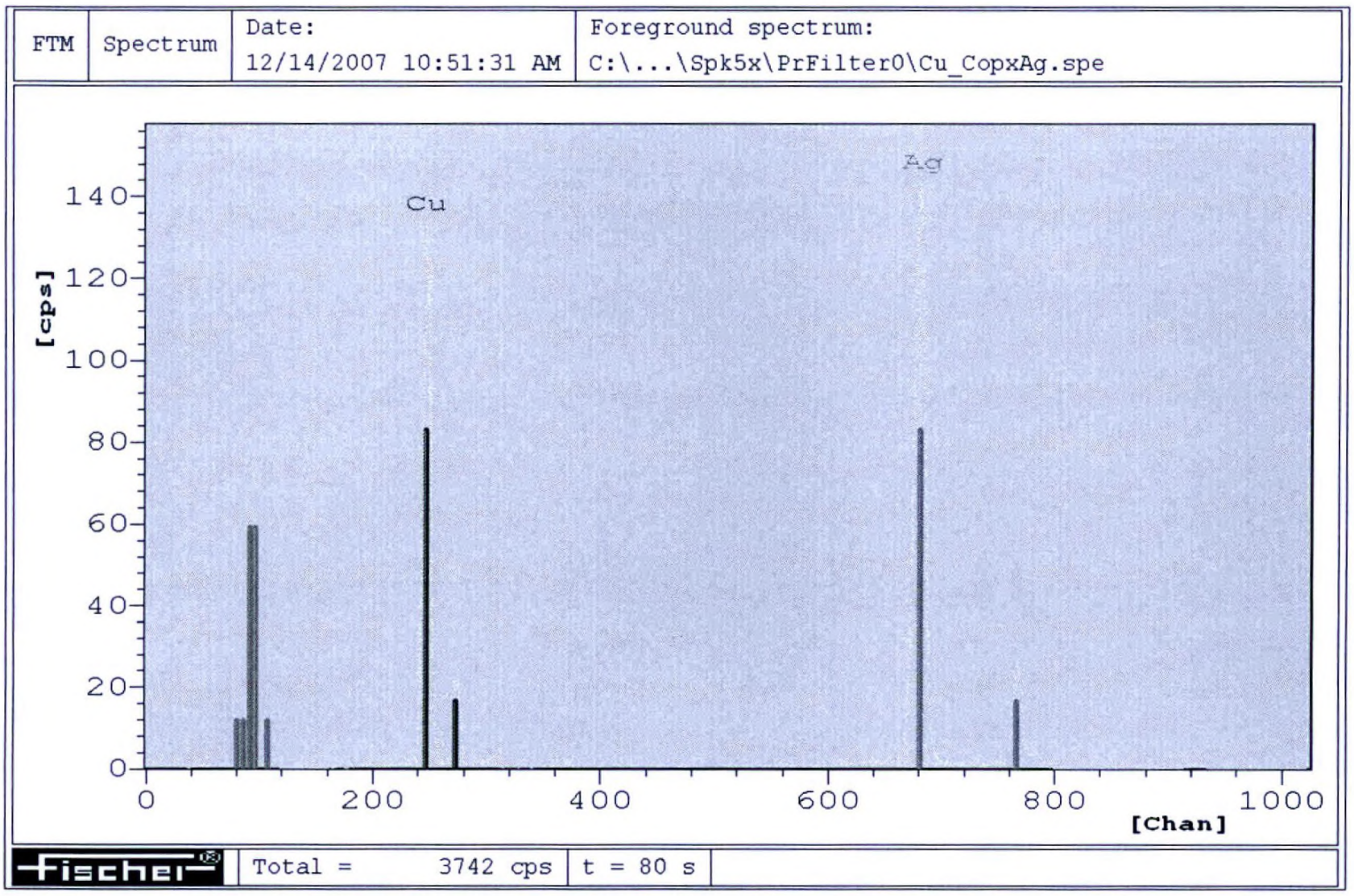

Meas. para. (foreground spectrum):
High voltage = 50 kV (875) Prim. Filter = Ni
Collimator 2 = 0.60 Dm. Anode current 900 uA
Meas. distance = 0.87 mm

Notes:
Cu 30.94
Ag 69.06

List of spectra:
Foreground: C:\...\Spk5x\PrFilter0\Cu_CopxAg.spe

Fig.18 XRF spectrum after passing Ag (I) through Cu-B

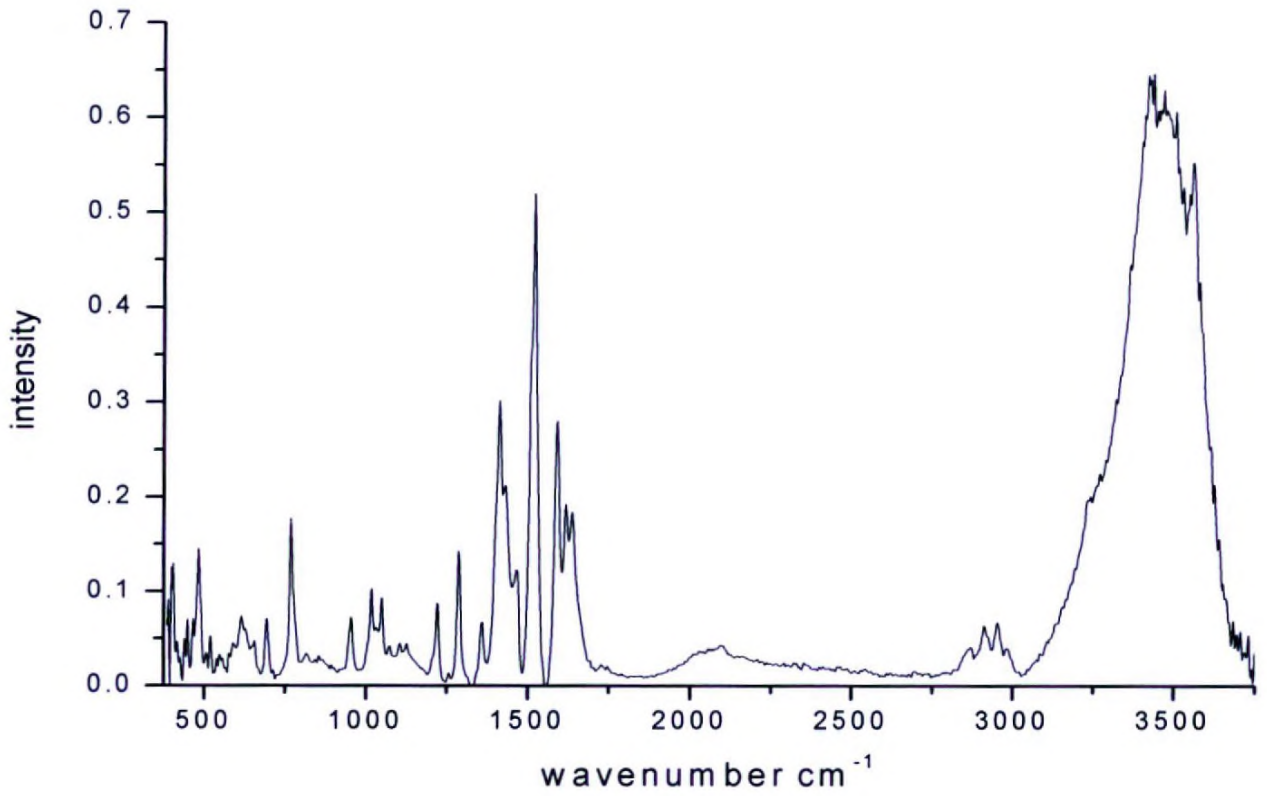

Fig. 19. IR Spectrum of N,N- ethylenebis(acetylacetoneiminato)Ni(II) complex

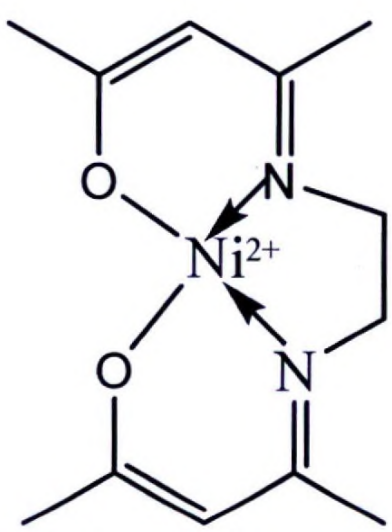

Fig. 20. The X-Ray crystal structure of the Ni-en-acac complex

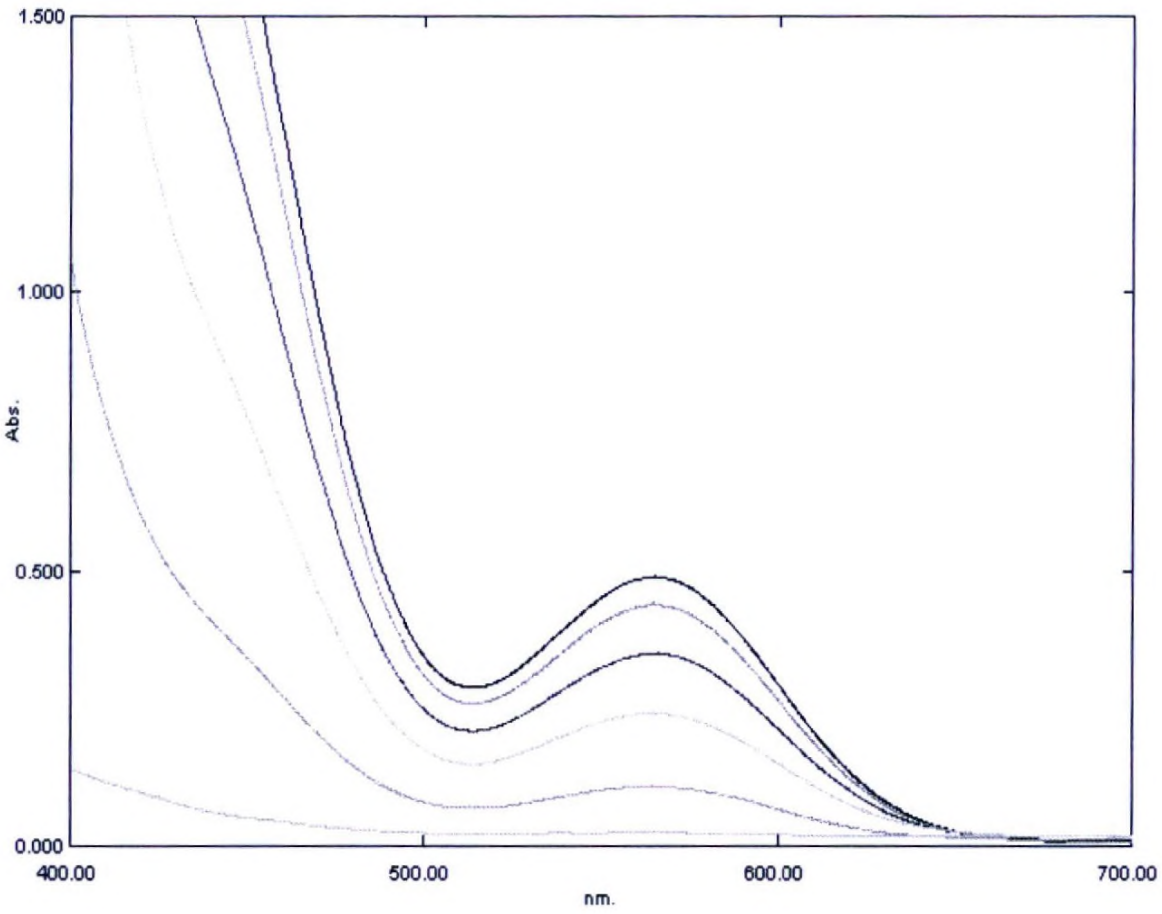

(a)

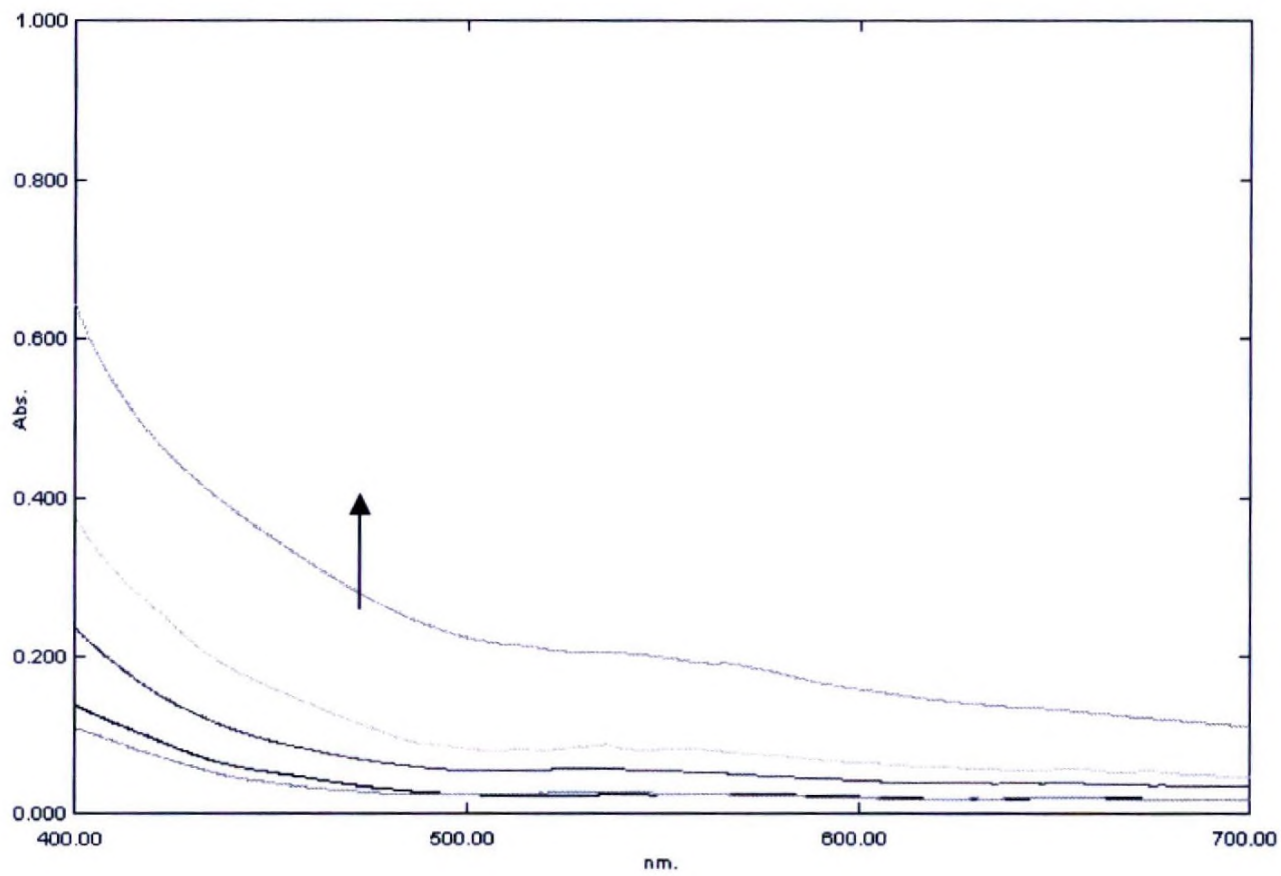

(b)

(a) UV-Visible spectra with the addition of 0.1M HCl (a) micro drop wise into a methanolic solution of the N,N- ethylenebis(acetylacetoneiminato)Ni(II) complex
(b) **UV-Visible spectra with the addition of 0.1 M NaOH micro drop wise into the same (acidified) solution of N,N- ethylenebis(acetylacetoneiminato)Ni(II) complex**

Fig. 21

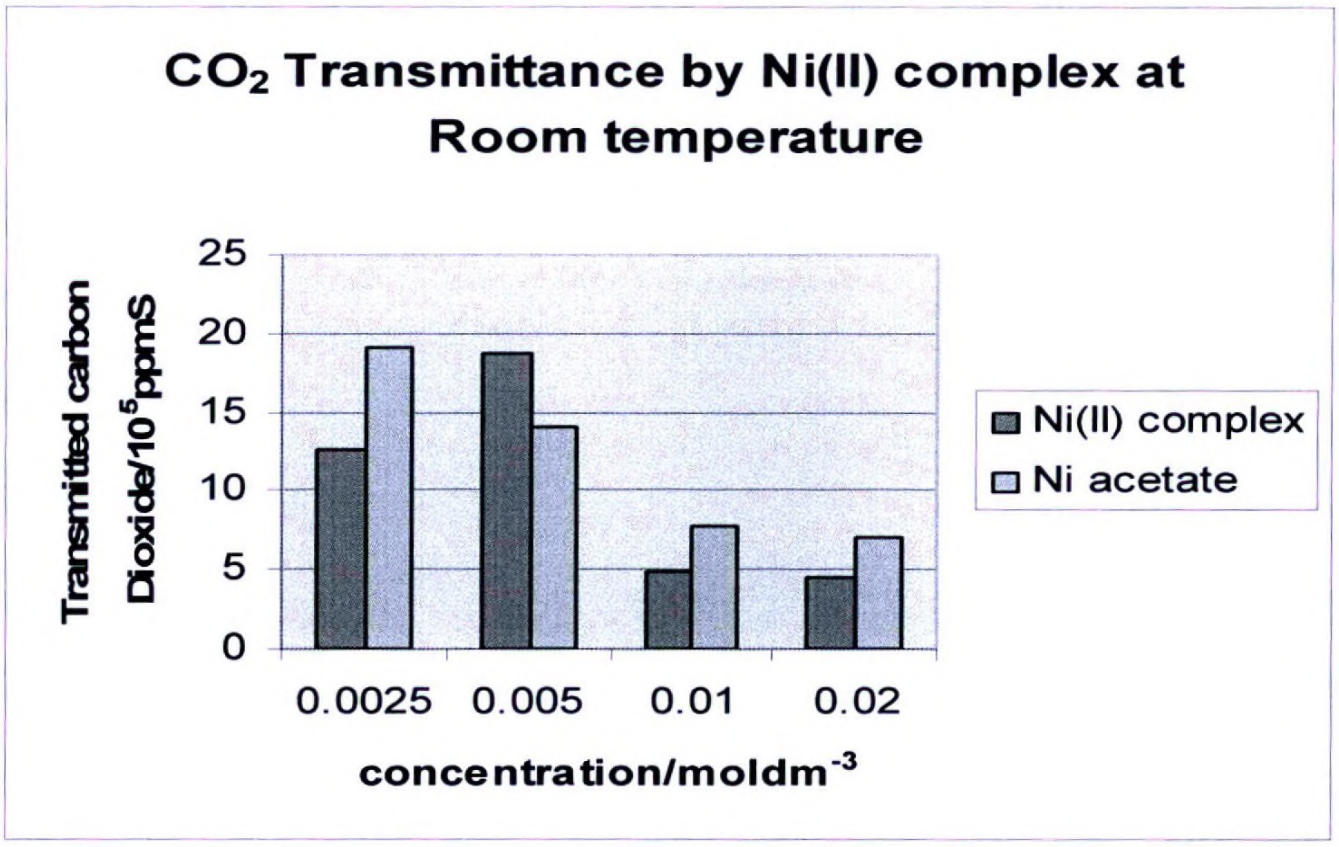

Fig 22: CO_2 transmittance by the various concentrations of N,N-ethylenebis(acetylacetoneiminato)Ni(II) complex at RT for 300 s.

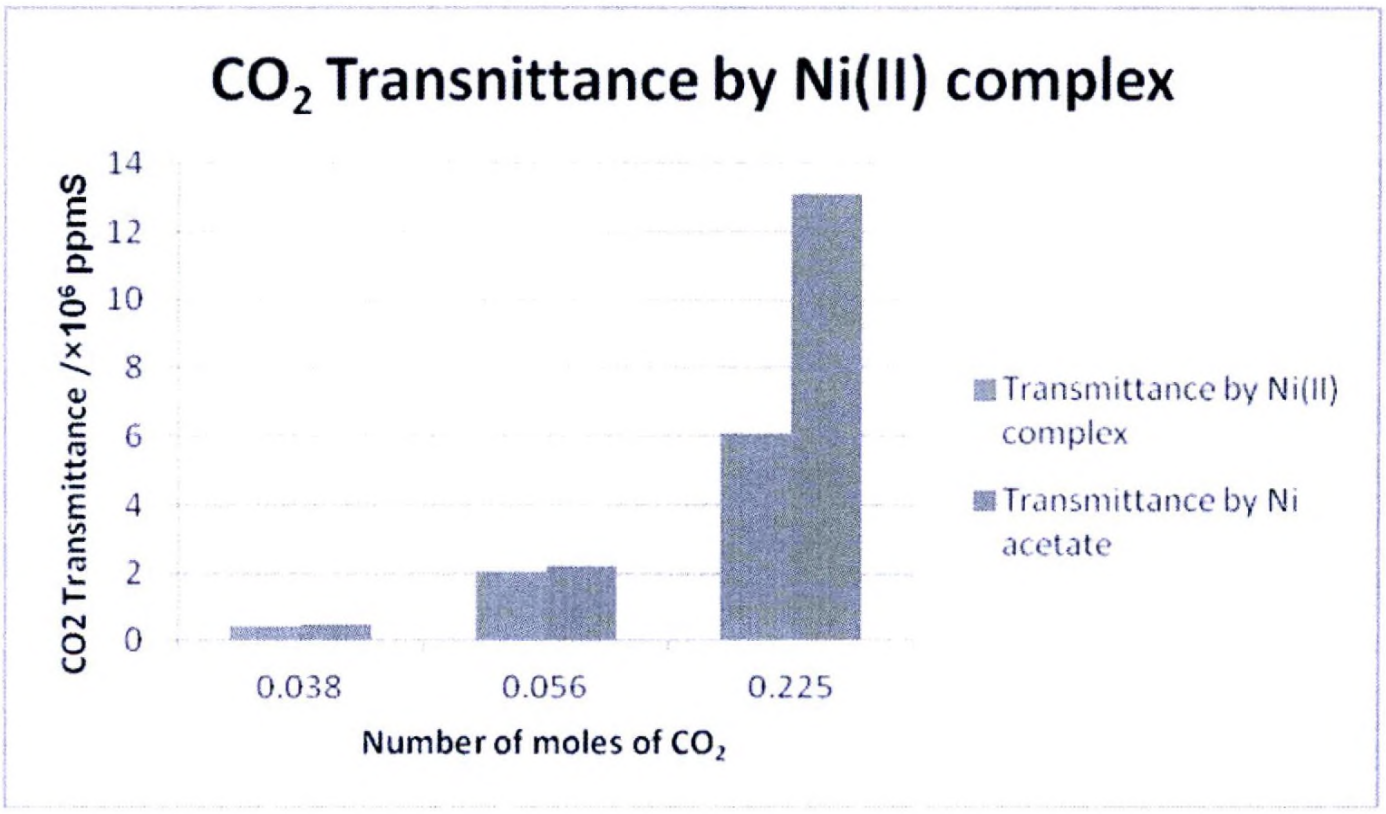

Fig 23: The amount of CO_2 Transmitted by 0.005 mol dm^{-3} of Ni(II) complex and Ni(II) acetate with increasing amounts of CO_2 gas at room temperature for 300 s.

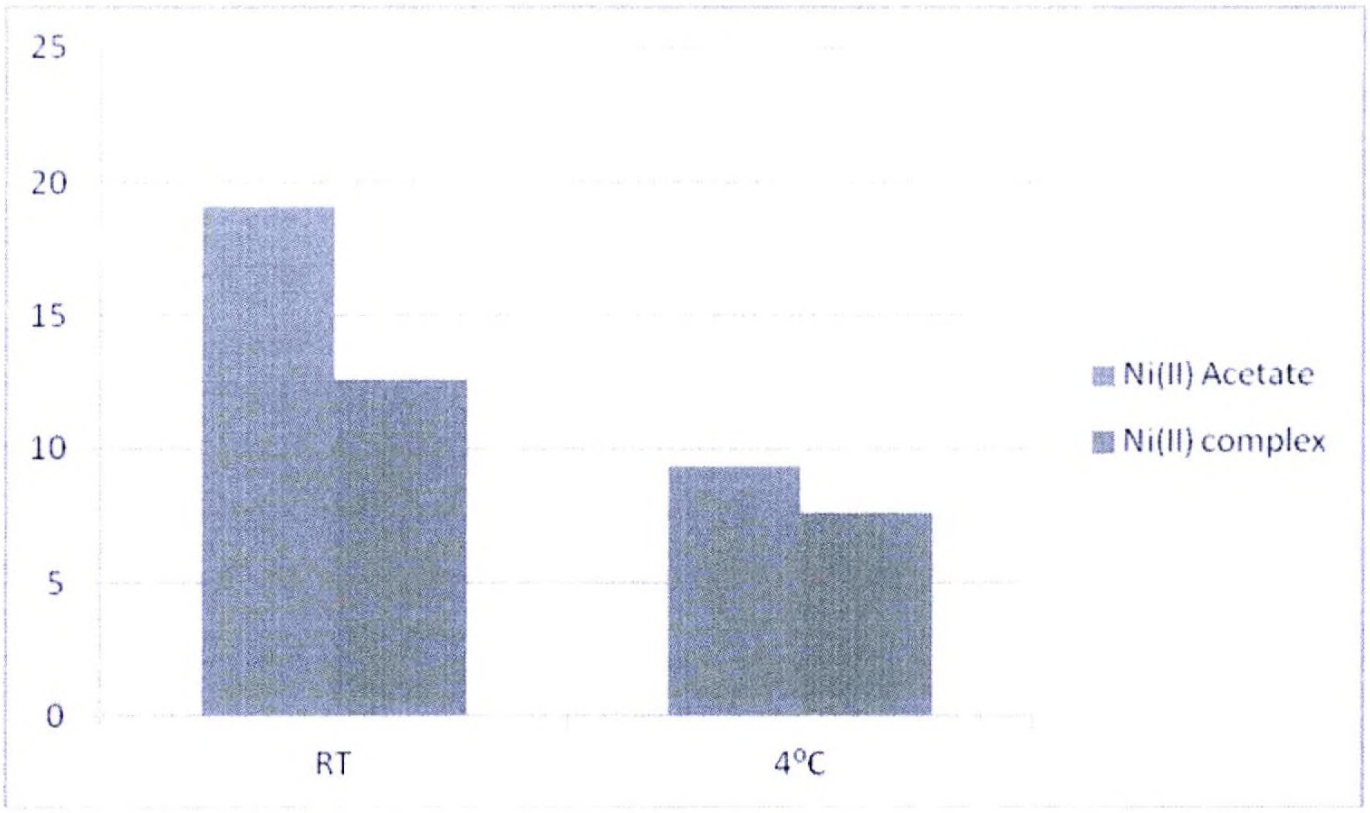

Fig 24: CO_2 transmittance for 0.0025 M concentrations of Ni(II) complex at RT and 4 °C

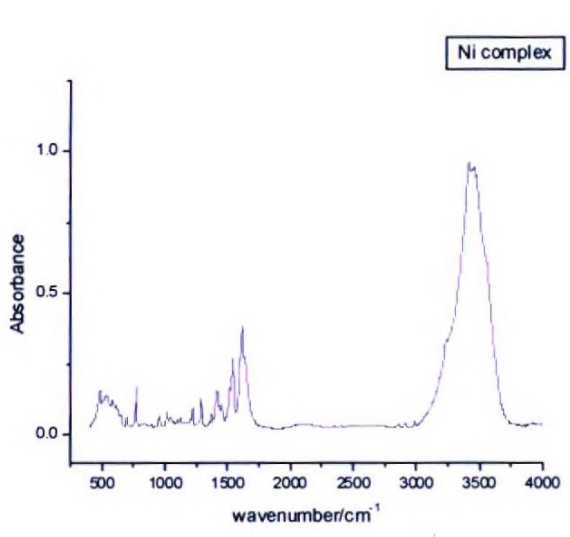

Fig.25.a: FTIR spectrum of Ni (II)complex

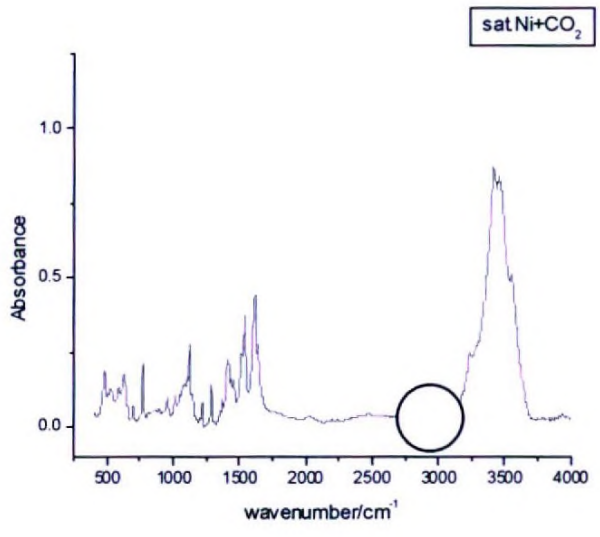

Fig.25.b: FTIR spectrum of saturated Ni (II) complex after passing CO_2 gas

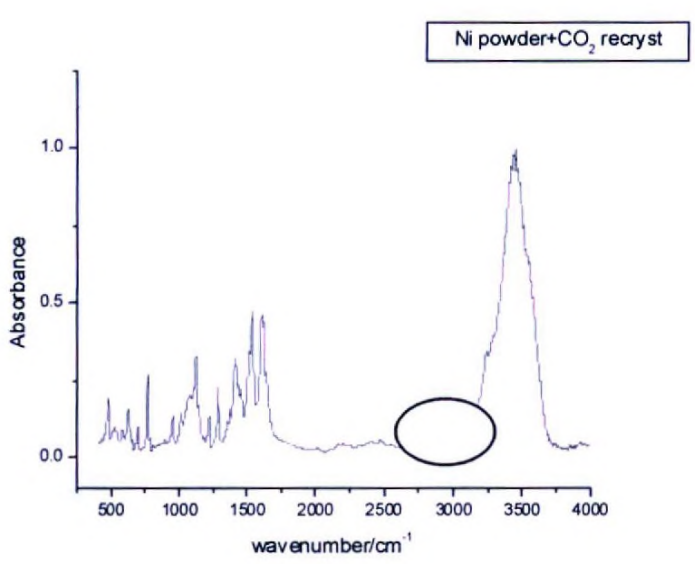

Fig.25. c: FTIR spectrum of Ni (II) complex (Recrystalized solid) after passing CO_2 gas

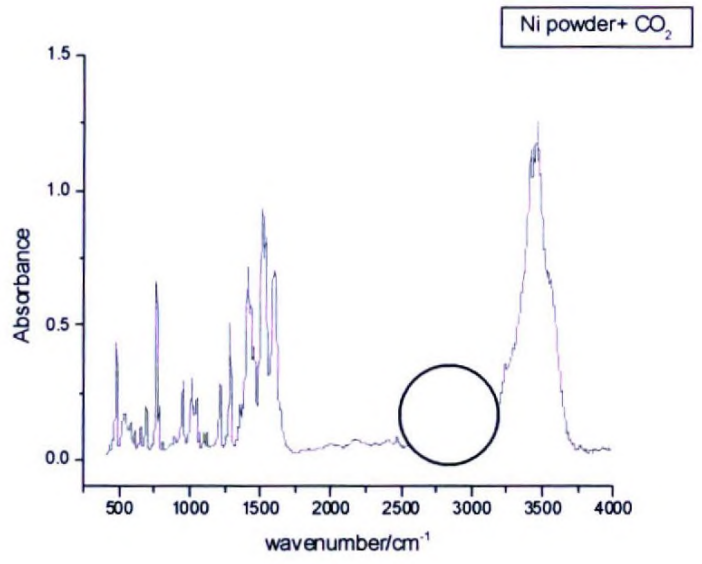

Fig.25.d FTIR spectrum of Ni(II) complex (original solid) after passing CO_2 gas

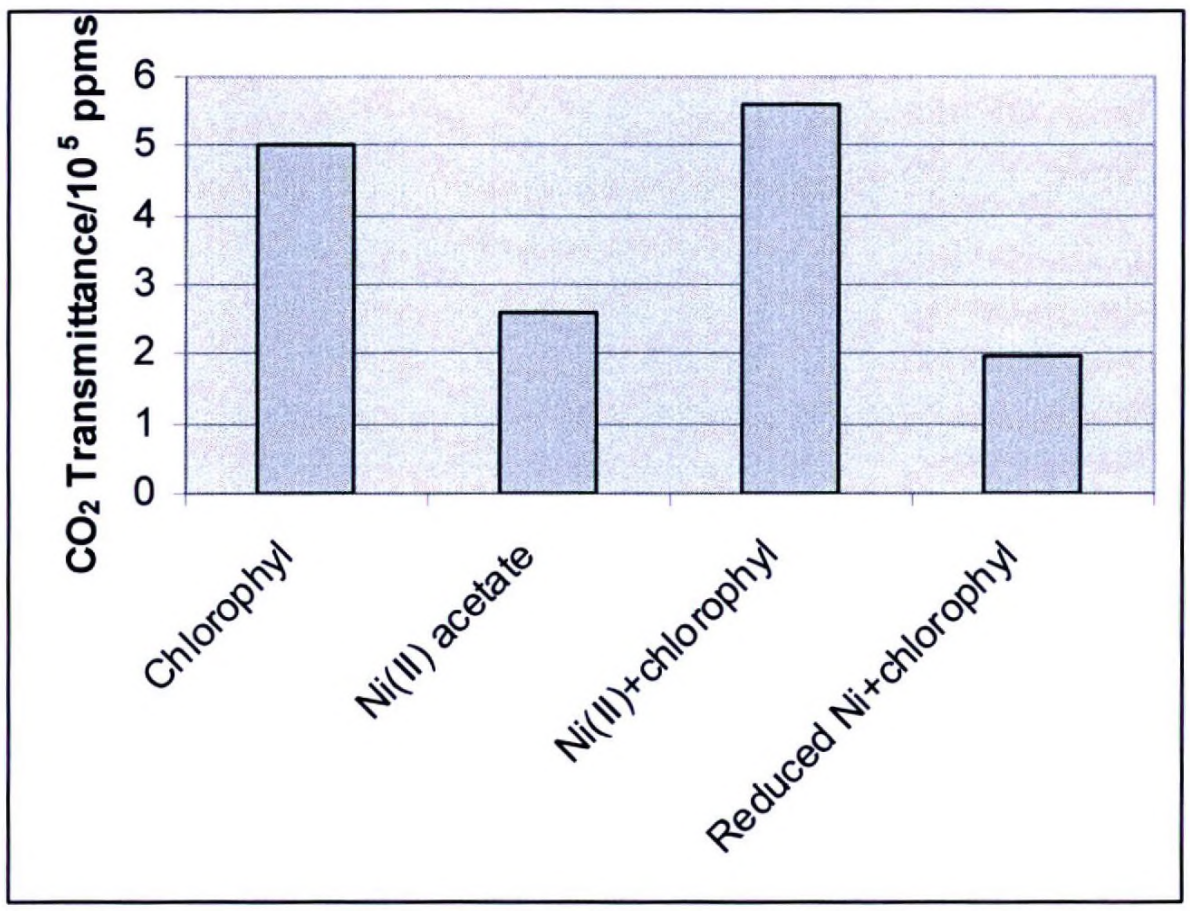

Fig.26: CO_2 Transmittance by natural and modified chlorophyll asystems.

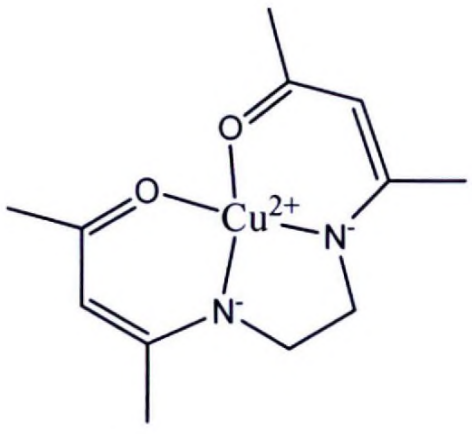

Fig.27 The single crystal X-ray structure of N,N- ethylenebis(acetylacetoneiminato) Cu(II) complex

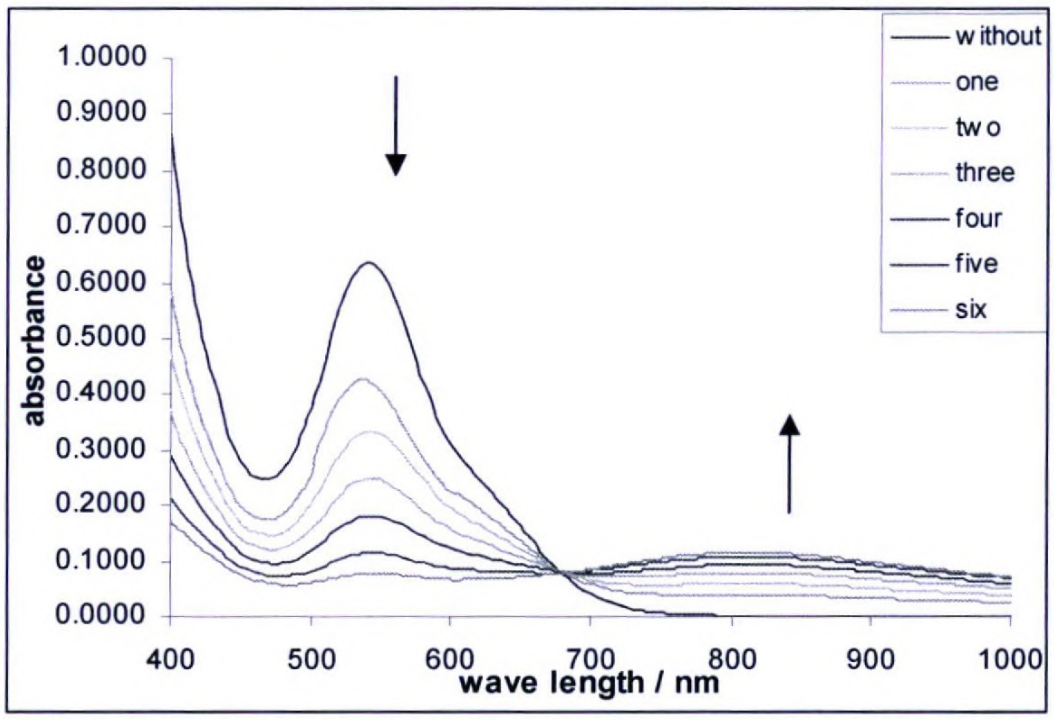

Fig. 28. UV-Visible spectra with the addition of 0.1 M HCl micro drop wise into an ethanolic solution of N,N- ethylenebis(acetylacetoneiminato)Cu(II) complex

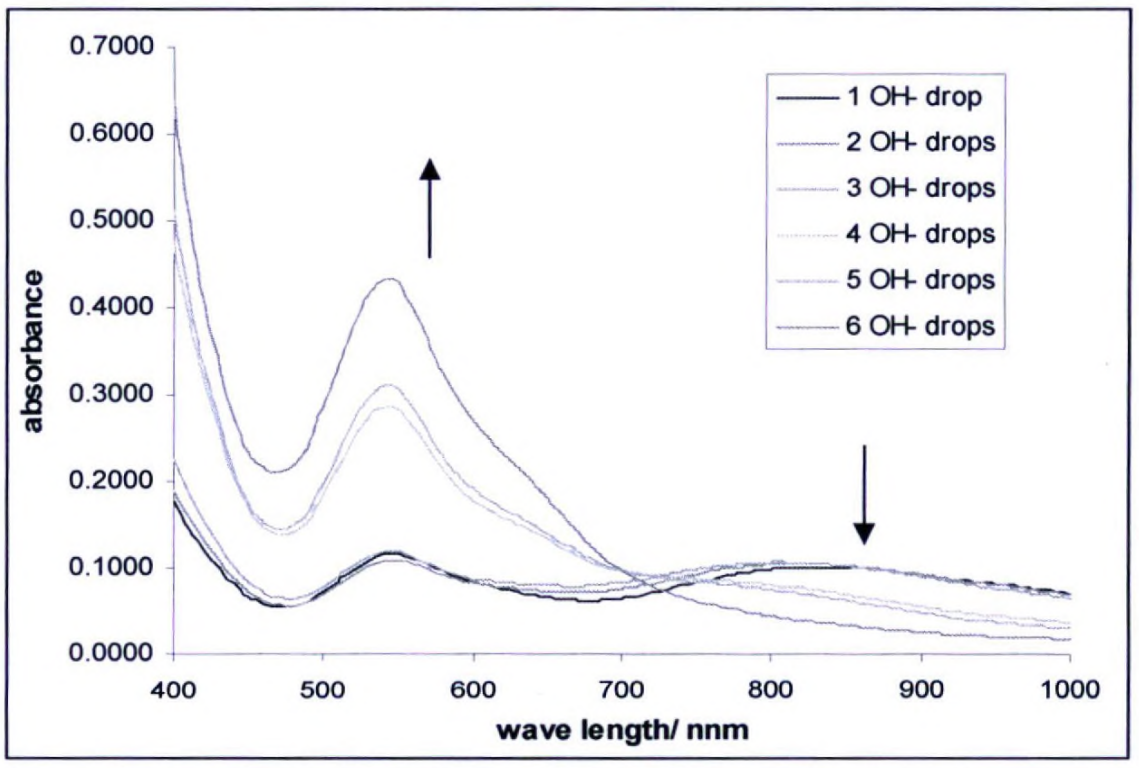

Fig. 29. UV-Visible spectra with the addition of 0.1 M NaOH micro drop wise into the same N,N- ethylenebis(acetylacetoneiminato)Cu(II) complex solution mixture

Table 5. Colour of the N,N- ethylenebis(acetylacetoneiminato)Cu(II) complex in different pH values

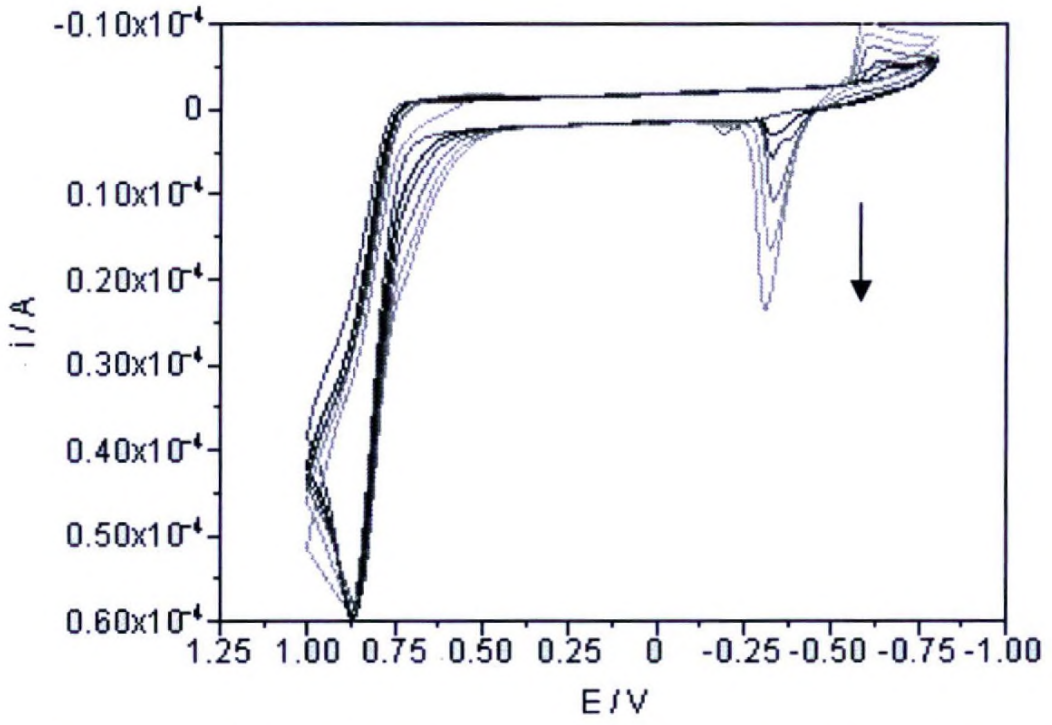

Fig. 30. CV with the addition of 1.0 M HCl to an ethanolic solution of N,N-ethylenebis(acetylacetoneiminato)Cu(II) complex

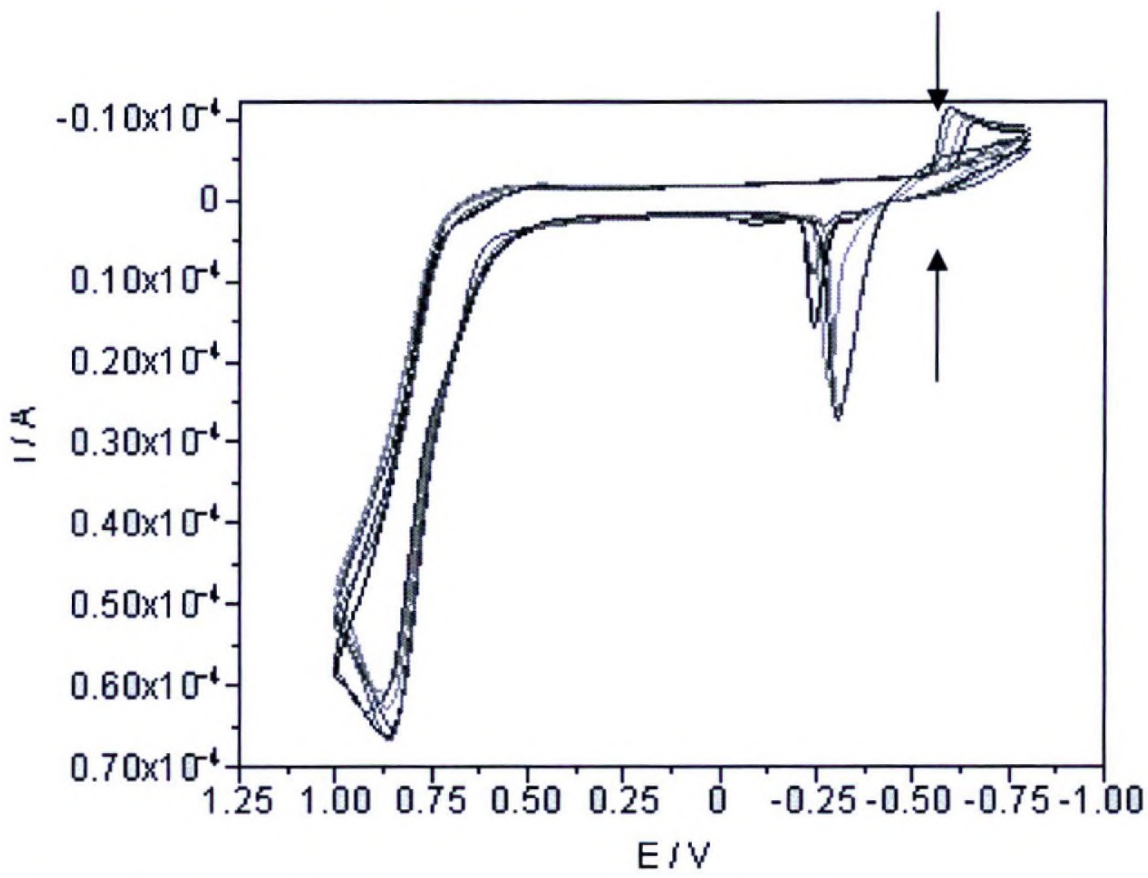

Fig. 31 CV with the addition of 1.0 M NaOH to the same ethanolic solution of N,N-ethylenebis(acetylacetoneiminato)Cu(II) complex

.

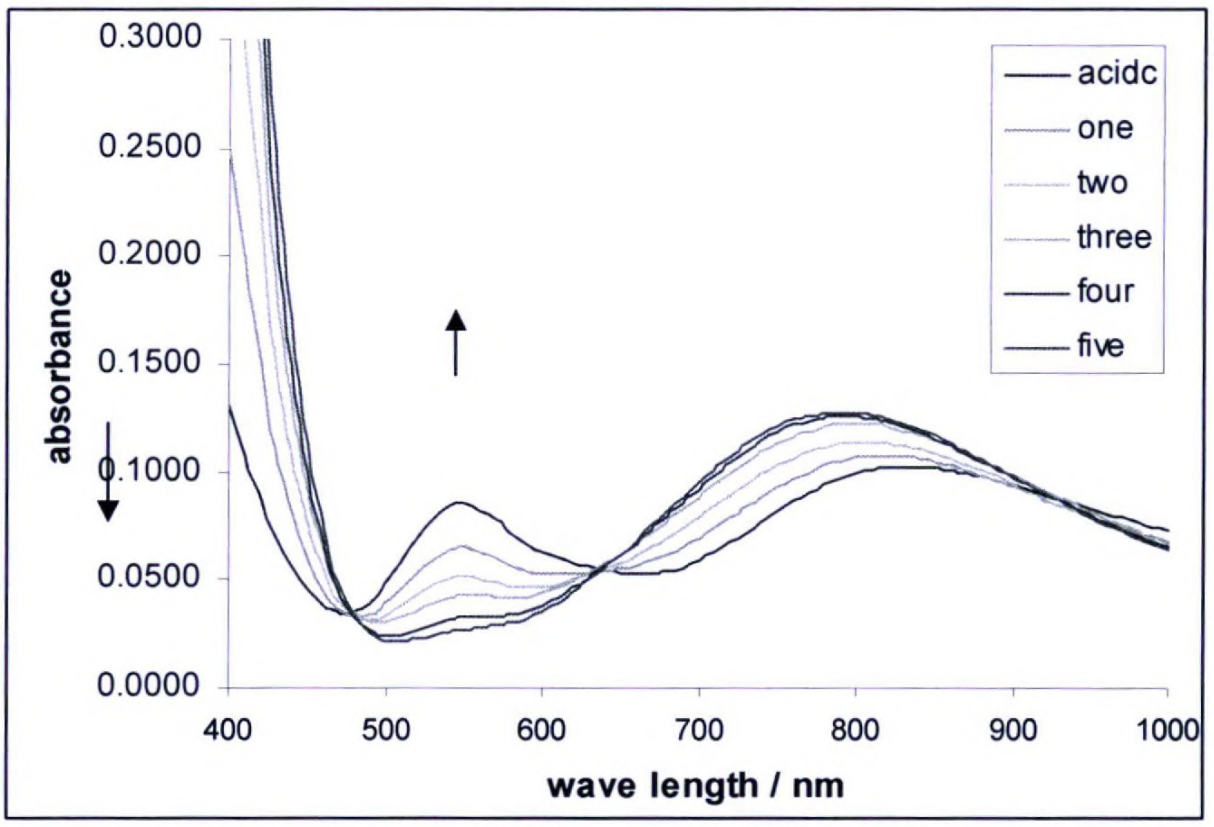

Fig. 32 UV-visible spectra with the stepwise addition of 1.0 M SCN^- to acidic ethanolic solution of N,N- ethylenebis(acetylacetoneiminato)Cu(II) complex

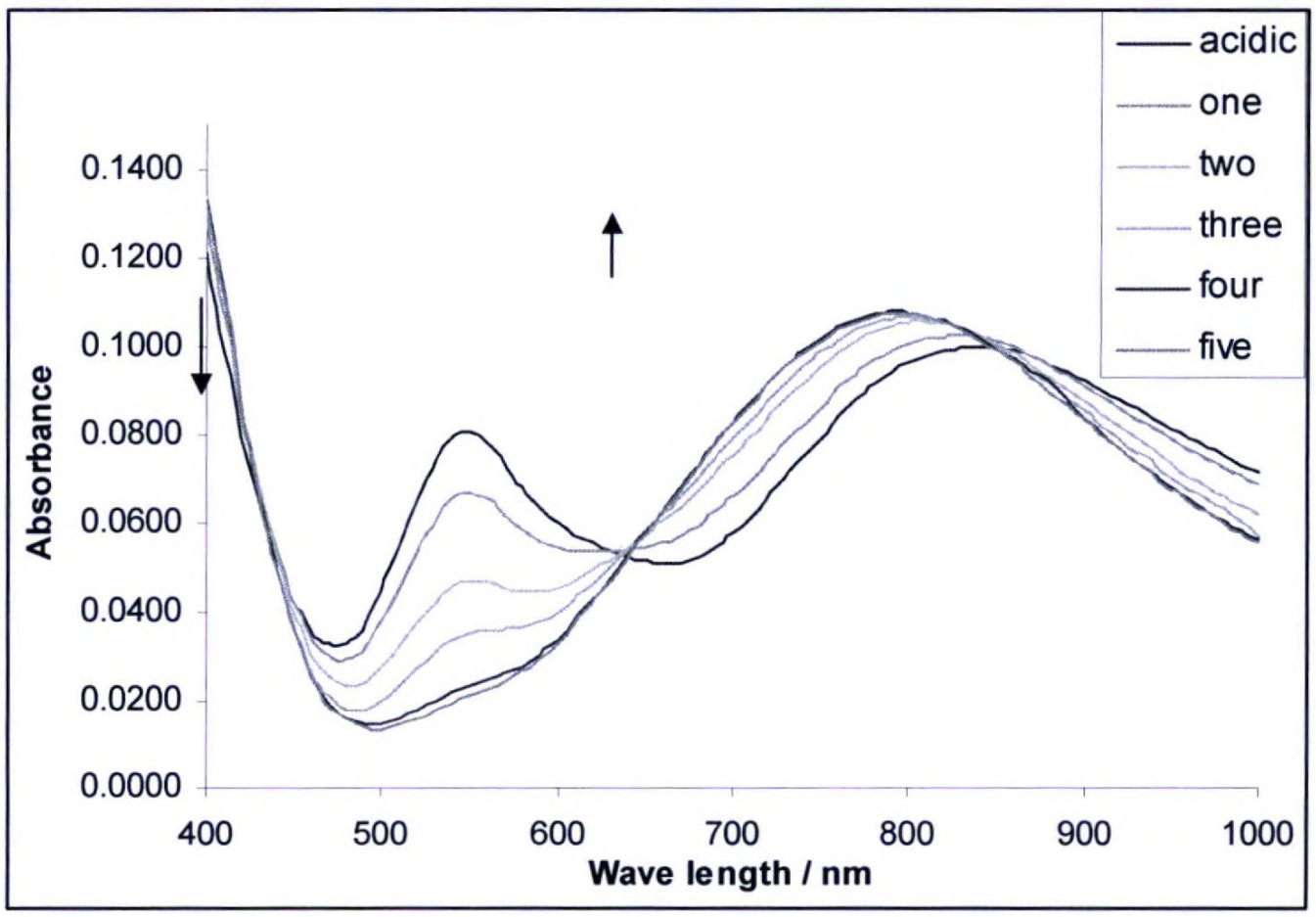

Fig. 33 UV-visible spectra with the stepwise addition of 1.0 M Br^- to acidic ethanolic solution of N,N- ethylenebis(acetylacetoneiminato)Cu(II) complex

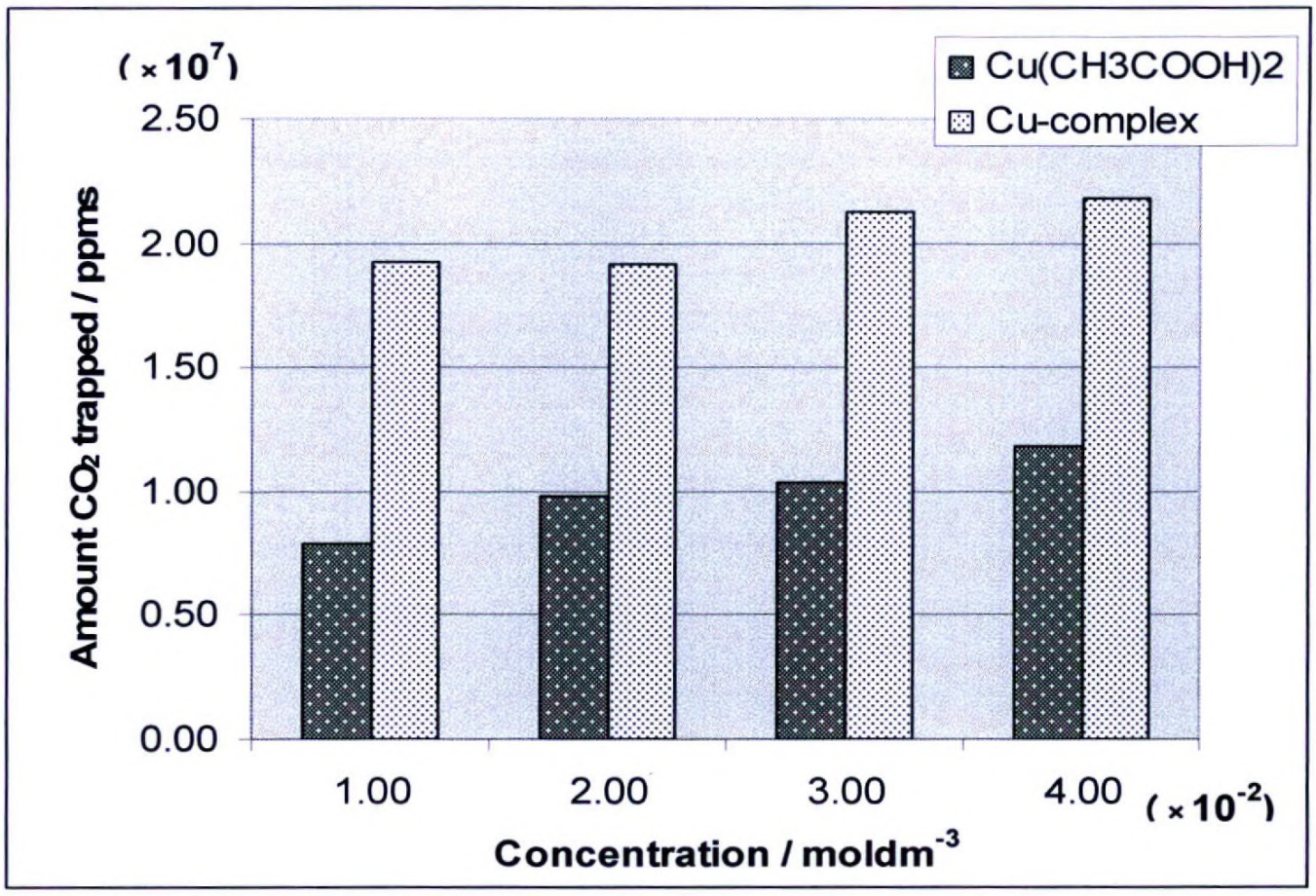

Fig. 34. Amount of CO_2 trapped by the N,N- ethylenebis(acetylacetoneiminato) Cu(II) complex complex and $Cu(CH_3COO)_2$ at RT

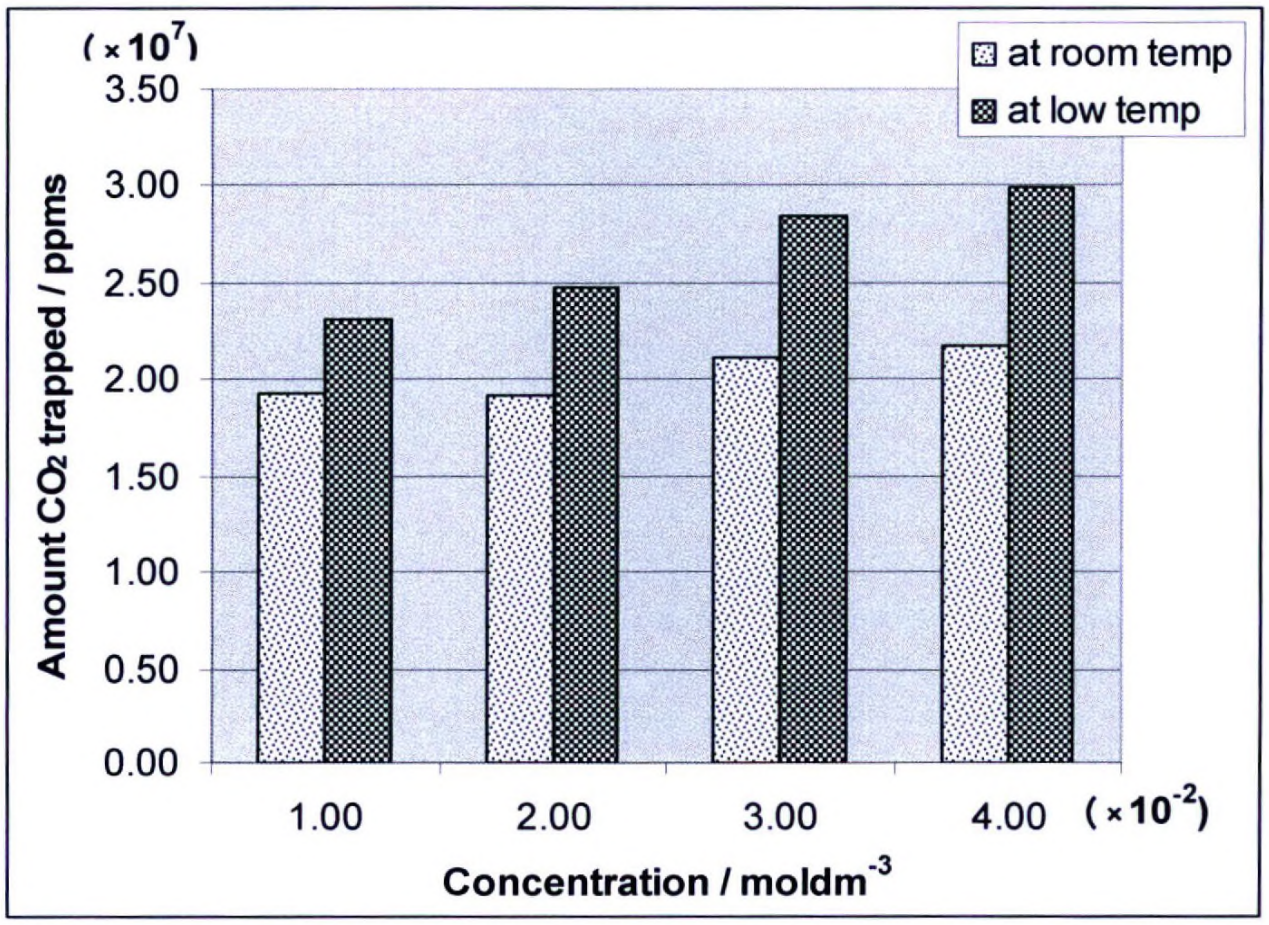

Fig. 35. Amount of CO_2 trapped by the N,N- ethylenebis(acetylacetoneiminato) Cu(II) complex at different temp.

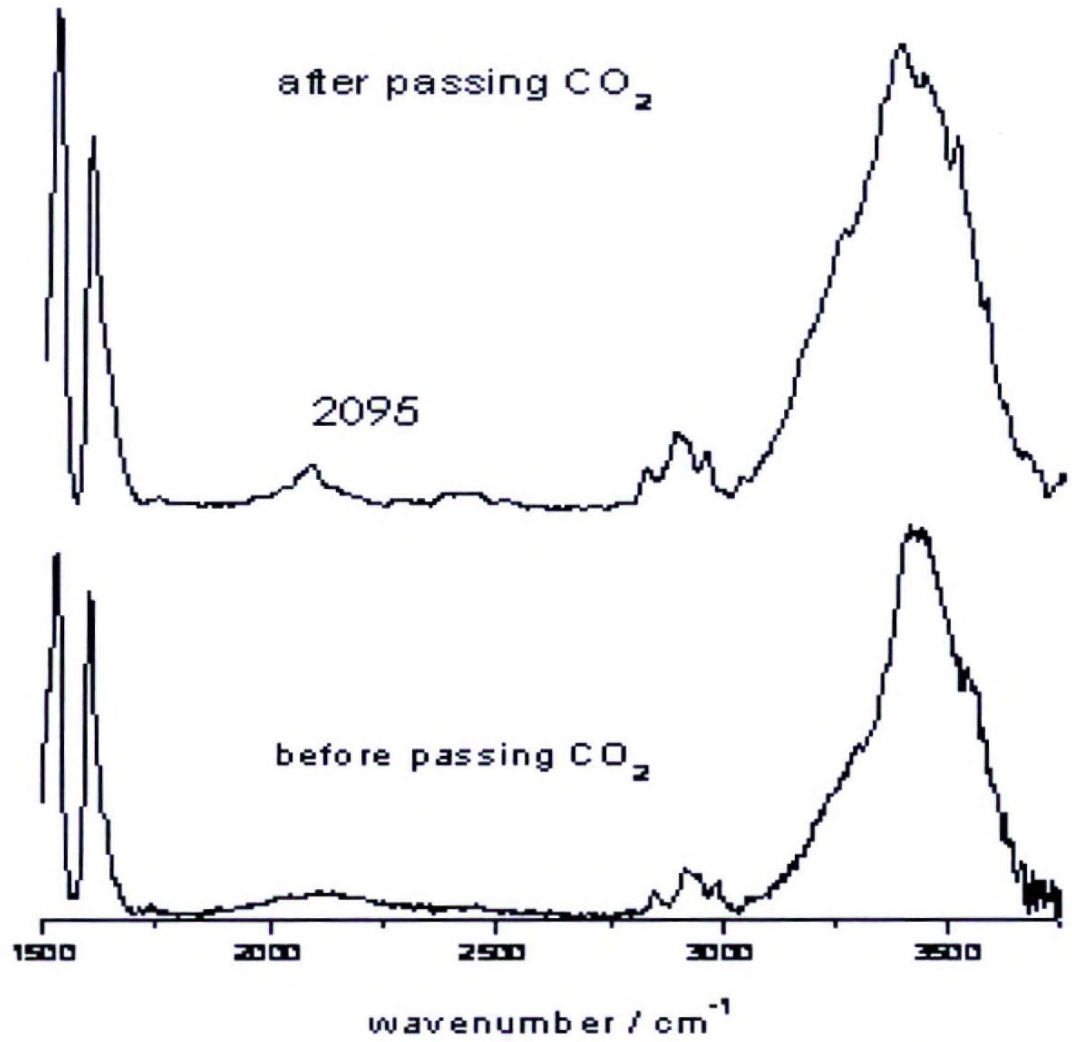

Fig. 36. IR spectra of the N,N- ethylenebis(acetylacetoneiminato)Cu(II) complex before and after passing CO_2 through a solid sample of the complex

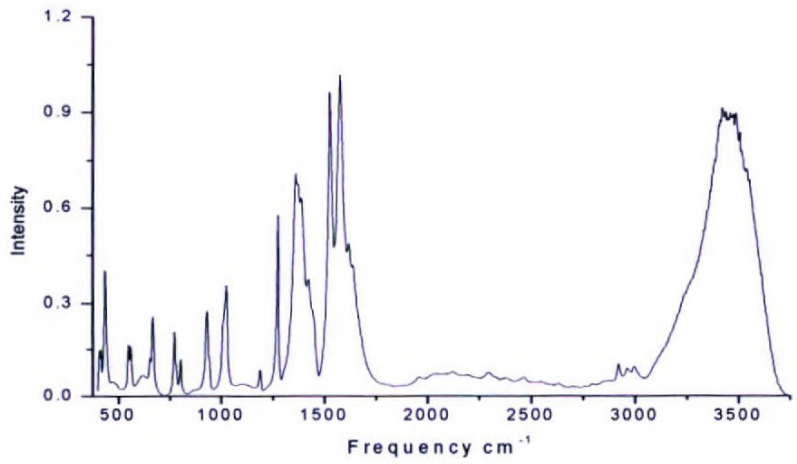

Fig. 37. IR spectrum of Fe-en-acac-R

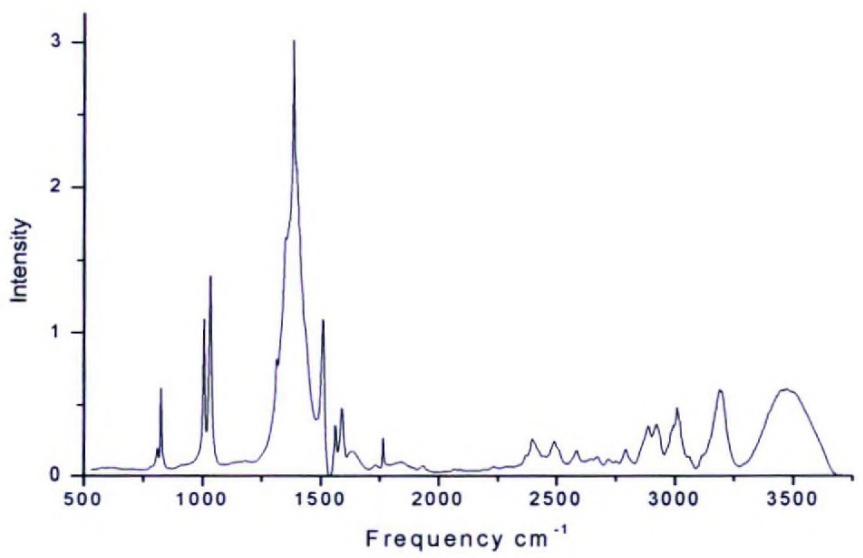

Fig. 38 IR spectrum of Fe-en-acac-Y

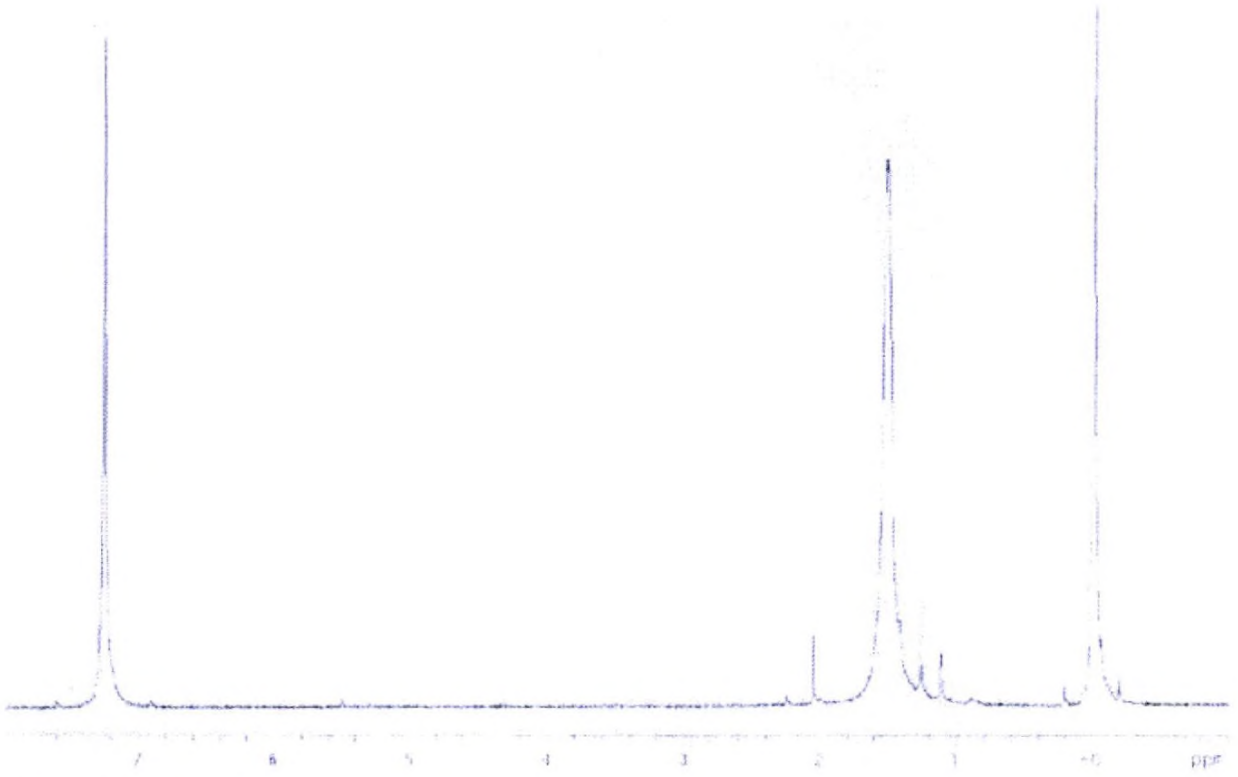

(a)1H NMR spectrum of Fe-en-acac-Y ;

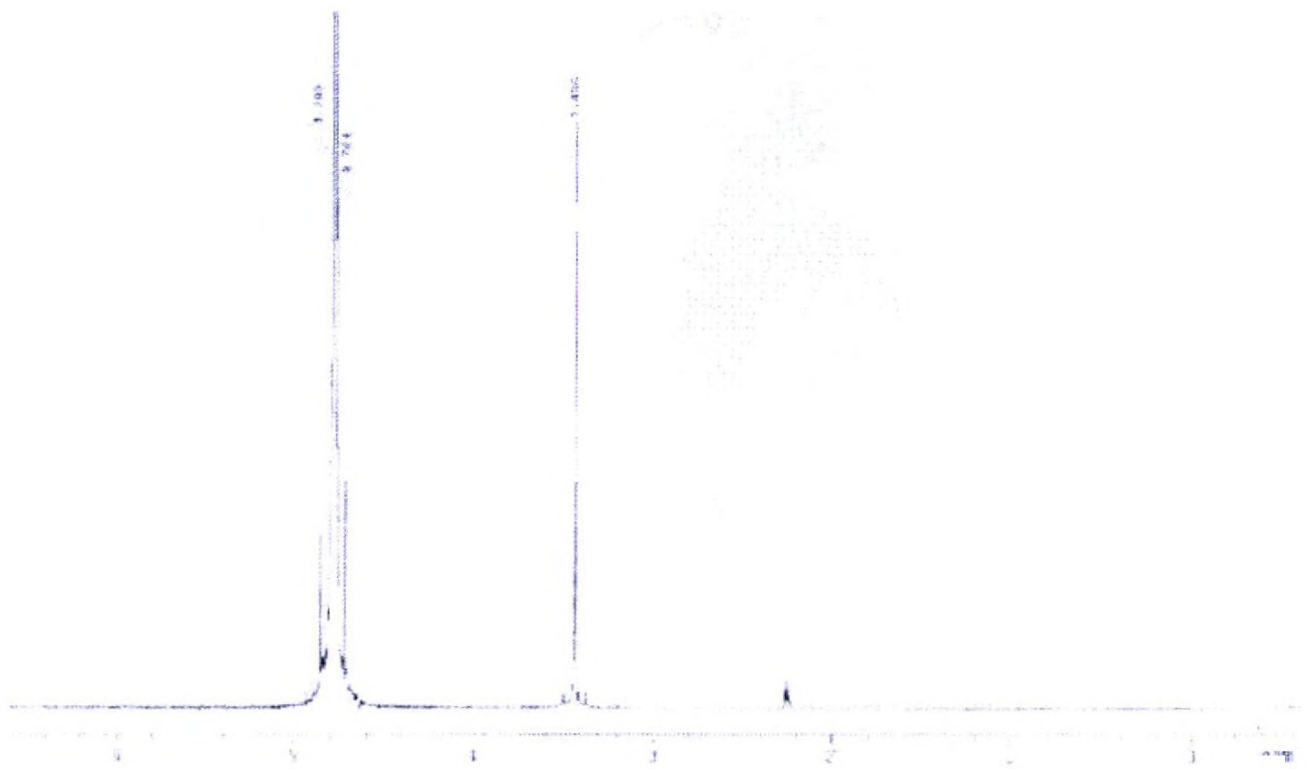

(b) **^{1}H NMR spectrum of Fe-en-acac-Y**

Fig. 39

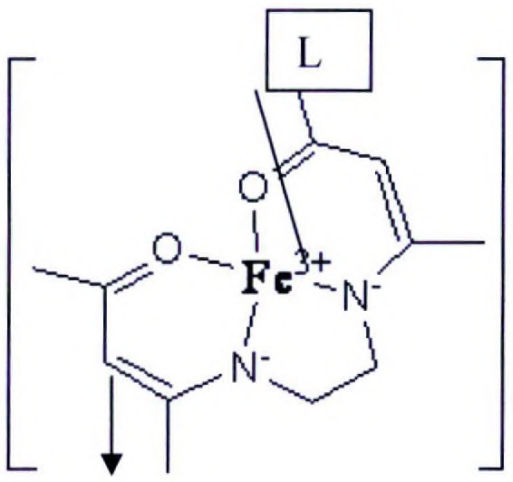

Fig. 40 Predicted structure of Fe-en-acac-R complex

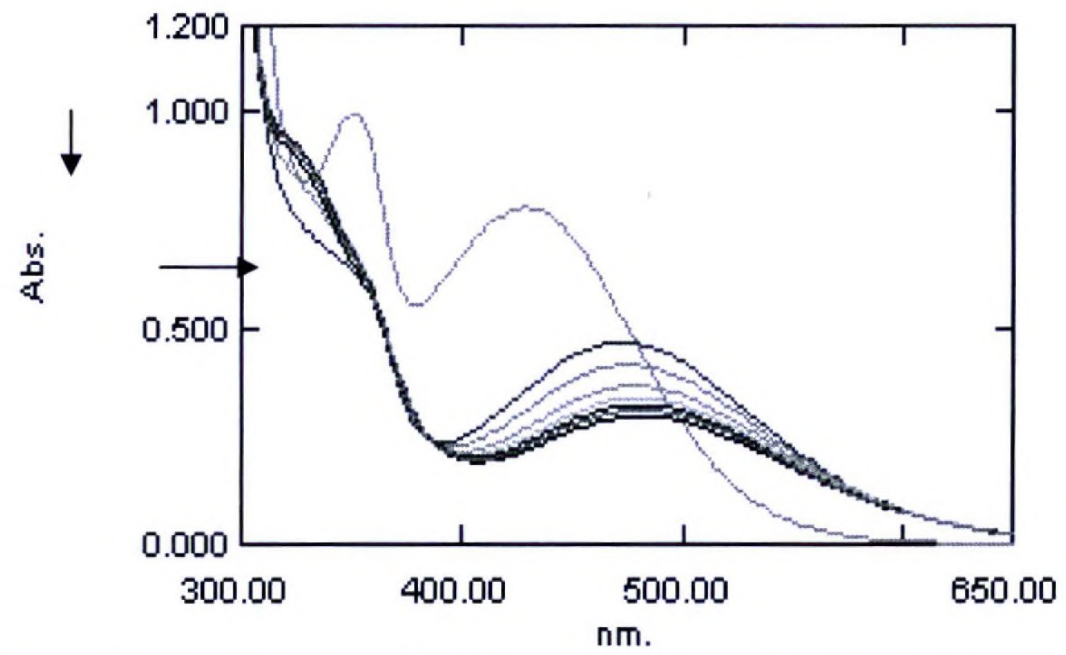

Fig. 41 UV-visible spectra with the stepwise addition of 0.1 M HCl into ethanolic Fe-en-acac-R

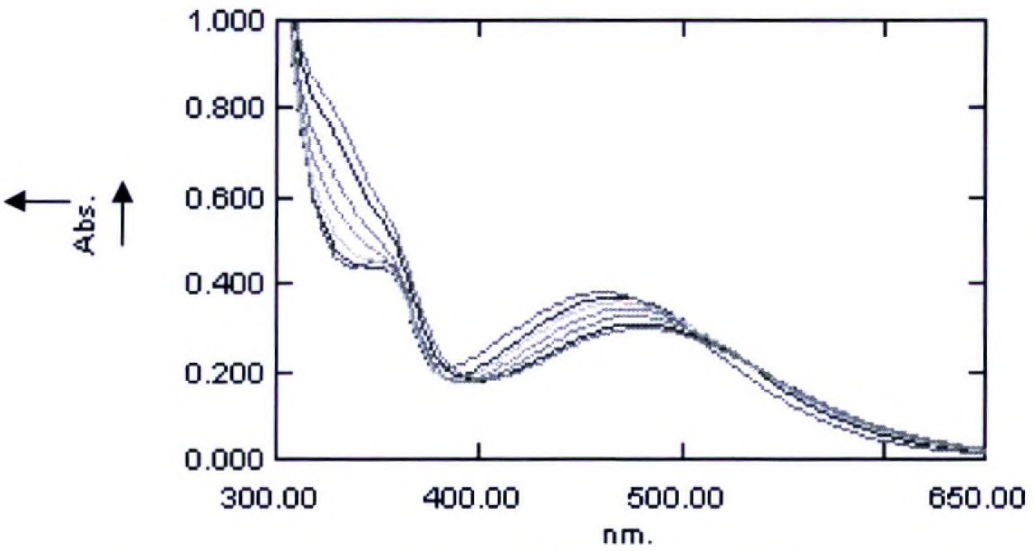

Fig. 42. UV-visible spectra with stepwise addition of 0.1 M NaOH into same solution of Fe-en-acac-R

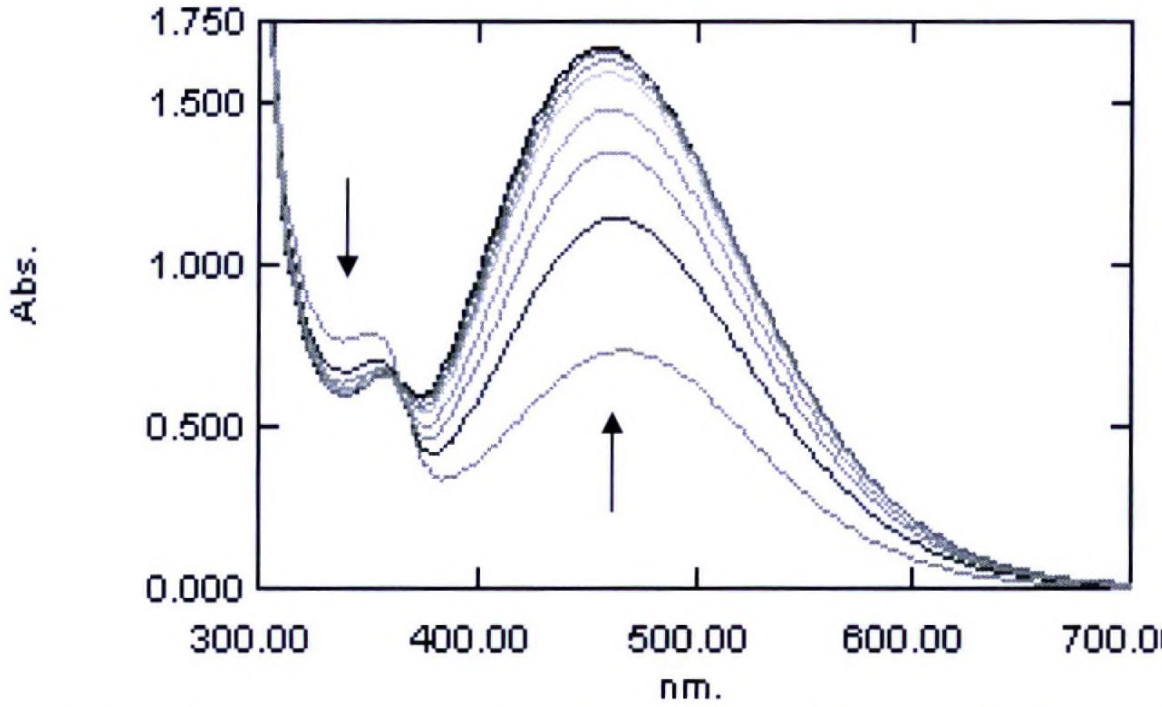

Fig. 43. UV-visible spectra with the stepwise addition of 1.0 moldm^{-3} SCN$^-$ into acidified ethanolic solution of Fe-en-acac-R

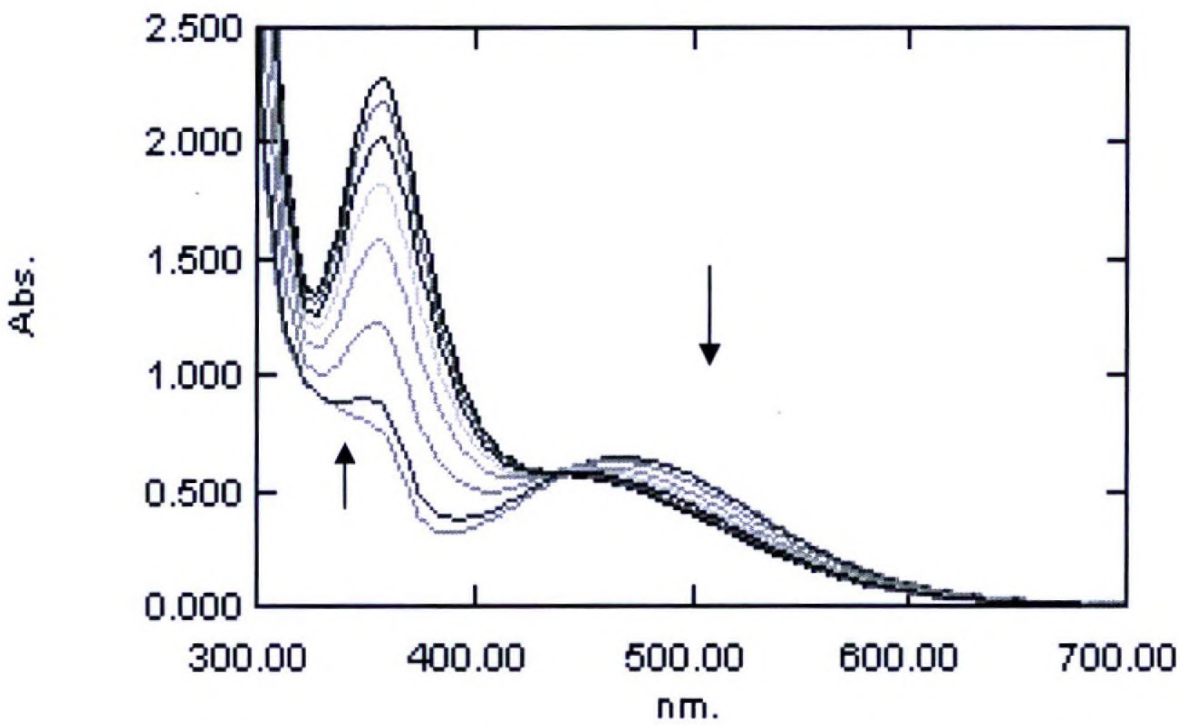

Fig. 44. UV-visible spectra with the stepwise addition of 1.0 moldm^{-3} I$^-$ into acidified ethanolic solution of Fe-en-acac-R

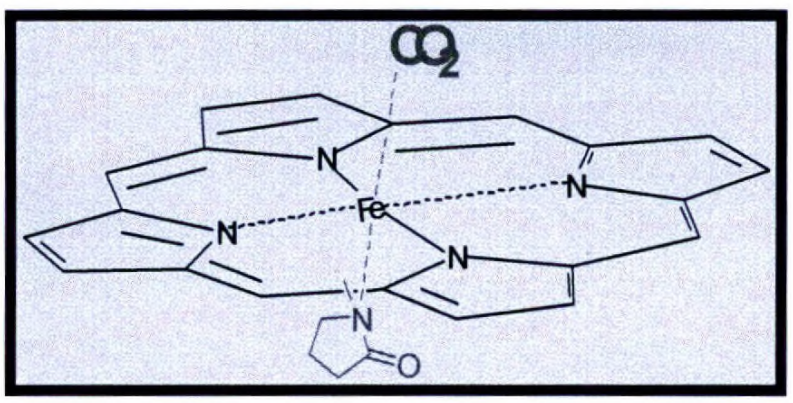

Fig.45

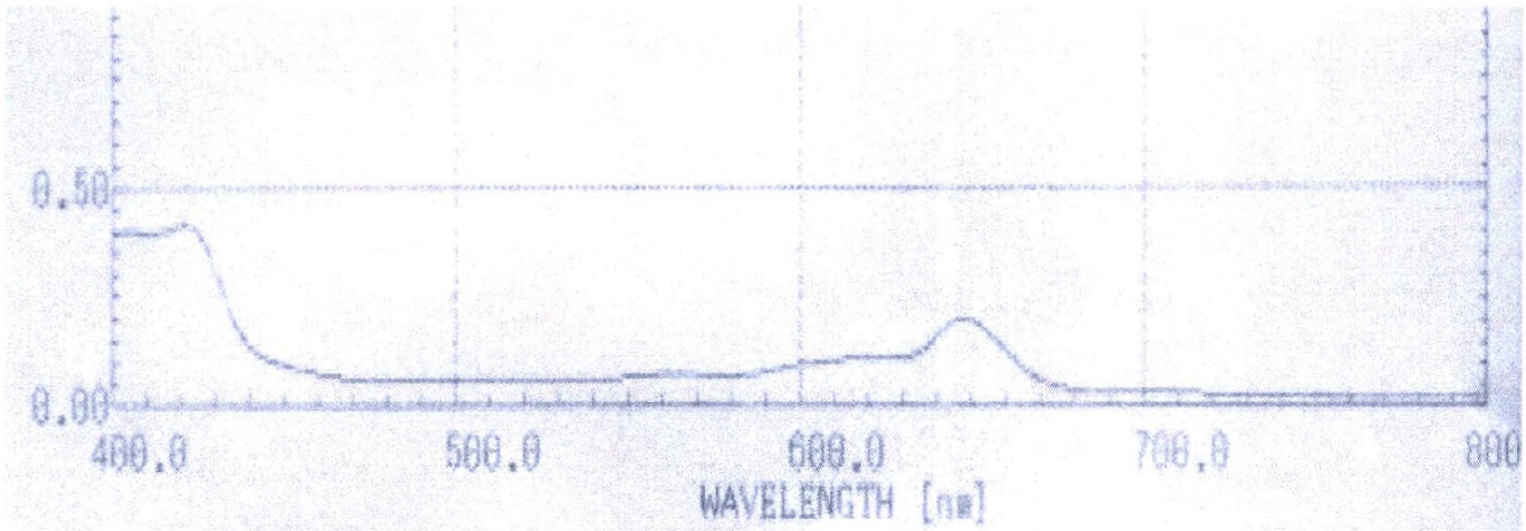

Fig. 46 UV-VIS spectrum of the liquid Fe(ii) Porphyrin using methanol

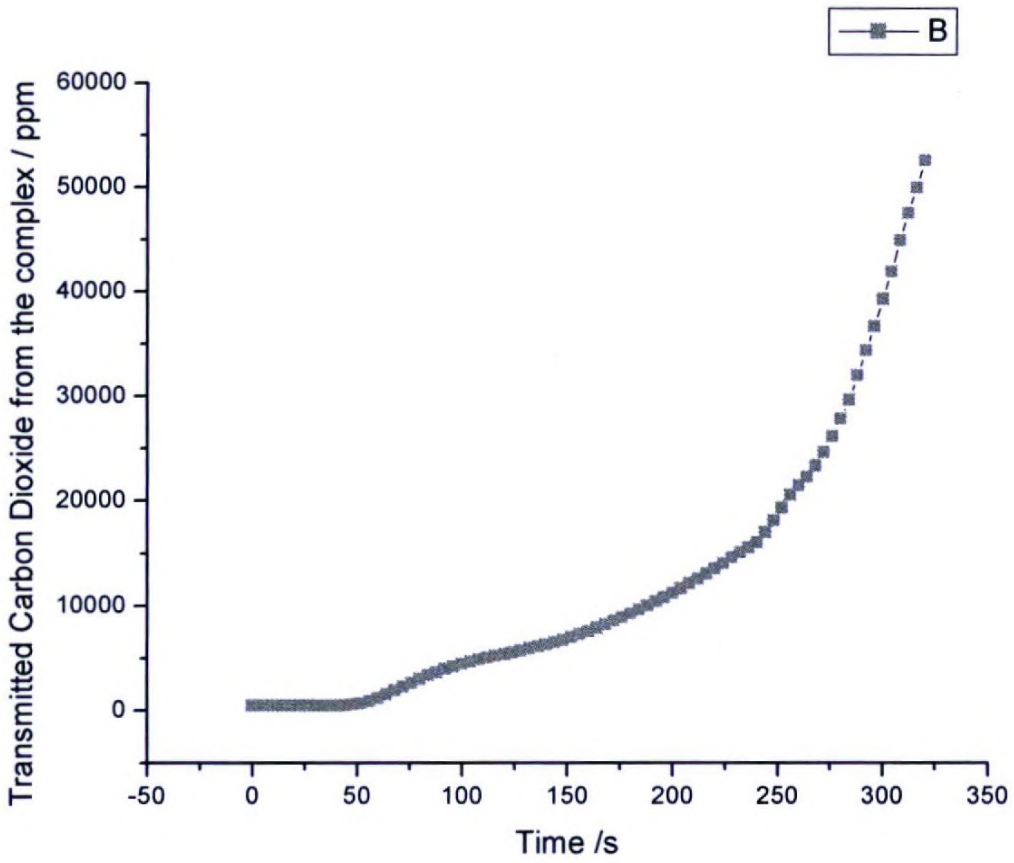

Fig.47CO2 transmittance from Fe(II)complex with time

Fig.48 CO_2 transmittance for complexes

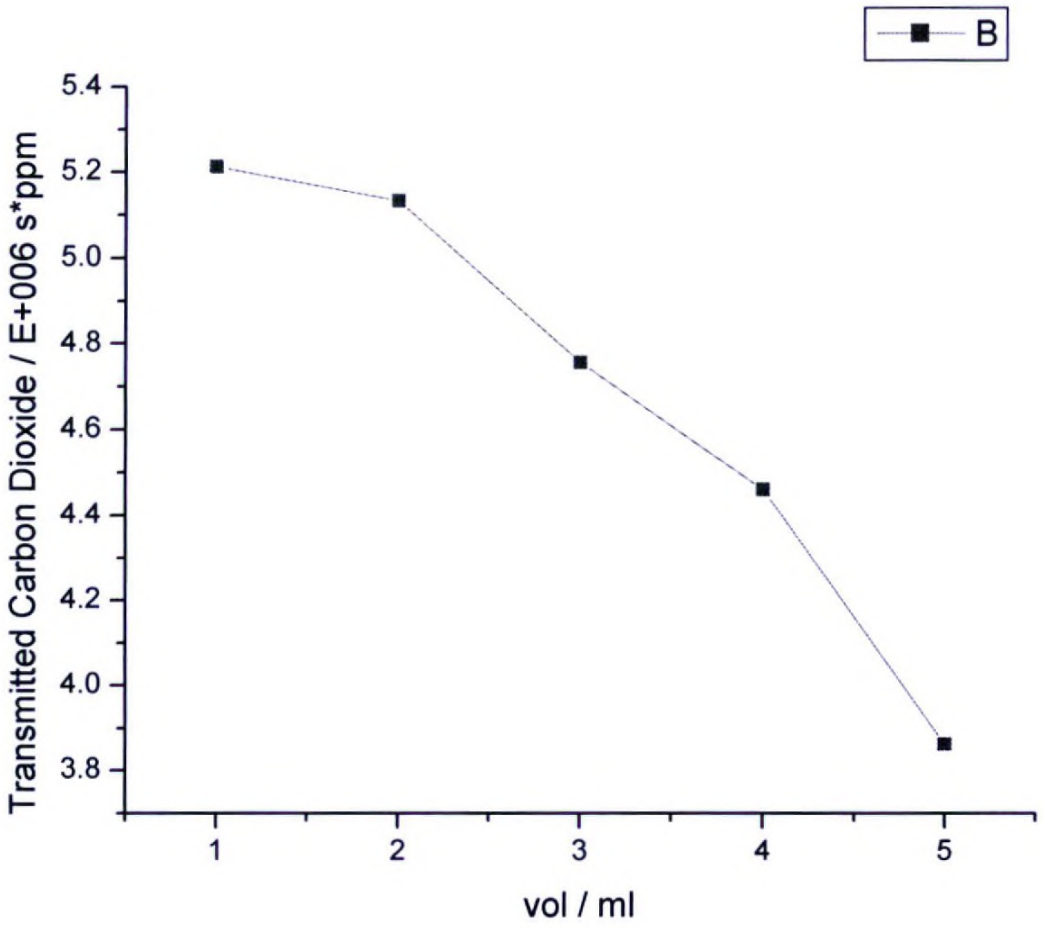

Fig.49 CO_2 transmittance with increasing [Fe(II)complex]

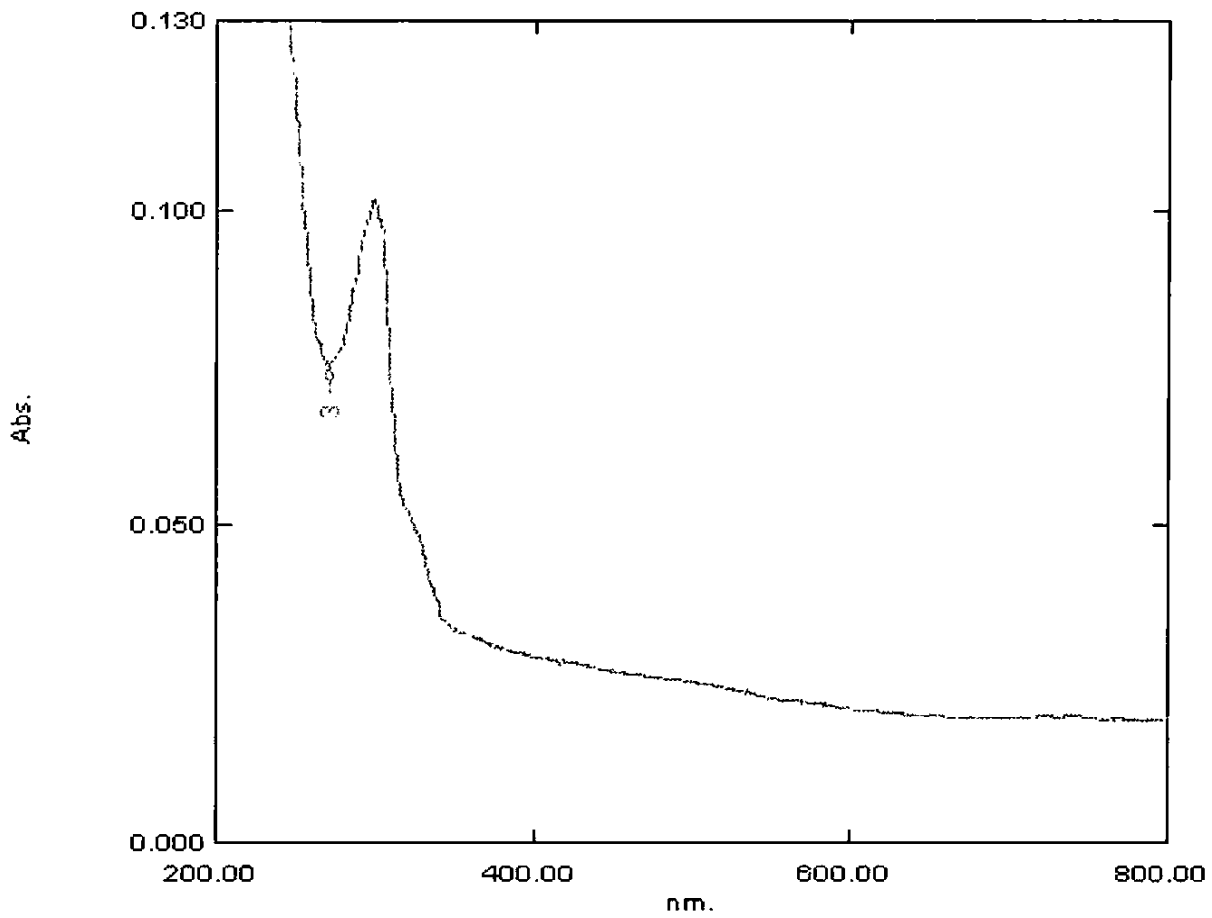

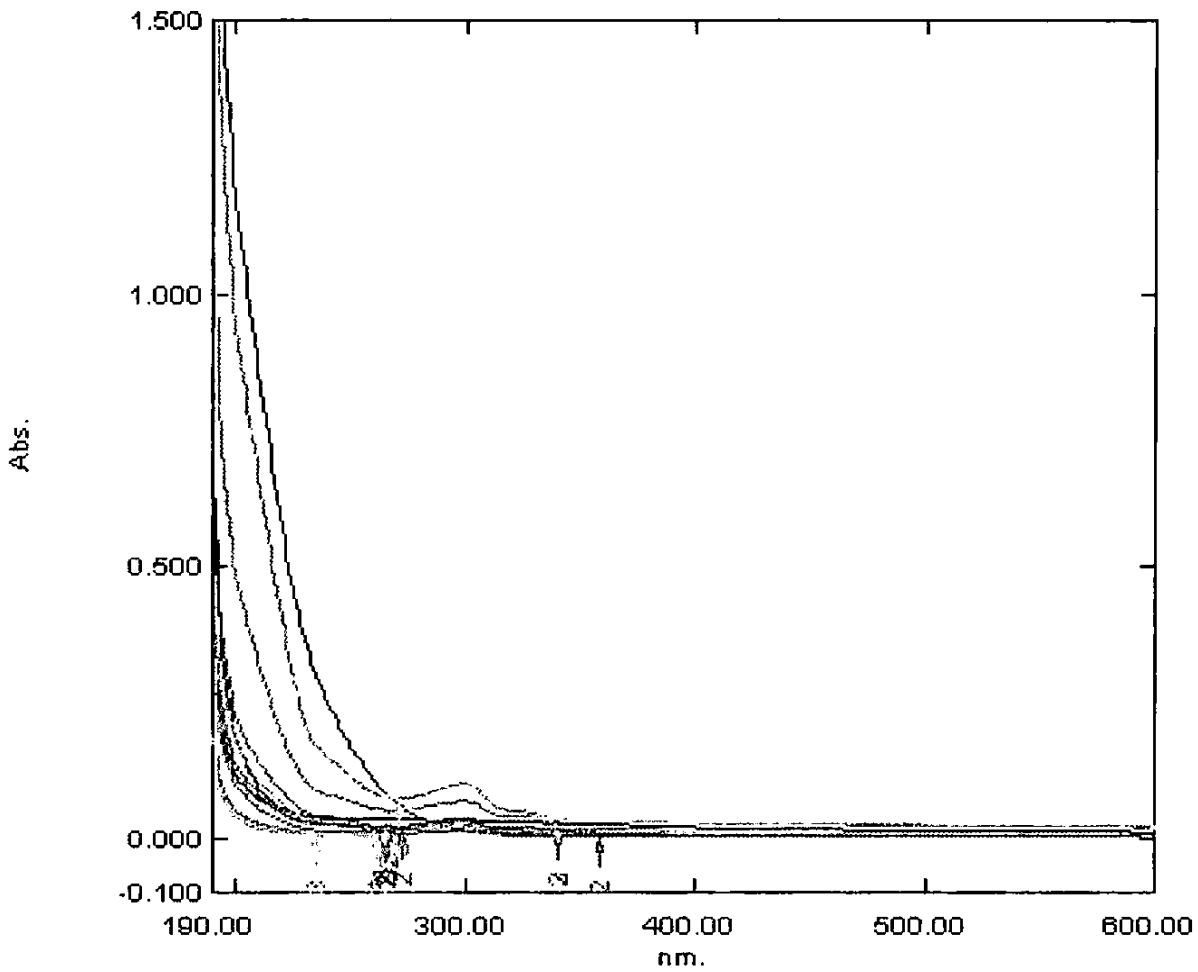

(a) (b)

Fig. 50 UV-VIS spectra of the solution (a) after 165 min of addition of Cu^{2+} (b) after each 15 min. of addition.

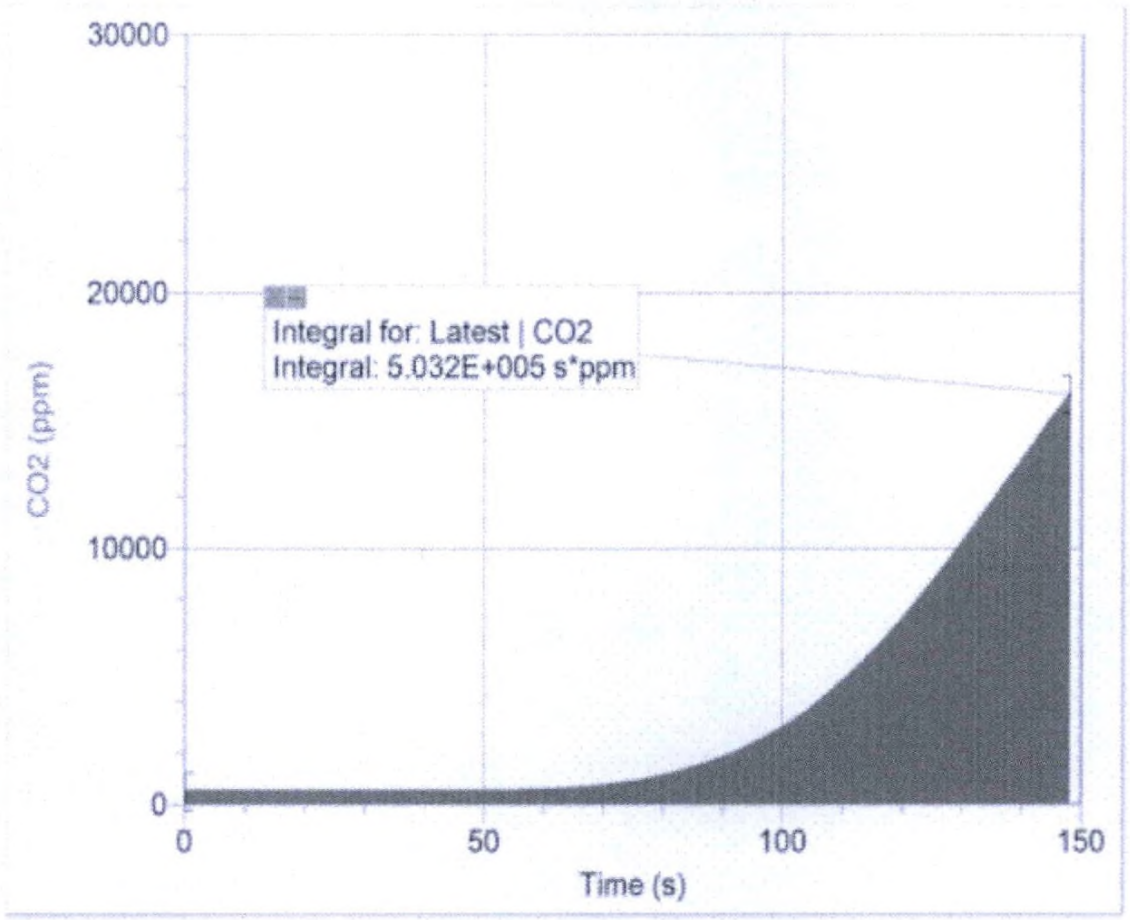

Fig.51 CO_2 transmittance of Fe(II)Chlorophyll complex.

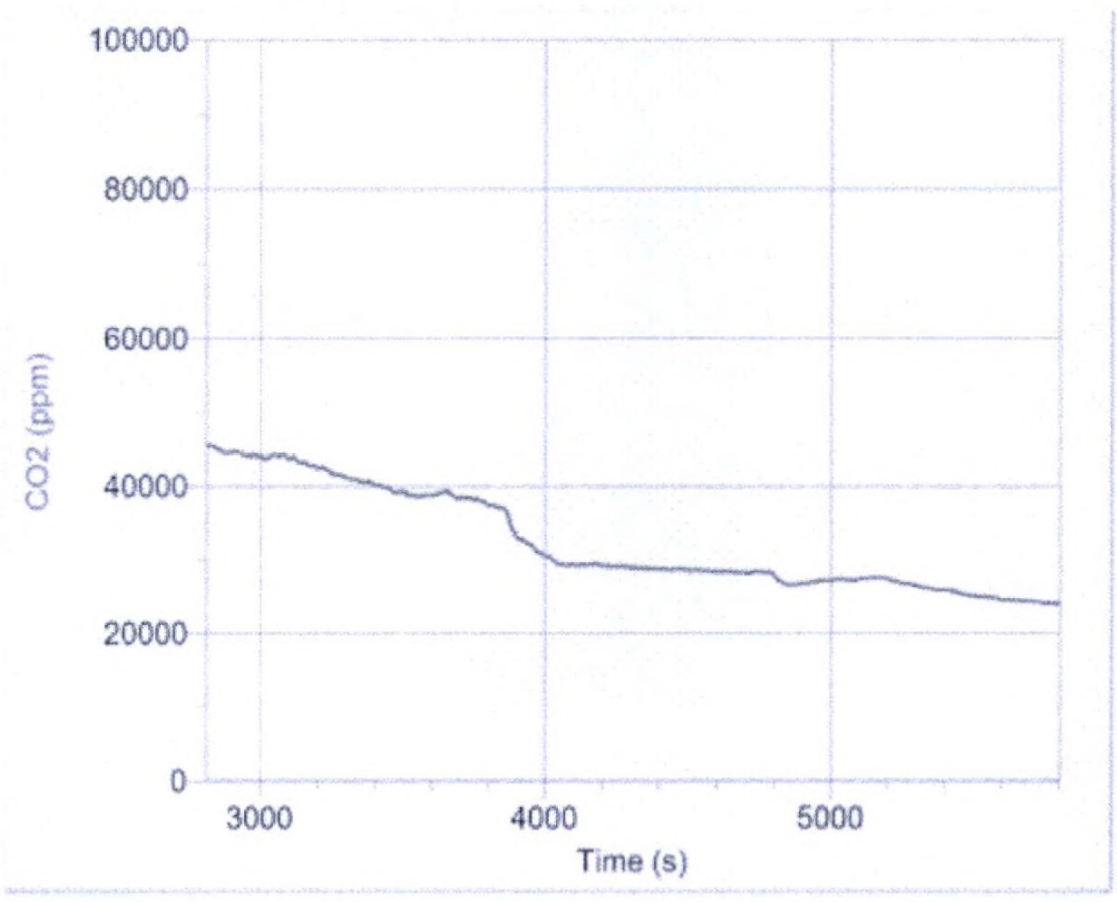

Fig. 52 Change in amount of CO_2 in the flask with the irradiation for Fe(III)Chlorophyll ;(trial1).

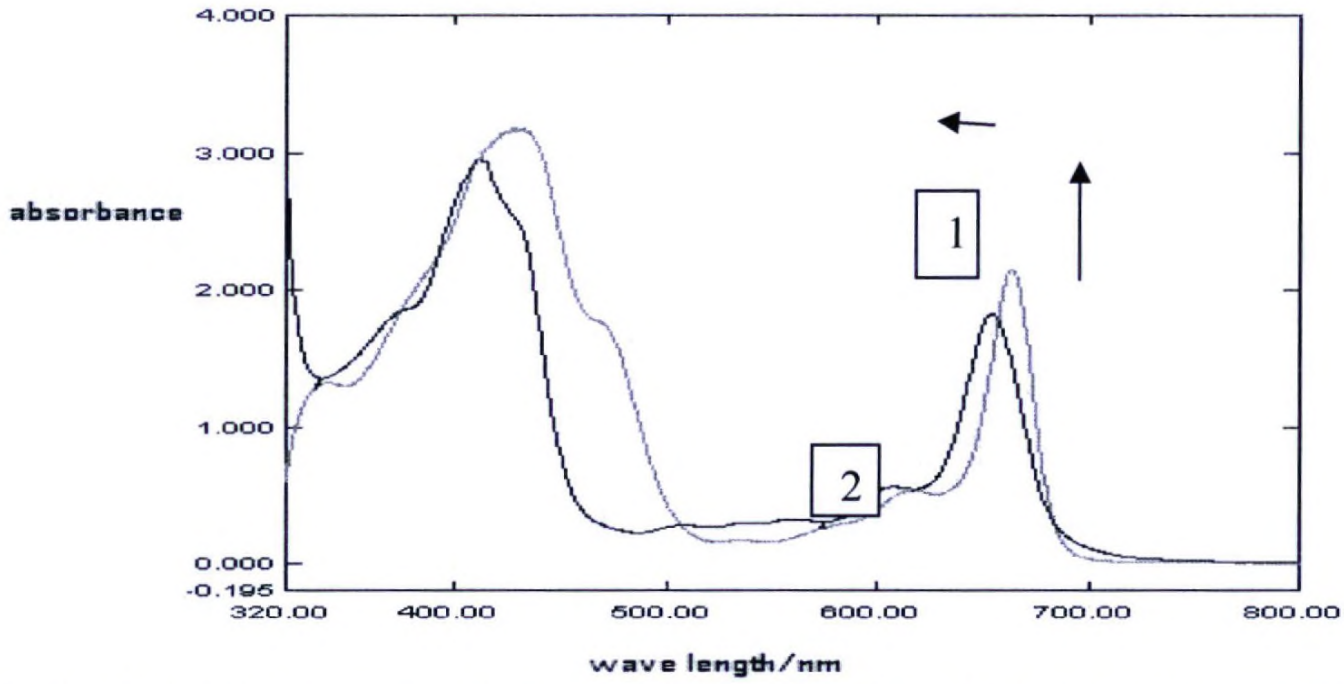

Fig.53.UV-Visible spectra of chlorophyll-a (1) and Co(II) Porphyrin complex (2)

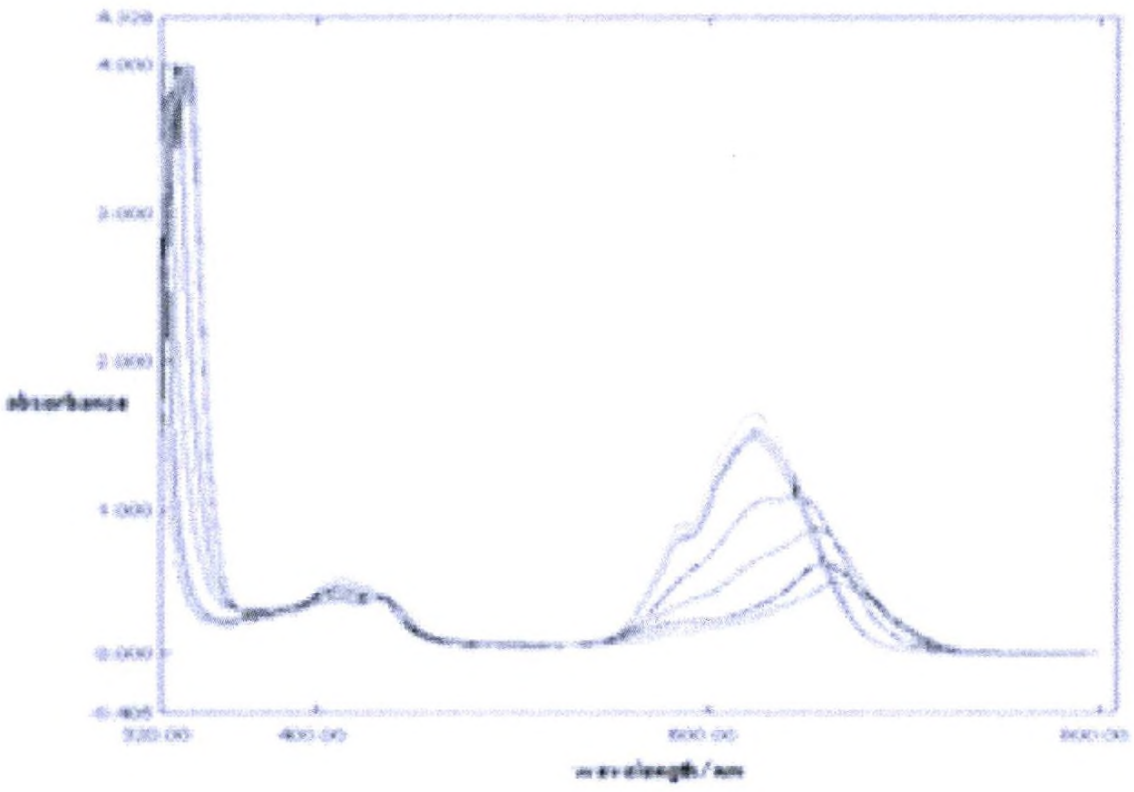

Fig.54.UV-visible spectra Co(II)Porphyrin complex with the addition of SCN-

National Digitization Project

National Science Foundation

Institute : National Science Foundation

1. Place of Scanning : Sanje (Private) Ltd, Hokandara
2. Date Scanned : 2017/04/18
3. Name of Digitizing Company : Sanje (Private) Ltd, No 435/16, Kottawa Rd, Hokandara North, Arangala, Hokandara
4. Scanning Officer

Name : H.P.A.V. Caldera

Signature : .....

Certification of Scanning

I hereby certify that the scanning of this document was carried out under my supervision, according to the norms and standards of digital scanning accurately, also keeping with the originality of the original document to be accepted in a court of law.

Certifying Officer

Designation : Information Officer

Name : Renuka Sugathadasa

Signature : .....

Date : .....

"This document/publication was digitized under National Digitization Project of the National Science Foundation, Sri Lanka"